

Anomalous contribution to galactic rotation curves due to stochastic spacetime

Jonathan Oppenheim¹ and Andrea Russo¹

¹*Department of Physics and Astronomy, University College London,
Gower Street, London WC1E 6BT, United Kingdom*

We consider a proposed alternative to quantum gravity, in which the spacetime metric is treated as classical, even while matter fields remain quantum. Consistency of the theory necessarily requires that the metric evolve stochastically. Here, we show that this stochastic behaviour leads to a modification of general relativity at low accelerations. In the low acceleration regime, the variance in the acceleration produced by the gravitational field is high in comparison to that produced by the Newtonian potential, and acts as an entropic force, causing a deviation from Einstein's theory of general relativity. We show that in this "diffusion regime", the entropic force acts from a gravitational point of view, as if it were a contribution to the matter distribution. We compute how this modifies the expectation value of the metric via the path integral formalism, and find that an entropic force driven by a stochastic cosmological constant can explain galactic rotation curves without needing to evoke dark matter. We caution that a greater understanding of this effect is needed before conclusions can be drawn, most likely through numerical simulations, and provide a template for computing the deviation from general relativity which serves as an experimental signature of the Brownian motion of spacetime.

According to the standard model of cosmology, Λ CDM, visible matter makes up only 5% of its contents, with dark energy or a cosmological constant Λ and cold dark matter (CDM) making up the remaining part. There is strong evidence for this. Dark energy or a cosmological constant appears to drive the expansion of the universe, while dark matter can account for the flatness of galactic rotation curves [1], is seen in the CMB power-spectrum [2, 3], by gravitational lensing [4], through dispersion relations of elliptical galaxies [5], mass estimates of galaxy clusters [6], and appears to be required for the formation of galaxies in the early universe [7]. But despite large scale efforts, neither dark energy or dark matter have been directly detected. Their apparent existence is only felt through their gravitational field. Discoveries in physics are often indirect. The neutrino was conjectured by Pauli to exist in 1939 in order to account for energy conservation in β -decay, and only gave a signal in a particle detector 26 years later. But in the absence of any direct evidence for dark energy or dark matter it is natural to wonder whether they may be unnecessary scientific constructs like celestial spheres, ether, or the planet Vulcan, all of which were superseded by simpler explanations. Gravity has a long history of being a trickster.

In 1983 Milgrom [8] found that if a theory had the property that either the law of inertia were modified, or Newton's theory of gravity was modified at low acceleration such that

$$a = \begin{cases} a_N & \text{when } a \gg a_0, \\ \sqrt{a_0 a_N} & \text{when } a \ll a_0. \end{cases} \quad (1)$$

with a_N the Newtonian acceleration, and a_0 a parameter of order 10^{-10} m/s^2 , then the flatness of rotation curves and the Tully-Fischer relation [9] would follow. These are effects currently attributed to dark matter. He called this Modified Newtonian Dynamics (MOND) [10–12]. Here, we would like to point out that this behaviour is reminiscent of Brownian motion, with a mean of a_N , and standard deviation of $\sqrt{a_N}$, a statement which we hope becomes clearer as we progress. In 1983 Milgrom also observed [8] that the MOND acceleration (in the units of this article, $c = \hbar = 1$), is given by

$$a_0 \approx \frac{1}{2\pi} \sqrt{\frac{\Lambda}{3}}, \quad (2)$$

a coincidence that has yet to be explained. A number of theories have been proposed to reproduce MOND phenomenology [11, 12], but thus far no satisfying fundamental theory which reproduces this behavior has been found. The problem is that while it is easier to modify a theory at high energy, modifying a theory at low energy while still respecting current experimental bounds is difficult.

We here calculate the effect on rotation curves due to a recently proposed alternative to quantum gravity [13, 14]. We will, in particular, use the path integral formulation developed in [14, 15], with Zach Weller-Davies. The theory was not developed to explain dark matter, but rather, to reconcile quantum theory with gravity. However, it was already noted in [13], that diffusion in the metric could result in stronger gravitational fields when one might otherwise expect none to be present, and that this raised the possibility that gravitational diffusion may explain galactic rotation curves and galaxy formation without the need for dark matter. Here, we will confirm this intuition and find that,

Listening to the Noise: Blind Denoising with Gibbs Diffusion

David Heurtel-Depeiges¹ Charles C. Margossian² Ruben Ohana² Bruno Régaldo-Saint Blancard²

Abstract

In recent years, denoising problems have become intertwined with the development of deep generative models. In particular, diffusion models are trained like denoisers, and the distribution they model coincide with denoising priors in the Bayesian picture. However, denoising through diffusion-based posterior sampling requires the noise level and covariance to be known, preventing *blind denoising*. We overcome this limitation by introducing Gibbs Diffusion (GDiff), a general methodology addressing posterior sampling of both the signal and the noise parameters. Assuming arbitrary parametric Gaussian noise, we develop a Gibbs algorithm that alternates sampling steps from a conditional diffusion model trained to map the signal prior to the family of noise distributions, and a Monte Carlo sampler to infer the noise parameters. Our theoretical analysis highlights potential pitfalls, guides diagnostic usage, and quantifies errors in the Gibbs stationary distribution caused by the diffusion model. We showcase our method for 1) blind denoising of natural images involving colored noises with unknown amplitude and spectral index, and 2) a cosmology problem, namely the analysis of cosmic microwave background data, where Bayesian inference of “noise” parameters means constraining models of the evolution of the Universe.

1. Introduction

Denoising is an old problem in signal processing, which has experienced significant advancements in the last decade, propelled by the advent of deep learning (Tian et al., 2020; Elad et al., 2023). Convolutional neural networks have led to the emergence of state-of-the-art image denoisers (e.g., Zhang et al., 2017; 2022), by learning complex prior dis-

¹Ecole Polytechnique, Institut Polytechnique de Paris
²Flatiron Institute. Correspondence to: David Heurtel-Depeiges <david.heurtel-depeiges@polytechnique.edu>, Bruno Régaldo-Saint Blancard <brégaldo@flatironinstitute.org>.

Preprint. Under review.

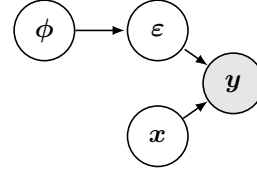


Figure 1. Graphical model: we observe $y = x + \varepsilon$ and aim to infer both x and ϕ in a Bayesian framework.

tributions of target signals implicitly. Denoisers were also found to be powerful tools for generative modeling, as strikingly demonstrated by diffusion models (Ho et al., 2020; Song et al., 2021; Saharia et al., 2022; Rombach et al., 2022). Considerable effort has been devoted to recovering highly accurate, noise-free versions of contaminated signals, often at the expense of fully addressing the noise’s complexity. In numerous practical scenarios, both in industry and scientific research, accurately characterizing the noise itself is of paramount importance (e.g., medical imaging, astronomy, speech recognition, financial market analysis). This paper addresses the challenge of *blind denoising*, with the objective of simultaneously recovering both the signal and the noise characteristics.

We formalize the problem as follows. We observe a signal $y \in \mathbb{R}^d$ that is an additive mixture of an arbitrary signal x and a Gaussian signal ε with covariance $\Sigma_\phi \in \mathbb{R}^{d \times d}$:

$$y = x + \varepsilon, \text{ with } \varepsilon \sim \mathcal{N}(0, \Sigma_\phi), \quad (1)$$

where $\phi \in \mathbb{R}^K$ is an unknown vector of parameters (see Fig. 1 for a graphical model). The functional form of Σ_ϕ can be arbitrary, although computational constraints would typically require that the number of parameters K remains reasonable. For example, the vector ϕ would typically include a parameter $\sigma > 0$ controlling the overall noise amplitude, but could also encompass parameters describing the local variations or spectral properties of the noise (cf Sect. 3). We frame the problem in a Bayesian picture, where prior information on x and ϕ is given, representing some pre-existing knowledge or assumptions on the target data. We will assume that the prior information over ϕ takes the form of an analytical prior distribution $p(\phi)$. Crucially, although the prior distribution $p(x)$ on the signal x is typically analytically intractable, we assume access to a set of examples x_1, \dots, x_N drawn from $p(x)$. In this Bayesian

Testing gravitational waveforms in full General Relativity

Fabio D'Ambrosio,^{1,*} Francesco Gozzini,^{2,†} Lavinia Heisenberg,^{2,‡}
Henri Inchauspé,^{2,§} David Maibach,^{2,¶} and Jann Zosso^{1,**}

¹*Institute for Theoretical Physics, ETH Zurich, Wolfgang-Pauli-Strasse 27, CH-8093 Zurich, Switzerland*
²*Institute for Theoretical Physics, University of Heidelberg, Philosophenweg 16 D-69120 Heidelberg Germany*
(Dated: March 1, 2024)

We perform a comprehensive analysis of state-of-the-art waveform models, focusing on their predictions concerning kick velocity and inferred gravitational wave memory. In our investigation we assess the accuracy of waveform models using energy-momentum balance laws, which were derived in the framework of full, non-linear General Relativity. The numerical accuracy assessment is performed for precessing as well as non-precessing scenarios for models belonging to the *EOB*, *Phenom*, and *Surrogate* families. We analyze the deviations of these models from each other and from Numerical Relativity waveforms. Our analysis reveals statistically significant deviations, which we trace back to inaccuracies in modelling subdominant modes and inherent systematic errors in the chosen models. We corroborate our findings through analytical considerations regarding the mixing of harmonic modes in the computed kick velocities and inferred memories.

I. INTRODUCTION

The first direct detection of gravitational waves (GWs) from the merger of two black holes in 2015 [1] marked a milestone in the field of astrophysics, confirming a key prediction of Einstein's General Theory of Relativity (GR) and ushering in a new era of observational astronomy. The waveforms matched against the GW signal encode a wealth of information, including the masses and spins of the binaries, the distances to the sources, and the geometry of their motion. By analyzing these waveforms, astrophysicists can uncover the underlying physical processes, discern the properties of exotic objects, and validate theoretical models with unprecedented precision. To date, the process of parameter estimation and the testing of GR necessitate numerical modeling of gravitational waveforms across a wide range of source parameters, including masses, spins, and other relevant factors pertaining to the merging objects. These modelled waveforms are used as fitting templates with respect to actual data. The effectiveness of this template-to-signal match hinges on the precision of the estimated waveforms. Therefore, in order to extract meaningful information from signals, it is crucial to construct comprehensive and accurate waveform templates that faithfully capture the physics of GR. This requirement is further substantiated by the expected increase in signal-to-noise-ratio of future GW observatories such as LISA [2], the Einstein Telescope [3], and the Cosmic Explorer [4]. Their increased resolution and sensitivity opens them up to more subtle effects like the gravitational memory [5–10] and they may even reveal physics beyond GR [11].

However, deviations between templates and the actual waveforms contained in the observational data introduce systematic biases, compromising the reliability of the information extracted from the signal. To counteract such biases, a diverse set of template waveforms is employed when analyzing data from GW instruments. Among these template waveforms, the ones obtained from Numerical Relativity (NR) simulations are the most reliable. Their disadvantage, however, is their consumption of vast amounts of computational resources for each simulation, i.e., for each choice of parameters describing an individual merging scenario. This time-consuming and resource-intensive process poses a significant challenge, particularly as the volume of data to be processed is expected to increase drastically in the upcoming years with the advent of multiple ground- and space-based instruments like LISA [12] and LIGO/Virgo [13, 14]. Furthermore, as the measuring precision advances, deviations from GR [11] may reveal themselves in the observed data. Detecting such deviations necessitates an expanded parameter space to account for alternative descriptions of gravity, which consequently amplifies the number of waveforms against which the data must be tested.

To address these challenges, and in particular to tackle the efficiency issue of the waveform generation process, multiple alternatives to NR simulations were established. Prominent representatives of alternative waveform models are the *Surrogate* models [15–17], phenomenological models [18–21] and effective-one-body simulations [22–27]. To obtain reliable results within reasonable timescales, the models adopt distinct strategies to compute the gravitational strain. Each model focuses on different physical aspects of compact binary coalescence and is capable of producing a waveform within certain parameter ranges in an efficient manner. To understand what distinguishes the different approximant families, it is helpful to divide the compact binary coalescence into three phases: the inspiral, the merger, and the ring-down phase. The objective of each approximant family is to generate waveforms that replicate NR without re-

* fabio.dambrosio@gmx.ch

† gozzini@thphys.uni-heidelberg.de

‡ l.heisenberg@thphys.uni-heidelberg.de

§ h.inchauspe@thphys.uni-heidelberg.de

¶ d.maibach@thphys.uni-heidelberg.de

** zosso.jann@bluewin.ch

Revisiting string-inspired running-vacuum models under the lens of light primordial black holes

Theodoros Papanikolaou^{a,b,c} Charalampos Tzerefos^{d,c}
 Spyros Basilakos^{c,e,f} Emmanuel N. Saridakis^{c,g,h}
 Nick E. Mavromatos^{i,j}

^aScuola Superiore Meridionale, Largo San Marcellino 10, 80138 Napoli, Italy

^bIstituto Nazionale di Fisica Nucleare (INFN), Sezione di Napoli, Via Cinthia 21, 80126 Napoli, Italy

^cNational Observatory of Athens, Lofos Nymfon, 11852 Athens, Greece

^dDepartment of Physics, National & Kapodistrian University of Athens, Zografou Campus GR 157 73, Athens, Greece

^eAcademy of Athens, Research Center for Astronomy and Applied Mathematics, Soranou Efessiou 4, 11527, Athens, Greece

^fSchool of Sciences, European University Cyprus, Diogenes Street, Engomi, 1516 Nicosia, Cyprus

^gCAS Key Laboratory for Researches in Galaxies and Cosmology, Department of Astronomy, University of Science and Technology of China, Hefei, Anhui 230026, P.R. China

^hDepartamento de Matemáticas, Universidad Católica del Norte, Avda. Angamos 0610, Casilla 1280 Antofagasta, Chile

ⁱPhysics Division, School of Applied Mathematical and Physical Sciences, National Technical University of Athens, Zografou Campus, Athens 157 80, Greece

^jTheoretical Particle Physics and Cosmology group, Department of Physics, King's College London, London WC2R 2LS, UK

E-mail: t.papanikolaou@ssmeridionale.it, chtzeref@phys.uoa.gr,
svasil@academyofathens.gr, msaridak@noa.gr, mavroman@mail.ntua.gr

Abstract. Light primordial black holes (PBHs) with masses $M_{\text{PBH}} < 10^9 \text{g}$ can interestingly dominate the Universe's energy budget and give rise to early matter-dominated (eMD) eras before Big Bang Nucleosynthesis (BBN). During this eMD era, one is met with an abundant production of induced gravitational waves (GWs) serving as a portal to constrain the underlying theory of gravity. In this work, we study this type of induced GWs within the context of string-inspired running-vacuum models (StRVMs), which, when expanded around de Sitter backgrounds, include logarithmic corrections of the space-time curvature. In particular, we discuss in detail the effects of StRVMs on the source as well as on the propagation of these PBH-induced GWs. Remarkably, under the assumption that the logarithmic terms represent quantum gravity corrections in the PBH era, we show that GW overproduction can be avoided if one assumes a coefficient of these logarithmic corrections that is much larger than the square of the reduced Planck mass. The latter cannot characterise quantum gravity corrections, though, prompting the need for revision of the quantisation of StRVMs in different than de Sitter backgrounds, such as those characterising PBH-driven eMD eras. This non trivial result suggests the importance of light PBHs as probes of new physics.

Keywords: primordial black holes, running vacuum models, gravitational waves/theory

Dark energy and dark matter configurations for wormholes and solitonic hierarchies of nonmetric Ricci flows and $F(R, T, Q, T_m)$ gravity

Laurențiu Bubuianu*

SRTV - Studioul TVR Iași and University Appolonia, 2 Muzicii street, Iași, 700399, Romania

Sergiu I. Vacaru †

*Department of Physics, California State University at Fresno, Fresno, CA 93740, USA;
Institute of Applied-Physics and Computer Sciences, Yu. Fedkovych University, Chernivtsi, 58012, Ukraine;
CAS Center for Advanced Studies, Ludwig-Maximilians-Universität, Seestrasse 13, München, 80802, Germany*

Elşen Veli Veliev ‡

Department of Physics, Kocaeli University, 41380, Izmit, Turkey

Assel Zhamysheva §

Department of General and Theoretical Physics, Eurasian National University, Astana, 010000, Kazakhstan

accepted by EPJC: February 6, 2024

Abstract

We extend the anholonomic frame and connection deformation method, AFCDM, for constructing exact and parametric solutions in general relativity, GR, to geometric flow models and modified gravity theories, MGTs, with nontrivial torsion and nonmetricity fields. Following abstract geometric or variational methods, we can derive corresponding systems of nonmetric gravitational and matter field equations which consist of very sophisticated systems of coupled nonlinear PDEs. Using nonholonomic frames with dyadic spacetime splitting and applying the AFCDM, we prove that such systems of PDEs can be decoupled and integrated in general forms for generic off-diagonal metric structures and generalized affine connections. We generate new classes of quasi-stationary solutions (which do not depend on time like coordinates) and study the physical properties of some physically important examples. Such exact or parametric solutions are determined by nonmetric solitonic distributions and/or ellipsoidal deformations of wormhole hole configurations. It is not possible to describe the thermodynamic properties of such solutions in the framework of the Bekenstein-Hawking paradigm because such metrics do not involve, in general, certain horizons, duality, or holographic configurations. Nevertheless, we can always elaborate on associated Grigori Perelman thermodynamic models elaborated for nonmetric geometric flows. In explicit form, applying the AFCDM, we construct and study the physical implications of new classes of traversable wormhole solutions describing solitonic deformation and dissipation of non-Riemannian geometric objects. Such models with nontrivial gravitational off-diagonal vacuum are important for elaborating models of dark energy and dark matter involving wormhole configurations and solitonic- type structure formation.

Keywords: exact and parametric solutions; modified gravity; nonholonomic geometric flows; dark energy; dark matter; wormholes

*email: laurentiu.bubuianu@tvr.ro and laurfb@gmail.com

†emails: sergiu.vacaru@fulbrightmail.org ; sergiu.vacaru@gmail.com ; *Address for correspondence in 2024 as a visiting fellow at CAS LMU, Munich, Germany and YF CNU, Chernivtsi, Ukraine:* Vokzalna street, 37-3, Chernivtsi, Ukraine, 58008

‡email: elsen@kocaeli.edu.tr and elsenveli@hotmail.com

§email: assel.zhamysheva1@gmail.com

Infinite Order Hydrodynamics: an Analytical Example

L. Gavassino

Department of Mathematics, Vanderbilt University, Nashville, TN, USA

We construct a kinetic model for matter-radiation interactions where the hydrodynamic gradient expansion can be computed analytically up to infinite order in derivatives, in the fully non-linear regime, and for arbitrary flows. The frequency dependence of the opacity of matter is chosen to mimic the relaxation time of a self-interacting scalar field. In this way, the transient sector simulates that of a realistic quantum field theory. As expected, the gradient series is divergent for most flows. We identify the mechanism at the origin of the divergence, and we provide a successful regularization scheme. Additionally, we propose a universal qualitative framework for predicting the breakdown of the gradient expansion of an arbitrary microscopic system undergoing a given flow. This framework correctly predicts the factorial divergence of the gradient expansion in most non-linear flows and its breakdown due to stochastic fluctuations. It also predicts that jets may induce an ultraviolet divergence in the gradient expansion of quark matter hydrodynamics.

Introduction - The most pressing open question in relativistic fluid mechanics is: “How far can we push hydrodynamics before it breaks down?” [1–20]

Let us make this question precise. The Knudsen number $\text{Kn} = \lambda/L$ is the ratio between the particles’ mean free path λ (defining the microscopic scale) and the characteristic length scale L of the flow of interest [21, 22]. It is common knowledge [23] that, if $\text{Kn} \rightarrow 0$, we can model the system as an ideal fluid, while when $\text{Kn} \gtrsim 1$, we need to rely on microphysics. Thus, there is some value of $\text{Kn} \in (0, 1]$ at which hydrodynamics stops working. Can we identify it precisely?

The answer depends on which hydrodynamic theory one is using. The ideal fluid breaks down at any finite value of Kn , since it is non-dissipative, and it predicts that waves survive forever. These issues are fixed in Navier-Stokes theory, whose breakdown is conventionally set at $\text{Kn} = 0.1$ [24]. However, one may try to do even better. Most derivations of hydrodynamics from kinetic theory [25, 26] and holography [27, 28] express the stress-energy tensor $T^{\mu\nu}$ of a fluid as a formal power series in Kn , known as the “gradient expansion” [29],

$$T^{\mu\nu}(\text{Kn}) = T_{\text{ID}}^{\mu\nu} + T_1^{\mu\nu}\text{Kn} + T_2^{\mu\nu}\text{Kn}^2 + \dots, \quad (1)$$

where the zeroth order is the ideal fluid, the first order is Navier-Stokes, the second order is the Burnett equation [30], and higher orders correspond to fluid theories with higher derivative corrections. One hopes that, by adding more and more powers of Kn , the regime of applicability of hydrodynamics will expand more and more, increasing the accuracy of hydrodynamics for all Kn up to the radius of convergence Kn^* of the series (1). Following this line of thought, it would then be natural to conclude that such radius Kn^* is what ultimately marks the rigorous breakdown of hydrodynamics [31].

Unfortunately, reality turns out to be more complicated. First, there are indications that, in most realistic scenarios, $\text{Kn}^* = 0$ [10, 13, 32]. This means that, if we keep adding higher and higher orders in Kn , at some point the region of applicability of (1) shrinks instead of expanding. Secondly, equation (1) makes sense only if the

function $T^{\mu\nu}(\text{Kn})$ is analytic in Kn . In principle, there may be non-smooth corrections like $\text{Kn}^{3/2}$ [33], or non-perturbative corrections like $e^{-1/\text{Kn}}$ [34]. Therefore, the breakdown scale of hydrodynamics remains unknown.

The dream of any fluid theorist would be to have a microscopic model where $T^{\mu\nu}(\text{Kn})$ can be computed exactly for arbitrary flow, at arbitrary Kn , in the fully non-linear regime, and where all the terms $T_n^{\mu\nu}$ in the series (1) have exact analytical formulas. Such model should have realistic interactions, to ensure that the dependence of $T^{\mu\nu}$ on Kn mimics the behavior of some microscopic quantum field theory. Finally, one should be able to extract from it general lessons about the expansion (1). In this Letter, we provide a model that fulfills all these requirements.

Notation: We work in Minkowski space, with signature $(-, +, +, +)$, and adopt natural units: $c = \hbar = k_B = 1$.

The kinetic model - Our model setup is a radiation-hydrodynamic system [35–41], namely a fluid mixture comprised of two substances: a material medium M with negligibly short mean free path (i.e. $\text{Kn}_M \equiv 0$), and a diluted radiation gas R with a finite, possibly large, mean free path (i.e. $\text{Kn}_R > 0$) [42, 43]. The former is modeled as an ideal fluid, with a well-defined temperature $T(x^\alpha)$ and flow velocity $u^\mu(x^\alpha)$. The latter can exist in far-from-equilibrium states, and we must track its kinetic distribution function $f_p(x^\alpha)$ [44, 45] (p = momentum). The total stress-energy tensor is the sum of a material non-viscous part and a radiation part:

$$T^{\mu\nu} = T_M^{\mu\nu} + \int \frac{d^3p}{(2\pi)^3 p^0} f_p p^\mu p^\nu. \quad (2)$$

The radiation particles do not interact with each other, but are randomly absorbed and emitted by the medium (neglecting scattering). Thus, the Boltzmann equation is of relaxation type [35, 46]. Taking the relaxation time to be $\tau_p = -u_\mu p^\mu / g$ (with $g > 0 = \text{constant}$), we have

$$p^\mu \partial_\mu f_p = -u_\mu p^\mu \frac{f_p^{\text{eq}} - f_p}{\tau_p} = g (f_p^{\text{eq}} - f_p). \quad (3)$$

Since τ_p grows linearly with $-u_\mu p^\mu$, our medium is opaque at low frequencies, and transparent at high frequencies [35]. The function f_p^{eq} is the value that f_p would

Calibrating gravitational-wave search algorithms with conformal prediction

Gregory Ashton,^{1,*} Nicolo Colombo,² Ian Harry,³ and Surabhi Sachdev⁴

¹*Department of Physics, Royal Holloway, Egham, TW20 0EX*

²*Department of Computer Science, Royal Holloway, Egham, TW20 0EX*

³*University of Portsmouth, Portsmouth, PO1 3FX, United Kingdom*

⁴*School of Physics, Georgia Institute of Technology, Atlanta, GW 30332, USA*

(Dated: March 1, 2024)

In astronomy, we frequently face the decision problem: does this data contain a signal? Typically, a statistical approach is used, which requires a threshold. The choice of threshold presents a common challenge in settings where signals and noise must be delineated, but their distributions overlap. Gravitational-wave astronomy, which has gone from the first discovery to catalogues of hundreds of events in less than a decade, presents a fascinating case study. For signals from colliding compact objects, the field has evolved from a frequentist to a Bayesian methodology. However, the issue of choosing a threshold and validating noise contamination in a catalogue persists. Confusion and debate often arise due to the misapplication of statistical concepts, the complicated nature of the detection statistics, and the inclusion of astrophysical background models. We introduce Conformal Prediction (CP), a framework developed in Machine Learning to provide distribution-free uncertainty quantification to point predictors. We show that CP can be viewed as an extension of the traditional statistical frameworks whereby thresholds are calibrated such that the uncertainty intervals are statistically rigorous and the error rate can be validated. Moreover, we discuss how CP offers a framework to optimally build a meta-pipeline combining the outputs from multiple independent searches. We introduce CP with a toy cosmic-ray detector, which captures the salient features of most astrophysical search problems and allows us to demonstrate the features of CP in a simple context. We then apply the approach to a recent gravitational-wave Mock Data Challenge using multiple search algorithms for compact binary coalescence signals in interferometric gravitational-wave data. Finally, we conclude with a discussion on the future potential of the method for gravitational-wave astronomy.

I. INTRODUCTION

The burgeoning field of gravitational-wave astronomy is in a state of rapid evolution. Second-generation detectors [1–3] have progressed from the first observation of a binary black hole merger [4] to the compilation of extensive transient event catalogues [5–7] including also binary neutron star and black-hole neutron-star mergers. With this progress, the methodologies for evaluating the statistical significance of Compact Binary Coalescence (CBC) signals have undergone notable transformations. While the significance of the initial detection [4] was assessed through the frequentist False Alarm Rate (FAR), contemporary catalogues [5–7] now use probabilistic Bayesian methods.

However, astrophysicists aiming to learn from gravitational-wave data are confronted with a challenge: the difficulty in identifying signals when their distribution and the noise distributions overlap. This issue is by no means unique in astronomy (see, e.g. Feigelson and Babu [8]). However, gravitational-wave astronomy is an especially intriguing case study because the Signal-To-Noise Ratio (SNR) ratio of sources is low, but the potential scientific reward is high. Moreover, much of the insights derive from studying the population of identified sources [9]. The events producing signals within

current sensitivities are isotropically distributed, so the number of detections scales with the cube of the horizon distance (a measure of the detector sensitivity). Therefore, there are always more events just beyond the horizon than within: increasing the horizon distance by just 25% will double the number of events. The conundrum facing anyone wishing to utilise the hundreds of sources now reported is how to select a threshold to cut between the signals and the noise. On the one hand, we can choose a conservative threshold, ensuring a high catalogue purity (the fraction of true signals). However, the conservative threshold also entails a loss of accuracy; after all, we must discard many low-significance astrophysical signals buried in the noise. On the other hand, choosing a liberal threshold would include a larger number of astrophysical signals but at the cost of bias induced by non-astrophysical catalogue contamination.

Along with the threshold problem, difficulties arise from concurrently applying multiple search algorithms (hereafter referred to as *pipelines*). The GWTC catalogues produced by the LIGO Scientific, Virgo, and KAGRA (LVK) collaborations (e.g. Abbott *et al.* [5]) include results from several independent pipelines (specifically, *GstLAL* [10–15], *MBTA* [16, 17], *PyCBC* [18–22], *SPIIR* [23, 24], and *Coherent WaveBurst* [25]). For a given candidate event, the significance between pipelines can vary substantially, reflecting inherent uncertainty in the significance estimate and varying pipeline performance. However, for those not intimately knowledgeable about the ever-evolving internal workings of the pipelines, it is

* gregory.ashton@rhul.ac.uk

A Multi-Model Ensemble System for the outer Heliosphere (MMESH): Solar Wind Conditions near Jupiter

M. J. Rutala¹, C. M. Jackman¹, M. J. Owens², C. Tao³, A. R. Fogg¹, S. A. Murray¹, L. Barnard²

¹School of Cosmic Physics, DIAS Dunsink Observatory, Dublin Institute for Advanced Studies, Dublin, Ireland

²Department of Meteorology, University of Reading, Earley Gate, PO Box 243, Reading RG6 6BB, UK

³Space Environment Laboratory, National Institute of Information and Communications Technology (NICT), Koganei, Japan

Key Points:

- The performance of several existing solar wind propagation models at the orbit of Jupiter is measured for multiple spacecraft epochs.
- A flexible system is developed to generate an ensemble of multiple propagation models so as to best leverage each input model's strengths.
- Over the epoch tested, the multi-model ensemble outperforms individual input models by 7% – 110% in forecasting the solar wind flow speed.

Corresponding author: M. J. Rutala, mrutala@cp.dias.ie

–1–

Abstract

How the solar wind influences the magnetospheres of the outer planets is a fundamentally important question, but is difficult to answer in the absence of consistent, simultaneous monitoring of the upstream solar wind and the large-scale dynamics internal to the magnetosphere. To compensate for the relative lack of in-situ data, propagation models are often used to estimate the ambient solar wind conditions at the outer planets for comparison to remote observations or in-situ measurements. This introduces another complication: the propagation of near-Earth solar wind measurements introduces difficult-to-assess uncertainties. Here, we present the Multi-Model Ensemble System for the outer Heliosphere (MMESH) to begin to address these issues, along with the resultant multi-model ensemble (MME) of the solar wind conditions near Jupiter. MMESH accepts as input any number of solar wind models together with contemporaneous in-situ spacecraft data. From these, the system characterizes typical uncertainties in model timing, quantifies how these uncertainties vary under different conditions, attempts to correct for systematic biases in the input model timing, and composes a MME with uncertainties from the results. For the case of the Jupiter-MME presented here, three solar wind propagation models were compared to in-situ measurements from the near-Jupiter spacecraft *Ulysses* and *Juno* which span diverse geometries and phases of the solar cycle, amounting to more than 14,000 hours of data over 2.5 decades. The MME gives the most-probable near-Jupiter solar wind conditions for times within the tested epoch, outperforming the input models and returning quantified estimates of uncertainty.

Plain Language Summary

The sun interacts with all the planets in the solar system through the solar wind, a stream of charged particles which blow outwards from the sun in all directions, carrying the interplanetary magnetic field with them. Both the magnetic field and particles interact with planetary magnetic fields with dramatic effects, including the aurora which shine not only on the Earth, but on gas giants of the outer solar system, like Jupiter, too. Characterizing the relationship between the solar wind and planetary magnetic fields is easiest with direct spacecraft measurements of both. Spacecraft between the Earth and Sun measure the solar wind, providing valuable context for understanding its interaction with the Earth. Unfortunately, there are no such permanent spacecraft near the other planets. Instead, models can be used to estimate the solar wind at these planets; however, these models can have significant, difficult-to-characterize uncertainties. Here we present the Multi-Model Ensemble System for the outer Heliosphere (MMESH), a framework designed to measure these uncertainties and attempt to correct for them by comparing multiple solar wind models to spacecraft measurements over a long time span. The final result here is an improved solar wind model, with estimated uncertainties, for Jupiter.

1 Background

The solar wind is a continuous stream of plasma emanating from the Sun in all directions which evolves as it travels through the heliosphere, interacting with every planetary magnetosphere in the solar system along the way. Near the Earth, the typical values of the solar wind flow speed $u_{mag,\oplus}$ (324–584 km/s), proton density n_{\oplus} (2.2–12.7 cm⁻³), dynamic (ram) pressure $p_{dyn,\oplus}$ (0.86–3.92 nPa), and interplanetary magnetic field (IMF) magnitude $B_{mag,\oplus}$ (3.1–9.7 nT) have all been statistically characterized by the expansive OMNI dataset (King & Papitashvili, 2005; N. E. Papitashvili & King, 2020), with values here spanning the start of OMNI2 to the start of 2023 (1963/11/27 – 2023/01/01) and characterizing 80% (10th–90th percentiles) of all measurements. The OMNI dataset is a composite of many near-Earth observations encompassing some 19 total spacecraft over its full time domain, including most recently *Wind* (Lepping et al., 1995; Kasper,

–2–

Search for Axion dark matter with the QUAX–LNF tunable haloscope

A. Rettaroli,^{1,*} D. Alesini,¹ D. Babusci,¹ C. Braggio,^{2,3} G. Carugno,² D. D’Agostino,^{4,5} A. D’Elia,¹ D. Di Gioacchino,¹ R. Di Vora,⁶ P. Falferi,^{7,8} U. Gambardella,^{4,5} C. Gatti,¹ G. Iannone,^{4,5} C. Ligi,¹ A. Lombardi,⁶ G. Maccarrone,¹ A. Ortolan,⁶ G. Ruoso,⁶ S. Tocci,^{1,†} and G. Vidali^{9,1}

¹*INFN, Laboratori Nazionali di Frascati, Frascati, Roma, Italy*

²*INFN, Sezione di Padova, Padova, Italy*

³*Dipartimento di Fisica e Astronomia, Padova, Italy*

⁴*Dipartimento di Fisica E.R. Caianiello, Fisciano, Salerno, Italy*

⁵*INFN, Sezione di Napoli, Napoli, Italy*

⁶*INFN, Laboratori Nazionali di Legnaro, Legnaro, Padova, Italy*

⁷*Istituto di Fotonica e Nanotecnologie, CNR Fondazione Bruno Kessler, I-38123 Povo, Trento, Italy*

⁸*INFN, TIFPA, Povo, Trento, Italy*

⁹*Dipartimento di Fisica, Università La Sapienza, Rome, Italy*

(Dated: March 1, 2024)

We report the first experimental results obtained with the new haloscope of the QUAX experiment located at Laboratori Nazionali di Frascati of INFN (LNF). The haloscope is composed of a OFHC Cu resonant cavity cooled down to about 30 mK and immersed in a magnetic field of 8 T. The cavity frequency was varied in a 6 MHz range between 8.831496 and 8.83803 GHz. This corresponds to a previously unprobed mass range between 36.52413 and 36.5511 μeV . We don’t observe any excess in the power spectrum and set limits on the axion-photon coupling in this mass range down to $g_{a\gamma\gamma} < 0.861 \times 10^{-13} \text{ GeV}^{-1}$ with the confidence level set at 90%.

I. INTRODUCTION

In recent years, we witnessed an increasing growth in the research of light Dark Matter (DM) candidates, addressing in particular axions and axion-like particles (ALPs). If axions are found to exist, they would untie the long-standing DM problem [1, 2], after being originally postulated as a solution to the strong CP problem [3, 4]. The nature of a pseudoscalar, electrically neutral and feebly interacting particle make the axion a strong DM candidate [5], and its cosmological evolution and astrophysical constraints indicate a favorable mass range between $1 \mu\text{eV} < m_a < 10 \text{ meV}$ [6].

The research efforts are now spread over many different detection approaches, but the paradigm has become the haloscope design proposed by Sikivie [7, 8], which probes axions from the DM halo of the Galaxy. Currently operating haloscopes are ADMX [9–12], HAYSTAC [13, 14], ORGAN [15], CAPP-8T [16, 17], CAPP-9T [18], CAPP-PACE [19], CAPP-18T [20], CAST-CAPP [21], GrA-Hal [22], RADES [23–25], TASEH [26] and QUAX [27–32], whereas among the proposed experiments are FLASH [33], ABRACADABRA [34], DM-Radio [35, 36], CADEX [37], MADMAX [38] and ALPHA [39].

The axion observation technique is based upon its inverse Primakoff conversion into one photon, stimulated by a static magnetic field. The essential elements required to run a haloscope are a superconducting magnet to generate a strong magnetic field, a microwave resonant cavity where the electromagnetic field excitation builds

up, an ultra-low noise receiver, a tuning mechanism to scan over the axion mass range and a cryogenic system to grant operation at low temperature. The two figures of merit in the axion search are the power of the produced photon [40]

$$P_{a\gamma} = \left(\frac{g_{a\gamma\gamma}^2}{m_a^2} \hbar^3 c^3 \rho_a \right) \left(\frac{\beta}{1+\beta} \omega_c \frac{1}{\mu_0} B_0^2 V C_{010} Q_L \right) \times \left(\frac{1}{1 + (2Q_L \Delta\omega/\omega_c)^2} \right), \quad (1)$$

and the scan rate [41]

$$\frac{df}{dt} = g_{a\gamma\gamma}^4 \frac{\rho_a^2}{m_a^2} \frac{1}{\text{SNR}^2} \left(\frac{B_0^2 V C_{010}}{k_B T_{\text{sys}}} \right)^2 \times \frac{\beta^2}{(1+\beta)^2} Q_a \min(Q_L, Q_a). \quad (2)$$

We assume a local DM density $\rho_a = 0.45 \text{ GeV}/\text{cm}^3$ [42], m_a is the axion mass and $g_{a\gamma\gamma}$ is its coupling constant to photons. B_0 is the applied magnetic field; $\omega_c = 2\pi\nu_c$, V , Q_L , β are respectively the resonance angular frequency of the cavity, the volume, the loaded quality factor and the antenna coupling to the cavity. The relation $Q_L = Q_0/(1+\beta)$ holds, with Q_0 the intrinsic quality factor. C_{010} is a mode dependent geometrical factor, about 0.6 for the TM010 resonant mode of a cylindrical cavity, and $\Delta\omega_c = \omega_c - \omega_a$ is the detuning between the cavity and the axion angular frequency defined as $\omega_a = m_a c^2/\hbar$. The quality factor $Q_a \approx 10^6$ [43] is related to the energy spread in the cold dark matter halo. In Eq. 2, the signal-to-noise ratio, SNR, is defined as the ratio between the signal power and the uncertainty of

* alessio.rettaroli@lnf.infn.it

† simone.tocci@lnf.infn.it

Dynamics of holographic dark energy with apparent-horizon cutoff and non-minimal derivative coupling gravity in non-flat FLRW universe

Amornthep Tita,^{1,2,*} Burin Gumjudpai,^{2,†} and Pornrad Srisawad^{3,‡}

¹*The Institute for Fundamental Study “The Tah Poe Academia Institute”,
Naresuan University, Phitsanulok 65000, Thailand*

²*NAS, Centre for Theoretical Physics & Natural Philosophy, Mahidol University,
Nakhonsawan Campus, Phayuha Khiri, Nakhonsawan 60130, Thailand*

³*Department of Physics, Faculty of Science, Naresuan University, Phitsanulok 65000, Thailand*
(Dated: March 1, 2024)

Background cosmological dynamics for a universe with matter, a scalar field non-minimally derivative coupling to Einstein tensor under power-law potential and holographic vacuum energy is considered here. The holographic IR cutoff scale is apparent horizon which, for accelerating universe, forms a trapped null surface in the same spirit as blackhole’s event horizon. For non-flat case, effective gravitational constant can not be expressed in the Friedmann equation. Therefore holographic vacuum density is defined with standard gravitational constant in stead of the effective one. Dynamical and stability analysis shows four independent fixed points. One fixed point is stable and it corresponds to $w_{\text{eff}} = -1$. One branch of the stable fixed-point solutions corresponds to de-Sitter expansion. The others are either unstable or saddle nodes. Numerical integration of the dynamical system are performed and plotted confronting with $H(z)$ data. It is found that for flat universe, $H(z)$ observational data favors large negative value of κ . Larger holographic contribution, c , and larger negative NMDC coupling increase slope and magnitude of the w_{eff} and $H(z)$. Negative NMDC coupling can contribute to phantom equation of state, $w_{\text{eff}} < -1$. The NMDC-spatial curvature coupling could also have phantom energy contribution. Moreover, free negative spatial curvature term can also contribute to phantom equation of state, but only with significantly large negative value of the spatial curvature.

PACS numbers: 98.80.Cq

I. INTRODUCTION

Present acceleration is a puzzle of contemporary cosmology. Dark energy or modification of general relativity could result in the acceleration [1–9]. The acceleration corresponds to negative equation of state, $w < -1/3$ and the observational favored value is $w \approx -1$ [10–17]. Dark energy (DE) is hypothetical energy with repulsive pressure. It could be cosmological constant or dynamical scalar fields. Having dark energy content in the universe is equivalent to adding of extra degree of freedom to the matter Lagrangian. Alternative way of achieving late acceleration is the modification of general relativity, i.e. modifying the left side of the Einstein field equation, that is, the gravitational sector. There are many ways of gravitational modifying such as considering function of Ricci scalar [18], function of Ricci tensor and Riemann tensor instead of using the Einstein-Hilbert Lagrangian [19]. Many other models are of mixed types that allow couplings among barotropic fluid, scalar and gravitational sectors. As a result, there are rich implications of these couplings in scalar-tensor theories [1, 20, 21] such as mediation of long-range fifth force when coupling between matter and scalar field is allowed. In this case, chameleon screening mechanism is considered to evade the fifth force problem [22]. It is found that only $R\phi_{,\mu}\phi^{,\mu}$ and $R^{\mu\nu}\phi_{,\mu}\phi_{,\nu}$ terms are necessary in the coupling sector [23, 24]. These couplings are motivated in lower energy limits of higher dimensional theories or in conformal supergravity [25, 26]. Combining the two terms into the Einstein tensor coupling to derivative of scalar field as $G_{\mu\nu}(\nabla^\mu\phi)(\nabla^\nu\phi)$ gives rise to the non-minimal derivative coupling (NMDC) gravity model and it can result in de-Sitter expansion as seen in literatures [27–50]. Further generalization of scalar-tensor theories, with at most second-order derivative with respect to dynamical variables, are such as galileons [51–53], Fab-Four [54], Horndeski action [55–57] and GLPV theories [58]. The $G_{\mu\nu}(\nabla^\mu\phi)(\nabla^\nu\phi)$ term is a sub-class (the G_5 term) of the Horndeski action.

Action of the NMDC coupling to gravity with other matters, e.g. dark matter (DM), matter fields and cosmological

* amornthept58@email.nu.ac.th

† Corresponding: burin.gum@mahidol.ac.th

‡ pornrads@nu.ac.th

Analytic solutions for the linearized first-order magnetohydrodynamics and implications for causality and stability

Zhe Fang^a Koichi Hattori^{a,b} Jin Hu^c

^a*Zhejiang Institute of Modern Physics, Department of Physics, Zhejiang University, Hangzhou, Zhejiang 310027, China*

^b*Research Center for Nuclear Physics, Osaka University, 10-1 Mihogaoka, Ibaraki, Osaka 567-0047, Japan*

^c*Department of Physics, Fuzhou University, Fujian 350116, China*

E-mail: koichi.hattori@zju.edu.cn, hu-j23@fzu.edu.cn

ABSTRACT: We solve the first-order relativistic magnetohydrodynamics (MHD) within the linear-mode analysis performed near an equilibrium configuration in the fluid rest frame. We find two complete sets of analytic solutions for the four and two coupled modes with seven dissipative transport coefficients. The former set has been missing in the literature for a long time. Our method provides a simple and general algorithm for the solution search on an order-by-order basis in the derivative expansion, and can be applied to general sets of hydrodynamic equations. We also find that the small-momentum expansions of the solutions break down when the momentum direction is nearly perpendicular to an equilibrium magnetic field due to the presence of another small quantity, that is, a trigonometric function representing the anisotropy. We elaborate on the angle dependence of the solutions and provide alternative series representations that work near the right angle. Finally, we discuss the issues of causality and stability based on our analytic solutions and recent developments in the literature.

Anisotropic solutions for R^2 gravity model with a scalar field

Vsevolod R. Ivanov*

Physics Department, Lomonosov Moscow State University,

Leninskie Gory 1, 119991 Moscow, Russia

Sergey Yu. Vernov†

Skobeltsyn Institute of Nuclear Physics, Lomonosov Moscow State University,

Leninskie Gory 1, 119991, Moscow, Russia

We study anisotropic solutions for the pure R^2 gravity model with a scalar field in the Bianchi I metric. The evolution equations have a singularity at zero value of the Ricci scalar R for anisotropic solutions, whereas these equations are smooth for isotropic solutions. So, there is no anisotropic solution with the Ricci scalar smoothly changing its sign during evolution. We have found anisotropic solutions using the conformal transformation of the metric and the Einstein frame. The general solution in the Einstein frame has been found explicitly. The corresponding solution in the Jordan frame has been constructed in quadratures.

PACS numbers: 98.80.-k, 04.50.Kd, 04.20.Jb

I. INTRODUCTION

The observable Universe is homogenous and isotropic at large scale and there are strong limits on anisotropic models from observations [1, 2]. For that reason, the Friedmann–Lemaître–Robertson–Walker (FLRW) metric plays the central role in the description of the global evolution of the Universe. Models with scalar fields are actively investigated, because they can describe the observable evolution of the Universe as the dynamics of FLRW background and cosmological perturbations.

The mechanism of isotropization of anisotropic solutions is an important question. The Wald theorem [3] proves that all initially expanding Bianchi models except type IX ap-

* vsvd.ivanov@gmail.com

† svernov@theory.sinp.msu.ru

Impact of weak lensing on bright standard siren analyses

Charlie T. Mpetha^{1,*}, Giuseppe Congedo¹, Andy Taylor¹, and Martin A. Hendry²

¹*Institute for Astronomy, School of Physics and Astronomy, University of Edinburgh,
Royal Observatory, Blackford Hill, Edinburgh, EH9 3HJ, United Kingdom*

²*SUPA, School of Physics and Astronomy, University of Glasgow, Glasgow G12 8QQ, United Kingdom*

(Dated: March 1, 2024)

Gravitational waves from binary mergers at cosmological distances will experience weak lensing by large scale structure. This causes a (de-)magnification, μ , of the wave amplitude, and a completely degenerate modification to the inferred luminosity distance d_L . The customary method to address this is to increase the uncertainty on d_L according to the dispersion of the magnification distribution at the source redshift, $\sigma_\mu(z)$. But this term is dependent on the cosmological parameters that are being constrained by gravitational wave “standard sirens”, such as the Hubble parameter H_0 , and the matter density fraction Ω_m . The dispersion $\sigma_\mu(z)$ is also sensitive to the resolution of the simulation used for its calculation. Tension in the measured value of H_0 from independent datasets, and the present use of weak lensing fitting functions calibrated using outdated cosmological simulations, suggest $\sigma_\mu(z)$ could be underestimated. This motivates an investigation into the consequences of mischaracterising $\sigma_\mu(z)$. We consider two classes of standard siren, supermassive black hole binary and binary neutron star mergers. Underestimating H_0 and Ω_m when calculating $\sigma_\mu(z)$ increases the probability of finding a residual lensing bias on these parameters greater than 1σ by $1.5 - 3$ times. Underestimating $\sigma_\mu(z)$ by using low resolution/small sky-area simulations can also significantly increase the probability of biased results, the probability of a 1σ (2σ) bias in H_0 and Ω_m found from binary neutron star mergers is 54% (19%) in this case. For neutron star mergers, the mean bias on H_0 caused by magnification selection effects is $\Delta H_0 = -0.1 \text{ km s}^{-1} \text{ Mpc}^{-1}$. The spread around this mean bias—determined by assumptions on $\sigma_\mu(z)$ —is $\Delta H_0 = \pm 0.25 \text{ km s}^{-1} \text{ Mpc}^{-1}$, comparable to the forecasted uncertainty. These effects do not impact merging neutron stars’ utility for addressing the H_0 tension, but left uncorrected they limit their use for precision cosmology. For supermassive black hole binaries, the spread of possible biases on H_0 is significant, $\Delta H_0 = \pm 5 \text{ km s}^{-1} \text{ Mpc}^{-1}$, but $\mathcal{O}(200)$ observations are needed to reduce the variance below the bias. To achieve accurate sub-percent level precision on cosmological parameters using standard sirens, first much improved knowledge on the form of the magnification distribution and its dependence on cosmology is needed.

I. INTRODUCTION

Waves propagating through the Universe are magnified by the gravitational potential of large scale structure. This *weak lensing* effect on light, observed through its effect on galaxy shapes, has been intensely studied as a source of cosmological information [1–5]. Similarly to light, gravitational wave weak lensing (GW-WL) modifies the observed wave amplitude h , to $h' = h\sqrt{\mu}$, where a prime denotes a lensed quantity [6–10]. The magnification μ depends on the matter along the line of sight where $\mu = 1$ corresponds to no effect, $\mu < 1$ a net underdensity of matter, and $\mu > 1$ a net overdensity.

The magnification distribution over the sky, $p(\mu, z)$, broadens towards higher redshifts, and is peaked at values below one as there are more voids than clusters. The tail of $p(\mu, z)$ is weighted towards values greater than one since clustered matter can have a larger effect on the magnification than voids. Gravitational waves from low redshift merging binaries, such as those observed using the LIGO-Virgo-Kagra (LVK) network [11–14], will not experience impactful weak lensing, though they may still be strongly lensed [15, 16]. The space-based GW detector LISA [17] expects to observe between a few and a few tens

of super massive black hole binary (SMBHB) mergers in the mid-2030’s over its nominal 5-year survey time with a duty cycle of 80% [18–20]. The effect of weak lensing on these observations will be significant, even for individual sources due to small uncertainties on their measured distances. A future network of 3rd generation ground-based detectors (3G), such as the Einstein Telescope [21] and Cosmic Explorer [22] is also anticipated to begin operations in the mid-2030’s. These detectors will observe binary neutron stars (BNSs) at $z \sim 2$ [23]. Weak lensing will not be as important for individual BNSs due to their larger distance uncertainties compared to those of SMBHBs. On the other hand, with the 3G network expected to detect many more BNSs than the numbers of SMBHBs observed by LISA, the effect of instrumental scatter on the cosmological parameters will be reduced. The bias due to lensing is likely to be even more significant.

For a single GW observation, the weak lensing effect can not be estimated from GW data alone. Past works have studied how successfully the GW can be “delensed” using external data to estimate μ for each observed source [24–26]. Ref. [26] found that sufficient delensing using galaxy surveys for all SMBHB mergers observed with LISA will be extremely challenging. For both SMBHBs and BNSs, we can not expect to remove or even meaningfully reduce the weak lensing effect, unless further advances are made in delensing methods.

* c.mpetha@ed.ac.uk

The effect of cloudy atmospheres on the thermal evolution of warm giant planets from an interior modelling perspective

A. J. Poser¹,^{*} R. Redmer¹

¹University of Rostock, Institute of Physics, D-18059 Rostock, Germany

Accepted 2024 February 28. Received 2024 February 21; in original form 2023 September 18

ABSTRACT

We are interested in the influence of cloudy atmospheres on the thermal radius evolution of warm exoplanets from an interior modelling perspective. By applying a physically motivated but simple parameterized cloud model, we obtain the atmospheric P - T structure that is connected to the adiabatic interior at the self-consistently calculated radiative-convective boundary. We investigate the impact of cloud gradients, with the possibility of inhibiting superadiabatic clouds. Furthermore, we explore the impact on the radius evolution for a cloud base fixed at a certain pressure versus a subsiding cloud base during the planets' thermal evolution. We find that deep clouds clearly alter the evolution tracks of warm giants, leading to either slower/faster cooling than in the cloudless case (depending on the cloud model used). When comparing the fixed versus dynamic cloud base during evolution, we see an enhanced behaviour resulting in a faster or slower cooling in the case of the dynamic cloud base. We show that atmospheric models including deep clouds can lead to degeneracy in predicting the bulk metallicity of planets, Z_p . For WASP-10b, we find a possible span of $\approx Z_p^{+0.10}_{-0.06}$. For TOI-1268b, it is $\approx Z_p^{+0.10}_{-0.05}$. Further work on cloud properties during the long-term evolution of gas giants is needed to better estimate the influence on the radius evolution.

Key words: planets and satellites: gaseous planets – planets and satellites: atmospheres – planets and satellites: interiors – planets and satellites: individual (WASP-10b, TOI-1268b)

1 INTRODUCTION

Giant planets are essential for understanding how planets form and evolve because they hide important information within their interiors (e.g. [Turrini et al. 2018](#); [Helled et al. 2021](#)). In particular, both the mass of the heavy elements and their distribution within the planet are of interest, as the bulk and atmospheric composition of the planets are related to their formation and evolutionary history. For example, the heavy element content of the planet may be correlated with the star's metallicity, both forming from the same protostellar cloud (e.g. [Guillot et al. 2006](#); [Thorngren et al. 2016](#)).

Characterisation of the interior is initially based on observational parameters of the planet, such as planetary mass, radius, and stellar age, as a proxy for the age of the planetary system and the planet itself. The ensuing description of the current (today's) bulk structure then relies on purely numerical models and delivers, among other things, the desired heavy-element content. Making use of the full set of observational parameters, one has to couple atmosphere, interior, and thermal evolution models (e.g. [Fortney et al. 2007](#); [Baraffe et al. 2008](#); [Müller & Helled 2023a,b](#); [Poser et al. 2019](#)).

In this context, the atmosphere of the planet plays a unique role. It is critical for the planet's radiative budget, in particular for irradiated planets, as it serves as a bottleneck for both the incoming stellar irradiation and the emitted intrinsic flux. As a result, it has a direct impact on the planet's cooling behaviour because the intrinsic heat

from the inside is radiated away through the atmosphere over time.

Over the past years, several atmosphere models have been developed that account for stellar irradiation and intrinsic heat flux, including atmospheric characteristics such as grains, hazes, and clouds (e.g. [Guillot 2010](#); [Heng et al. 2012](#); [Baudino et al. 2017](#); [Mollière et al. 2015](#); [Malik et al. 2019](#)).

Few earlier works have investigated the impact of the atmospheric conditions including grains and clouds on the planets' long-term thermal evolution: For example, [Kurosaki & Ikoma \(2017\)](#) show that condensation in heavily enriched atmospheres of ice giants accelerates the cooling as the planet emits more energy due to latent heat release. In contrast, [Vazan et al. \(2013\)](#) show a delayed cooling due to an atmosphere enriched in grains for giant planets. For isolated, non-irradiated low-mass planets ($M_p < 0.6 M_J$), [Linder et al. \(2019\)](#) find that including clouds or using different atmospheric codes have only a limited influence on the evolution tracks.

In many atmospheric models, the stellar irradiation flux is considered to be the main driver of the physics of the upper atmosphere. [Fortney et al. \(2020\)](#) emphasise that not only the equilibrium temperature (T_{eq}) as a measure for the stellar irradiation characterises the atmosphere of giant planets - but also the heat flux from the deep interior (characterised by the intrinsic temperature T_{int}), stressing that the appearance of clouds might as well depend on the atmospheric pressure-temperature conditions (P - T) in the deep atmosphere.

In coupled atmosphere-interior models with convective interiors, the atmosphere connects to the inner envelope at the radiative-convective boundary (RCB) (e.g. [Thorngren & Fortney 2019](#); [Thorngren et al.](#)

* E-mail: anna.poser@uni-rostock.de

A Model for Pair Production Limit Cycles in Pulsar Magnetospheres

TAKUYA OKAWA¹ AND ALEXANDER Y. CHEN¹

¹*Physics Department and McDonnell Center for the Space Sciences, Washington University in St. Louis; MO, 63130, USA*

ABSTRACT

It was recently proposed that the electric field oscillation as a result of self-consistent e^\pm pair production may be the source of coherent radio emission from pulsars. Direct Particle-in-Cell (PIC) simulations of this process have shown that the screening of the parallel electric field by this pair cascade manifests as a limit cycle, as the parallel electric field is recurrently induced when pairs produced in the cascade escape from the gap region. In this work, we develop a simplified time-dependent kinetic model of e^\pm pair cascades in pulsar magnetospheres that can reproduce the limit-cycle behavior of pair production and electric field screening. This model includes the effects of a magnetospheric current, the escape of e^\pm , as well as the dynamic dependence of pair production rate on the plasma density and energy. Using this simple theoretical model, we show that the power spectrum of electric field oscillations averaged over many limit cycles is compatible with the observed pulsar radio spectrum.

Keywords: Radio pulsars — Plasma Astrophysics — Neutron stars — Radio sources


1. INTRODUCTION

Pulsars are rapidly rotating, highly magnetized neutron stars that produce coherent radio emission with enormous brightness temperature (see e.g. [Philippov & Kramer 2022](#) for a review). Very quickly after its discovery, it was realized that the magnetic field near the pulsar surface can be strong enough to ignite a QED e^\pm pair cascade ([Sturrock 1971](#)). It was believed that pulsars can fill their surroundings with plasma through this e^\pm pair production process, screening the electric field E_{\parallel} along the magnetic field, creating a smooth force-free magne-

tosphere ([Contopoulos et al. 1999](#); [Spitkovsky 2006](#)). The regions in the magnetosphere with unscreened $\mathbf{E} \cdot \mathbf{B}$ are called “gaps” and they are the main locations for pair production activity (see e.g. [Ruderman & Sutherland 1975](#); [Arons 1983](#); [Cheng et al. 1986](#)).

Arguably, the most important pair-producing gap is located at the pulsar polar cap, since it supplies the plasma on open field lines that is believed to be the source of coherent radio emission ([Sturrock 1971](#)). [Beloborodov \(2008\)](#) demonstrated theoretically that the pair production process at the polar cap must be inherently time-dependent when the magnetospheric current is spacelike, and [Levinson et al. \(2005\)](#) showed that this process tends to produce large-amplitude oscillations of the accelerating elec-

The nature of compact radio-loud AGN: a systematic look at the LOFAR AGN population

J. Chilufya,¹  M. J. Hardcastle,¹ J. C. S. Pierce,¹ J.H. Croston,² B. Mingo,² X. Zheng,^{3,5} R. D. Baldi,⁴ and H. J. A. Röttgering³

¹Centre for Astrophysics Research, Department of Physics, Astronomy and Mathematics, University of Hertfordshire, Hatfield AL10 9AB, UK

²School of Physical Sciences, The Open University, Walton Hall, Milton Keynes, MK7 6AA, UK

³Leiden Observatory, Leiden University, PO Box 9513, 2300 RA Leiden, The Netherlands

⁴INAF - Istituto di Radioastronomia, via Gobetti 101 40129 Bologna

⁵Key Laboratory for Research in Galaxies and Cosmology, Shanghai Astronomical Observatory, Chinese Academy of Sciences, 80 Nandan Road, Shanghai 200030, China

Accepted 2024 February 26. Received 2024 January 29; in original form 2023 November 06

ABSTRACT

We investigate the nature of low-luminosity radio-loud active galactic nuclei (RLAGN) selected from the LOFAR Two-metre Sky Survey (LoTSS) first data release (DR1). Using optical, mid-infrared, and radio data, we have conservatively selected 55 radiative AGN candidates from DR1 within the redshift range $0.03 < z < 0.1$. We show using high-frequency *Karl G. Jansky* Very Large Array (VLA) observations that 10 out of 55 objects show radio emission on scales $>1 - 3$ kpc, 42 are compact at the limiting resolution of 0.35 arcsec (taking an upper limit on the projected physical size, this corresponds to less than 1 kpc), and three are undetected. The extended objects display a wide range of radio morphologies: two-jet (5), one-jet (4), and double-lobed (1). We present the radio spectra of all detected radio sources which range from steep to flat/inverted and span the range seen for other compact radio sources such as compact symmetric objects (CSOs), compact steep spectrum (CSS) sources, and gigahertz peaked-spectrum (GPS) sources. Assuming synchrotron self-absorption (SSA) for flat/inverted radio spectrum sources, we predict small physical sizes for compact objects to range between 2 – 53 pc. Alternatively, using free-free absorption (FFA) models, we have estimated the free electron column depth for all compact objects, assuming a homogeneous absorber. We find that these objects do not occupy a special position on the power/linear size ($P - D$) diagram but some share a region with radio-quiet quasars (RQQs) and so-called ‘FR0’ sources in terms of radio luminosity and linear size.

Key words: galaxies: jets – galaxies: active – radio continuum: galaxies.

1 INTRODUCTION

Theoretical studies have proposed the existence of two main types of active galactic nuclei (AGN) feedback, the radiative (or quasar) mode and the kinetic (or jet) mode (e.g. Croton et al. 2006; McNamara & Nulsen 2007; Nesvadba et al. 2008; Hardcastle et al. 2012; Fabian 2012; Somerville & Davé 2015; Hardcastle & Croston 2020).

The quasar mode is often implemented in simulations (e.g. Faucher-Giguère & Quataert 2012; Somerville & Davé 2015; Costa et al. 2018) and is associated with periods of intense accretion unto a supermassive black hole (SMBH), leading to the formation of a quasar. The intense radiation emitted by quasars (i.e. radiatively efficient AGN; e.g. Hardcastle & Croston 2020) can heat and ionise the surrounding gas, creating strong winds of hot gas that can sweep material out of the host galaxy hence regulating the growth of the SMBH itself, and influencing star formation rates (SFRs; see e.g. Harrison 2017).

The jet mode, often associated with radiatively inefficient AGN

(e.g. Hardcastle et al. 2007), is well supported by observational evidence (e.g. Best et al. 2006; Fabian 2012; Hardcastle et al. 2012; Hardcastle & Croston 2020) which makes it the preferred feedback mechanism in the local Universe. The large-scale emission (jets and sometimes lobes) from powerful radio-loud AGN (RLAGN; blazars, radio galaxies, and radio quasars) often lead to heating of the surrounding gas, preventing cooling flows in galaxy clusters. They can also regulate star formation (SF) in galaxies by heating and disrupting the gas required for SF (e.g. Fabian 2012).

These feedback processes regulate SF, which has a direct consequence on the growth of massive galaxies. However, the extent to which these jets affect the interstellar medium (ISM) of the host galaxy, and how much they affect SFRs is as yet poorly understood. A better understanding of AGN feedback requires the study of RLAGN populations at both high and low luminosities and from the local Universe out to high redshifts.

Recently, an interest in studying physically small (less than 100 kpc) RLAGN and their impact on their surrounding environments has emerged (e.g. Bicknell et al. 2018; Jarvis et al. 2019; Ubertosi et al. 2021). These objects range from powerful yet compact RLAGN

* E-mail: j.chilufya@herts.ac.uk (JC)

A Newborn AGN in a Starforming Galaxy

P. Arévalo^{1,2}, E. López-Navas^{1,2}, M.L. Martínez-Aldama^{3,2}, P. Lira^{4,2}, S. Bernal^{1,2}, P. Sánchez-Sáez⁵, M. Salvato^{7,8},
L. Hernández-García^{1,6}, C. Ricci⁹, A. Merloni⁷, M. Krumpe¹⁰

¹ Instituto de Física y Astronomía, Universidad de Valparaíso, Gran Bretaña 1111, Valparaíso, Chile
e-mail: patricia.arevalo@uv.cl

² Millennium Nucleus on Transversal Research and Technology to Explore Supermassive Black Holes (TITANS)

³ Astronomy Department, Universidad de Concepción, Casilla 160-C, Concepción 4030000, Chile

⁴ Departamento de Astronomía, Universidad de Chile, Casilla 36D, Santiago, Chile

⁵ European Southern Observatory, Karl-Schwarzschild-Str. 2, 85748, Garching, Germany

⁶ Millennium Institute of Astrophysics (MAS), Monseñor Sotero Sanz 100, Providencia, Santiago, Chile

⁷ Max-Planck-Institut für extraterrestrische Physik, Giessenbachstr. 1, 85748 Garching, Germany

⁸ Exzellenzcluster ORIGINS, Boltzmannstr. 2, 85748 Garching, Germany

⁹ Instituto de Estudios Astrofísicos, Facultad de Ingeniería y Ciencias, Universidad Diego Portales, Av. Ejército Libertador 441, Santiago, Chile

¹⁰ Leibniz-Institut für Astrophysik Potsdam, An der Sternwarte 16, 14482 Potsdam, Germany

March 1, 2024

ABSTRACT

Aims. We report on the finding of a newborn AGN, i.e. current AGN activity in a galaxy previously classified as non-active, and characterize its evolution.

Methods. Black hole ignition event candidates were selected from a parent sample of spectrally classified non-active galaxies (2.394.312 objects), that currently show optical flux variability indicative of a type I AGN, according to the ALERCE light curve classifier. A second epoch spectrum for a sample of candidate newborn AGN were obtained with the SOAR telescope to search for new AGN features.

Results. We present spectral results for the most convincing case of new AGN activity, for a galaxy with a previous star-forming optical classification, where the second epoch spectrum shows the appearance of prominent, broad Balmer lines without significant changes in the narrow line flux ratios. Long term optical lightcurves show a steady increase in luminosity starting 1.5 years after the SDSS spectrum was taken and continuing for at least 7 years. MIR colors from the WISE catalog have also evolved from typical non active galaxy colors to AGN-like colors and recent X-ray flux detections confirm its AGN nature.

Key words. galaxies:active; quasars:supermassive black holes; accretion, accretion discs;

1. Introduction

Observations and models indicate that the fraction of active galaxies in the local Universe is about $\sim 10\%$ (Schulze & Wisotzki 2010; Shankar et al. 2013; Sun et al. 2015), which can be interpreted as a duty cycle, where 10% of galaxies are active at any given time. Indirect evidence also suggests that activity varies by several orders of magnitude in time scales of $\Delta t \sim 10^4 - 10^7$ yrs, effectively turning the active nuclei on and off (Hickox et al. 2014; Ichikawa et al. 2019, and references therein). Estimating this activation rate, or alternatively, how many times each galaxy has switched on and off, is important to constrain central black hole feeding mechanisms in galaxy evolution models.

Newborn AGN, which involve a galaxy transitioning from a quiescent or star-forming (SF) state to a type I Active Galactic Nucleus (AGN), are exceptionally challenging to detect. Part of the difficulty arises from the data available, since the largest spectroscopic survey, from SDSS, was originally shallow, it would target mostly galaxies that were bright at that time, and might have become dimmer, not the other way around. Among all the possible signatures of AGN activity, we will focus on optical spectral classification. This choice is justified by the avail-

ability of archival spectral data, and the ease of obtaining new spectra for a few sources. Moreover, AGN activity can be identified largely unambiguously through this approach. A key characteristic of Seyfert I galaxies and quasars, is the presence of broad emission lines in their optical spectra, with widths of thousands of km s^{-1} (Baldwin & Netzer 1978). Therefore, the identification of broad emission lines in a previously spectroscopically-classified quiescent galaxy could serve as compelling evidence for a black hole ignition event.

In the public archives, there are approximately two million galaxies with optical spectra showing no broad emission lines (or other features that identify them as AGN) obtained on average about a decade ago. Detecting ignition events within this vast dataset is possible if they occur more frequently than about 1/20,000,000 per year. Re-observing all of these galaxies, however, is impractical so alternative criteria for target selection are needed. Fortunately, there is another distinguishable characteristic of quasars and Seyfert I galaxies, which is their persistent and stochastic optical flux variability (e.g. MacLeod et al. 2010; Sánchez-Sáez et al. 2018). Such variations are considerably rare in even type II AGN (López-Navas et al. 2023), and even rarer in quiescent galaxies as discussed below.

Rapid Variability of Mrk 421 During Extreme Flaring as Seen Through the Eyes of *XMM-Newton*

A. Gokus,^{1,2,3*} J. Wilms,² M. Kadler,³ D. Dorner,^{4,3,†} M. A. Nowak,¹ A. Kreikenbohm,³ K. Leiter,³ T. Bretz,^{4,5,†} B. Schleicher,^{4,3,†} A. G. Markowitz,^{6,7} K. Pottschmidt,^{8,9} K. Mannheim,^{3,†} I. Kreykenbohm,² M. Langejahn,^{3,10} F. McBride,¹¹ T. Beuchert,² T. Dauser,² M. Kreter,¹² and the FACT Collaboration: J. Abhir,⁴ D. Baack,¹³ M. Balbo,¹⁴ A. Biland,⁴ K. Brand,³ J. Buss,¹³ L. Eisenberger,³ D. Elsaesser,¹³ P. Günther,³ D. Hildebrand,⁴ M. Linhoff,¹³ A. Paravac,³ W. Rhode,¹³ V. Sliusar,¹⁴ S. Hasan,⁴ R. Walter¹⁴

¹Department of Physics & McDonnell Center for the Space Sciences, Washington University in St. Louis, One Brookings Drive, St. Louis, MO 63130, USA

²Dr. Karl Remeis-Sternwarte & ECAP, Universität Erlangen-Nürnberg, Sternwartstr. 7, 96049 Bamberg, Germany

³Institut für Theoretische Physik und Astrophysik, Universität Würzburg, Emil-Fischer-Straße 31, 97074 Würzburg, Germany

⁴ETH Zürich, Institute for Particle Physics and Astrophysics, Otto-Stern-Weg 5, 8093 Zürich, Switzerland

⁵also at GSI Helmholtzzentrum für Schwerionenforschung GmbH, Darmstadt, Germany

⁶Nicolaus Copernicus Astronomical Center, Polish Academy of Sciences, ul. Bartycka 18, 00-716, Warszawa, Poland

⁷University of California, San Diego, Center for Astrophysics and Space Sciences, MC 0424, La Jolla, CA, 92093-0424, USA

⁸CRESSST and CSST, University of Maryland, Baltimore County, 1000 Hilltop Circle, Baltimore, MD 21250, USA

⁹Code 661 Astroparticle Physics Laboratory, NASA Goddard Space Flight Center, Greenbelt, MD 20771, USA

¹⁰Lehrstuhl für Data Science in Earth Observation, Technische Universität München, Arcisstraße 21, 80333 München, Germany

¹¹Department of Physics and Astronomy, Bowdoin College, Brunswick, ME 04011, USA

¹²Centre for Space Research, North-West University, Potchefstroom 2520, South Africa

¹³TU Dortmund, Experimental Physics 5, Otto-Hahn-Str. 4a, 44227 Dortmund, Germany

¹⁴University of Geneva, Department of Astronomy, Chemin d'Ecogia 16, 1290 Versoix, Switzerland

[†]also member of the FACT Collaboration

Accepted XXX. Received YYY; in original form ZZZ

ABSTRACT

By studying the variability of blazars across the electromagnetic spectrum, it is possible to resolve the underlying processes responsible for rapid flux increases, so-called flares. We report on an extremely bright X-ray flare in the high-peaked BL Lacertae object Mrk 421 that occurred simultaneously with enhanced γ -ray activity detected at very high energies (VHE) by FACT on 2019 June 9. We triggered an observation with *XMM-Newton*, which observed the source quasi-continuously for 25 hours. We find that the source was in the brightest state ever observed using *XMM-Newton*, reaching a flux of 2.8×10^{-9} erg cm⁻² s⁻¹ over an energy range of 0.3–10 keV. We perform a spectral and timing analysis to reveal the mechanisms of particle acceleration and to search for the shortest source-intrinsic time scales. Mrk 421 exhibits the typical harder-when-brighter behaviour throughout the observation and shows a clock-wise hysteresis pattern, which indicates that the cooling dominates over the acceleration process. While the X-ray emission in different sub-bands is highly correlated, we can exclude large time lags as the computed zDCFs are consistent with a zero lag. We find rapid variability on time scales of 1 ks for the 0.3–10 keV band and down to 300 s in the hard X-ray band (4–10 keV). Taking these time scales into account, we discuss different models to explain the observed X-ray flare, and find that a plasmoid-dominated magnetic reconnection process is able to describe our observation best.

Key words: BL Lacertae objects: individual: Markarian 421 – galaxies: active – X-rays: galaxies – acceleration of particles – relativistic processes

1 INTRODUCTION

Among active galactic nuclei (AGN), blazars show the strongest and the most rapid variability (e.g., Stein et al. 1976; Wagner & Witzel 1995; Ulrich et al. 1997). Their luminosity and extreme properties

originate from a collimated outflow, the so-called jet, of relativistically moving particles close to the line of sight (Antonucci 1993; Urry & Padovani 1995), and their emission is Doppler boosted towards the observer. Their characteristic broadband spectral energy distribution has a double-hump structure and sub-classes of blazars are broadly defined by their overall luminosity and the peak position of the first hump, which lies somewhere between near-IR to X-ray energies. The emission of the low-energy hump is typically strongly

* E-mail: gokus@wustl.edu, dr.andrea.gokus@gmail.com

Scattering model of scintillation arcs in pulsar secondary spectra

Tobias Kramer,^{1,2} Daniel Waltner,¹ Eric J. Heller,² and Dan R. Stinebring³

¹*Institute for Theoretical Physics, Johannes Kepler University Linz, Altenberger Str. 69, 4020 Linz, Austria*

²*Harvard Physics Department, 17 Oxford Street, Cambridge, MA 02138, USA*

³*Department of Physics and Astronomy, 110 No. Professor St., Oberlin College, Oberlin, OH 44074, USA*

1 March 2024

ABSTRACT

The dynamic spectra of pulsars frequently exhibit diverse interference patterns, often associated with parabolic arcs in the Fourier-transformed (secondary) spectra. In our approach, we extend beyond the traditional Fresnel-Kirchhoff method by using the Green’s function of the Helmholtz equation. Through advanced numerical techniques, we model both the dynamic and secondary spectra, providing a comprehensive framework that describes all components of the latter spectra in terms of physical quantities. Additionally, we provide a thorough analytical explanation of the secondary spectrum.

Key words: Radio pulsars (1353), Pulsars (1306)

1 INTRODUCTION

The first observation of radio pulsars goes back to [Hewish et al. \(1969\)](#). The electromagnetic signals of pulsars encounter on their way a varying electron density of the interstellar medium (ISM), resulting in deflection and scattering of the traveling electromagnetic waves. In addition, the relative motion of pulsar, ISM, and the observer’s antenna leads to a Doppler shift and time-varying phenomena. The dynamic spectra consist of the frequency resolved pulse sequences observed over a time-span of up to several hours. A two-dimensional (2D) Fourier transform of the dynamic spectra gives the secondary spectra. [Stinebring et al. \(2001\)](#) discovered parabolic arc structures in the secondary spectra, which result from the interference of multiple signal pathways at a specific distance between the pulsar and the observer. The recent catalog of scintillation arcs compiled by [Stinebring et al. \(2022\)](#) of 22 pulsars shows various structures and contains the basic physical parameters of the pulsar, such as distance and velocity. [Walker et al. \(2004\)](#) developed theoretical descriptions of the parabolic arcs starting from the Fresnel-Kirchhoff integral. Using Monte Carlo methods, [Walker et al. \(2004\)](#) then computed the locations of points in the secondary spectra. Similarly, [Cordes et al. \(2006\)](#) used a thin phase-changing screen approach to study the dynamic and secondary spectra. Since then there have been a variety of arc studies based on observations by different groups, e.g., [Hill et al. \(2003, 2005\)](#); [Wang et al. \(2005\)](#); [Bhat et al. \(2016\)](#); [Safutdinov et al. \(2017\)](#); [Wang et al. \(2018\)](#); [Stinebring et al. \(2019\)](#); [Reardon et al. \(2020\)](#); [Rickett et al. \(2021\)](#); [Yao et al. \(2021\)](#); [Chen et al. \(2022\)](#); [McKee et al. \(2022\)](#).

Here we put forward a different theoretical approach to treat scattering by the ISM using Green’s functions. This method is commonly applied to scattering problems in quantum mechanics; see [Kramer & Rodríguez \(2006\)](#) for an application to matter waves originating from a compact source. By solving Helmholtz’s equation in Cartesian coordinates using Green’s functions we determine the pulsar spectra received after scattering at the interstellar medium (dynamic spectrum) and its 2D Fourier transform with respect to time and frequency by high-precision numerics (secondary spectrum) for a given scattering configuration. In contrast to the Fresnel-Kirchhoff approach, our method enables the determination of the entire spectrum and relates the strengths of the individual components to physical quantities such as the refractive index and the wavenumber. Furthermore, we give a complete analytical description of the secondary spectra. [Walker et al. \(2004\)](#) obtained point-like peaks in the snapshot regime and determined their positions. We considerably extend this analysis by analytically determining also the peak extensions and the intensities.

In the second section we introduce our scattering approach and present our findings for an analytical description of the spectra in the third section. We conclude in the fourth section and relegate to the appendices some detailed explanations and technical details.

2 SOLUTION OF THE HELMHOLTZ EQUATION

In this section we propose a Green’s function method to describe the scattering of pulsar radiation in the ISM. The differences to the Fresnel-Kirchhoff approach are summarized in Appendix A. We consider scattering from an extended plasma cloud (see Fig. 1), described by a region with

$$V(\mathbf{r}') = \frac{1}{4\pi}(\epsilon(\mathbf{r}') - \epsilon_{\text{background}}) \neq 0. \quad (1)$$

A new analytical model of the cosmic-ray energy flux for Galactic diffuse radio emission

Andrea Bracco^{1,2}, Marco Padovani¹, and Daniele Galli¹

¹ INAF – Osservatorio Astrofisico di Arcetri, Largo E. Fermi 5, 50125 Firenze, Italy
e-mail: andrea.bracco@inaf.it

² Laboratoire de Physique de l’Ecole Normale Supérieure, ENS, Université PSL, CNRS, Sorbonne Université, Université de Paris, F-75005 Paris, France

Received 15 February 2024; accepted 29 February 2024

ABSTRACT

Low-frequency radio observations of diffuse synchrotron radiation offer a unique vantage point for investigating the intricate relationship between gas and magnetic fields in the formation of structures within the Galaxy, spanning from the diffuse interstellar medium (ISM) to star-forming regions.

Achieving this pivotal objective hinges on a comprehensive understanding of cosmic-ray properties, which dictate the effective energy distribution of relativistic electrons, primarily responsible for the observable synchrotron radiation. Notably, cosmic-ray electrons (CRE) with energies between 100 MeV and 10 GeV play a crucial role in determining the majority of the sky brightness below the GHz range. However, their energy flux (j_e) remains elusive due to solar modulation.

We propose deriving observational constraints on this energy gap of interstellar CRE through the brightness temperature spectral index of low-frequency radio emission, here denoted as β_{obs} . We introduce a new parametric analytical model that fits available data of j_e in accordance with the β_{obs} values measured in the literature between 50 MHz to 1 GHz for diffuse emission in the Milky Way. Our model allows to account for multiple observations considering magnetic-field strengths consistent with existing measurements below 10 μG . We present a first all-sky map of the average component of the magnetic field perpendicular to the line of sight and validate our methodology against state-of-the-art numerical simulations of the diffuse ISM.

This research makes headway in modeling Galactic diffuse emission with a practical parametric form. It provides essential insights in preparation for the imminent arrival of the Square Kilometre Array.

Key words. magnetic fields – radiation mechanisms: non-thermal – ISM: cosmic rays – radio continuum: ISM

1. Introduction

Low-frequency radio emission observations are paving the way for a comprehensive study of Galactic magnetic fields traced by synchrotron radiation. The breakthrough in sensitivity of current and upcoming radio telescopes, including the Low Frequency Array (LOFAR, van Haarlem et al. 2013), the Long Wavelength Array (LWA, Dowell et al. 2017), the New Extension in Nançay Upgrading LOFAR (NenuFAR, Zarka et al. 2012), the C-Band All-Sky Survey (Jones et al. 2018), and the Square Kilometre Array (SKA, Dewdney et al. 2009) along with its precursors, promises the most detailed multi-scale description of the Galactic magnetic field. This description encompasses both its topology and its strength, ranging from the diffuse interstellar medium (ISM) to star-forming regions (Heald et al. 2020).

Achieving this paramount objective, however, relies on the thorough characterization of cosmic-ray (CR) properties, acceleration, and propagation. These factors determine the effective energy distribution of relativistic electrons, which are primarily responsible for the observable synchrotron radiation¹ (e.g., Ginzburg & Syrovatskii 1964; Padovani & Galli 2018). In particular, low-energy cosmic-ray electrons (CRE) between 100 MeV and 10 GeV are those relevant for most of the radio emission

detected below the GHz range (Padovani et al. 2021, hereafter P21). Unfortunately, because of solar modulation, the energy flux of these electrons (j_e) cannot be measured from near-earth direct observations (e.g., Gabici 2022). Hence, j_e is usually interpolated in the GeV window (e.g., Orlando 2018; Padovani & Galli 2018; Padovani et al. 2018; Unger & Farrar 2023; Bracco et al. 2023) between the MeV range observed with the Voyager spacecrafts (Cummings et al. 2016; Stone et al. 2019) and the hundred-of-GeV range measured by facilities including Fermi LAT (Ackermann et al. 2010), Pamela (Adriani et al. 2011), and the Alpha Magnetic Spectrometer (AMS, Aguilar et al. 2014).

Building upon the pioneering works of Rockstroh & Webber (1978), Strong & Wolfendale (1978), and Strong et al. (2000), and following up the investigation conducted by P21, in this paper we propose that observational constraints on the missing energy window of interstellar CRE can be obtained through the spectral index of low-frequency radio emission, denoted as β_{obs} . We introduce a new analytical-parametric model that accurately fits j_e , considering the values of β_{obs} measured in the literature between 45 MHz and 408 MHz for Galactic diffuse emission. We use our models of j_e to estimate the strength of the Galactic magnetic field averaged along the line of sight. Our observational results are discussed through a comparison with synthetic data generated from state-of-the-art magneto-hydrodynamic (MHD) simulations of the diffuse ISM.

¹ Positrons and secondary electrons also contribute to synchrotron radiation but at a few % level (Orlando 2018; Ponnada et al. 2024)

jetsimpy: A Highly Efficient Hydrodynamic Code for Gamma-ray Burst Afterglow

HAO WANG ¹, RANADEEP G. DASTIDAR,¹ DIMITRIOS GIANNIOS ¹ AND PAUL C. DUFFELL¹

¹*Department of Physics and Astronomy, Purdue University, 525 Northwestern Avenue, West Lafayette, IN 47907, USA*

(Received xxx; Revised xxx; Accepted xxx; Published xxx)

Submitted to ApJS

ABSTRACT

Gamma-ray Burst afterglows are emissions from ultra-relativistic blastwaves produced by a narrow jet interacting with surrounding matter. Since the first multi-messenger observation of a neutron star merger, hydrodynamic modeling of GRB afterglows for structured jets with smoothly varying angular energy distributions has gained increased interest. While the evolution of a jet is well described by self-similar solutions in both ultra-relativistic and Newtonian limits, modeling the transitional phase remains challenging. This is due to the non-linear spreading of a narrow jet to a spherical configuration and the breakdown of self-similar solutions. Analytical models are limited in capturing these non-linear effects, while relativistic hydrodynamic simulations are computationally expensive which restricts the exploration of various initial conditions. In this work, we introduce a reduced hydrodynamic model that approximates the blastwave as an infinitely thin two-dimensional surface. Further assuming axial-symmetry, this model simplifies the simulation to one dimension and drastically reduces the computational costs. We have compared our modeling to relativistic hydrodynamic simulations, semi-analytic methods, and applied it to fit the light curve and flux centroid motion of GW170817. These comparisons demonstrate a high level of agreement and validate our approach. We have developed this method into a numerical tool, **jetsimpy**, which models the synchrotron GRB afterglow emission from a blastwave with arbitrary angular energy and Lorentz factor distribution. Although the code is built for GRB afterglow in mind, it is applicable to any relativistic jets. This tool is particularly useful in Markov Chain Monte Carlo studies and is provided to the community.

Keywords: Gamma-ray bursts, Hydrodynamics, Jets

1. INTRODUCTION

Gamma-ray Bursts (GRBs) are the most energetic catastrophic events in the Universe. Their tremendous explosive power provides a platform for scientific study of fundamental physical processes in extreme physical environments. One of the intriguing aspects of GRBs is their long-term, multi-waveband afterglow following the prompt emission. GRB afterglows are radiation from the ultra-relativistic blastwaves produced by the interaction of a narrow jet with the surrounding external medium. They are the promising sites to study the hydrodynamical interactions and microphysical processes

associated with some of the most extreme macroscopic bulk motions in the Universe. Recently, it has also been demonstrated that GRB afterglows could serve as probes to study the Universe’s expansion rate (see [Bulla et al. 2022](#) for a review), thereby helping to unravel the nature of the Hubble tension (see [Di Valentino et al. 2021](#) for a review).

To model the evolution of a narrow GRB jet, the angular energy profile is often approximated by a so-called “top-hat” model, where the energy is uniformly distributed within a narrow core, and sharply drops to zero at the edge. This model has been proven highly successful in accounting for the GRB phenomenology when the jet is observed from an on-axis direction, namely, when the observer’s line of sight lies within the jet core (see [Kumar & Zhang 2015](#) for a review). This is a nat-

Searching for NLTE effects in the high-resolution transmission spectrum of WASP-121 b with Cloudy for Exoplanets

M. E. Young^{1,2*}, E. F. Spring³ and J. L. Birkby¹

¹*Department of Physics, University of Oxford, Denys Wilkinson Building Keble Rd., Oxford OX1 3RH, UK*

²*School of Mathematics and Physics, Queen's University Belfast, Main Physics Building University Rd., Belfast BT7 1NN, UK*

³*Anton Pannekoek Instituut (API), Universiteit van Amsterdam, Science Park 904, 1098 XH Amsterdam, Netherlands*

Accepted XXX. Received YYY; in original form ZZZ

ABSTRACT

Ultra-hot Jupiters (UHJs) undergo intense irradiation by their host stars and are expected to experience non-local thermodynamic equilibrium (NLTE) effects in their atmospheres. Such effects are computationally intensive to model but, at the low pressures probed by high-resolution cross-correlation spectroscopy (HRCCS), can significantly impact the formation of spectral lines. The UHJ WASP-121 b exhibits a highly inflated atmosphere, making it ideal for investigating the impact of NLTE effects on its transmission spectrum. Here, we formally introduce *Cloudy for Exoplanets*, a *Cloudy*-based modelling code, and use it to generate 1-D LTE and NLTE atmospheric models and spectra to analyse archival HARPS WASP-121 b transmission spectra. We assessed the models using two HRCCS methods: i) Pearson cross-correlation, and ii) a method that aims to match the average observed line depth for given atmospheric species. All models result in strong detections of Fe I ($7.5 < S/N < 10.5$). However, the highest S/N model (LTE) does not agree with the best-matching model of the average line depth (NLTE). We also find degeneracy, such that increasing the isothermal temperature and metallicity of the LTE models can produce average line depths similar to cooler, less metal rich NLTE models. Thus, we are unable to conclusively remark on the presence of NLTE effects in the atmosphere of WASP-121 b. We instead highlight the need for standardised metrics in HRCCS that enable robust statistical assessment of complex physical models, e.g. NLTE or 3-D effects, that are currently too computationally intensive to include in HRCCS atmospheric retrievals.

Key words: planets and satellites: atmospheres – planets and satellites: gaseous planets – planets and satellites: composition

1 INTRODUCTION

WASP-121 b is one of the best studied examples of an ultra-hot Jupiter (UHJ), and the first exoplanet to have a stratosphere (thermal inversion) detected in its atmosphere (Evans et al. 2017). Recent JWST phase curve observations have revealed a day-side hot spot eastward of the substellar point, and are consistent with a cloudy night-side (Mikal-Evans et al. 2023). A number of works have also been published inventorying the chemical species in its atmosphere, using high-resolution transmission spectroscopy. Collectively, they have identified neutral atomic species such as H, Li, Na, Mg, K, Ca, Sc, V, Cr, Mn, Fe, Co, Ni, Cu, and Ba, as well as Ca II and Fe II (Gibson et al. 2020; Cabot et al. 2020; Hoeijmakers et al. 2020; Ben-Yami et al. 2020; Merritt et al. 2020, 2021; Borsa et al. 2021b; de Regt et al. 2022; Azevedo Silva et al. 2022; Gibson et al. 2022), although Fe II and neutral Mg are debated in the literature with non-detections in high-resolution (Hoeijmakers et al. 2020; Merritt et al.

2021). It is worth noting, however, that both Fe II and Mg II have been detected at UV wavelengths with low-resolution observations (Sing et al. 2019).

The advantage of high-resolution spectroscopy is that it is sensitive to the number of spectral lines and line depth ratios, information that might be missed in low-resolution, while also probing higher altitudes than low-resolution can reach. Unfortunately, unlike stellar high-resolution spectroscopy where individual spectral lines stand out well above the level of the noise, exoplanetary spectral features are generally of comparable signal to observational noise or are buried within it. Therefore, rather than study individual spectral lines, it is common to employ high-resolution cross-correlation spectroscopy (HRCCS), which involves cross-correlating a model template with a time series of observations to extract the planetary signal from within the noise.

It is common to make a number of assumptions when generating templates for HRCCS, and when modelling exoplanetary atmospheres in general. These can include: i) modelling the atmospheres in 1-D, ii) assuming they are isothermal, or iii) calculating

* E-mail: mitchell.young@physics.ox.ac.uk

Integral field spectroscopy supports atmospheric optics to reveal the finite outer scale of the turbulence

B. García-Lorenzo,^{1,2} D. Esparza-Arredondo,^{1,2} J.A. Acosta-Pulido,^{1,2} and J.A. Castro-Almazán^{1,2}

¹ Instituto de Astrofísica de Canarias, C/ Vía Láctea s/n, E-38205 La Laguna, Tenerife, Spain
e-mail: begona.garcia@iac.es

² Departamento de Astrofísica, Universidad de La Laguna, E-38200 La Laguna, Tenerife, Spain

Received October 24, 2023; accepted , 2024

ABSTRACT

Context. The spatial coherence wavefront outer scale (\mathcal{L}_0) characterizes the size of the largest turbulence eddies in Earth's atmosphere, determining low spatial frequency perturbations in the wavefront of the light captured by ground-based telescopes. Advances in adaptive optics (AO) techniques designed to compensate for atmospheric turbulence emphasize the crucial role of this parameter for the next generation of large telescopes.

Aims. The motivation of this work is to introduce a novel technique for estimating \mathcal{L}_0 from seeing-limited integral field spectroscopic (IFS) data. This approach is based on the impact of a finite \mathcal{L}_0 on the light collected by the pupil entrance of a ground-based telescope.

Methods. We take advantage of the homogeneity of IFS observations to generate band filter images spanning a wide wavelength range, enabling the assessment of image quality (IQ) at the telescope's focal plane. Comparing the measured wavelength-dependent IQ variation with predictions from Tokovinin (2002) analytical approach offers valuable insights into the prevailing \mathcal{L}_0 parameter during the observations. We applied the proposed technique to observations from the Multi Unit Spectroscopic Explorer (MUSE) in the Wide Field Mode obtained at the Paranal Observatory.

Results. Our analysis successfully validates Tokovinin's analytical expression, which combines the seeing (ϵ_0) and the \mathcal{L}_0 parameters, to predict the IQ variations with the wavelength in ground-based astronomical data. However, we observed some discrepancies between the measured and predictions of the IQ that are analyzed in terms of uncertainties in the estimated ϵ_0 and dome-induced turbulence contributions.

Conclusions. This work constitutes the empirical validation of the analytical expression for estimating IQ at the focal plane of ground-based telescopes under specific ϵ_0 and finite \mathcal{L}_0 conditions. Additionally, we provide a simple methodology to characterize the \mathcal{L}_0 and dome-seeing (ϵ_{dome}) as by-products of IFS observations routinely conducted at major ground-based astronomical observatories.

Key words. Atmospheric effects – Telescopes – Instrumentation: high angular resolution – Techniques: imaging spectroscopy – Site testing

1. Introduction

Earth's atmospheric turbulence significantly affects light propagation through it, distorting both intensities and wavefronts. Consequently, ground-based astronomical observations often produce blurred images compared to those obtained from space using identical telescopes and instruments.

Atmospheric turbulence results from stochastic fluctuations in the refractive index attributed to temperature variations. The strength of this turbulence can be quantified using the refractive index structure parameter (C_n^2), which is a function of the position. The Kolmogorov model provides a satisfactory description of the statistical properties of atmospheric turbulence, assuming that it is homogeneous and isotropic (e.g., Roddier 1981). This model pictures the turbulence as a cascade of energy, following a power-law distribution, from large- to small-scale turbulence eddies until dissipation. The Kolmogorov model applies only to the inertial range between inner (l_0) and outer (L_0) scales determined by the smallest and largest sizes of turbulence eddies. This model holds for any atmospheric turbulence layer that light passes through on its way to the pupil entrance of ground-based telescopes, each characterized by a C_n^2 and an L_0 depending on the local conditions at each layer height (h). Hence, the wavefront of the light reaching the telescope pupil will suffer pertur-

bations from the distinct atmospheric turbulence layers. We can define the spatial coherence wavefront outer scale (\mathcal{L}_0) as an equivalent outer scale determining the image quality (IQ) of any observation taken with that telescope (Borgnino 1990). \mathcal{L}_0 is related to the L_0 of the atmospheric turbulence layers as follows (e.g., Abahamid et al. 2004):

$$\mathcal{L}_0 = \left(\frac{\int L_0(h)^{-1/3} C_n^2(h) dh}{\int C_n^2(h) dh} \right)^{-3} \quad (1)$$

The \mathcal{L}_0 is a parameter independent of the wavelength of the observed light, representing a size and typically measured in meters. In many applications, equations are simplified by assuming infinite outer scales. Under this assumption, the full width at half maximum (FWHM) of the point spread function (PSF) in a long-exposure (LE) image, captured with a ground-based telescope limited by atmospheric turbulence, commonly referred to as the seeing-limited IQ (ϵ_{LE}), can be expressed in terms of the strength of atmospheric turbulence as follows:

$$\epsilon_{LE}(\lambda) \approx \epsilon_0(\lambda) = \frac{0.976\lambda}{r_0(\lambda)} \quad (2)$$

Connections between Planetary Populations and the Chemical Characteristics of their Host Stars

SOL YUN,¹ YOUNG SUN LEE,^{2,3} YOUNG KWANG KIM,⁴ TIMOTHY C. BEERS,^{3,5} BERFIN TOGAY,⁶ AND DONGWOOK LIM⁷

¹*Department of Astronomy, Space Science, and Geology, Chungnam National University, Daejeon 34134, South Korea; yunsol719@gmail.com*

²*Department of Astronomy and Space Science, Chungnam National University, Daejeon 34134, South Korea; youngsun@cnu.ac.kr*

³*Department of Physics and Astronomy, University of Notre Dame, Notre Dame, IN 46556, USA*

⁴*Department of Astronomy and Space Science, Chungnam National University, Daejeon 34134, South Korea*

⁵*Joint Institute for Nuclear Astrophysics – Center for the Evolution of the Elements (JINA-CEE), USA*

⁶*Department of Astronomy, Space Science, and Geology, Chungnam National University, Daejeon 34134, South Korea*

⁷*Department of Astronomy, Yonsei University, Yonsei-ro, Seodaemun-gu Seoul, 03722, South Korea*

ABSTRACT

Chemical anomalies in planet-hosting stars (PHSs) are studied in order to assess how the planetary nature and multiplicity affect the atmospheric chemical abundances of their host stars. We employ APOGEE DR17 to select thin-disk stars of the Milky Way, and cross-match them with the Kepler Input Catalog to identify confirmed PHSs, which results in 227 PHSs with available chemical-abundance ratios for six refractory elements. We also examine an ensemble of stars without planet signals, which are equivalent to the selected PHSs in terms of evolutionary stage and stellar parameters, to correct for Galactic chemical-evolution effects, and derive the abundance gradient of refractory elements over the condensation temperature for the PHSs. Using the Galactic chemical-evolution corrected abundances, we found that PHSs do not show a significant difference in abundance slope from the stars without planets. Furthermore, we examine the depletion trends of refractory elements of PHSs depending on total number of planets and their types, and find that the PHSs with giant planets are more depleted in refractory elements than those with rocky planets. Among the PHSs with rocky planets, the refractory-depletion trends are potentially correlated with the terrestrial planets' radii and multiplicity. In the cases of PHSs with giant planets, sub-Jovian PHSs demonstrated more depleted refractory trends than stars hosting Jovian-mass planets, raising questions on different planetary-formation processes for Neptune-like and Jupiter-like planets.

Keywords: Star-planet interactions (2177), Planetary system formation (1257), Chemical abundances (224), Stellar abundances (1577), Stellar kinematics (1608), Galaxy chemical evolution (580)

1. INTRODUCTION

A star and its planets are thought to have formed from the same molecular cloud. The composition of a star could influence the protoplanetary disk where planets form, and the accreting material from the protoplanetary disk onto the host star may be chemically imprinted in the atmosphere of the star. These interactions may result in an intricate relationship between the chemical composition of a star and the formation and evolution of its planets. Various approaches have been conducted to find such connections between the chemical composition of a planet-hosting star (PHS) and its planet formation and architecture. Notably, the amount of heavy elements in a stellar atmosphere, often characterized by metallicity ($[Fe/H]$), has received attention due to its expected implications for the occurrence and properties of planetary companions (e.g., [Gonzalez 1997](#); [Heiter & Luck](#)

[2003](#); [Santos, N. C. et al. 2004](#); [Fischer & Valenti 2005](#); [Udry & Santos 2007](#); [Adibekyan et al. 2012b](#)).

[Meléndez et al. \(2009\)](#) first reported, based on an analysis of 11 Solar twin stars, that the Sun's refractory elements (Mg, Al, Si, etc.), which have condensation temperatures (T_C) over 1200 K, are relatively depleted compared to those of the volatile elements (C, N, O, etc.). They suggested that refractory depletion is correlated with the presence of terrestrial planets; the material to form the rocky planet readily incorporates elements with high T_C in the solid phase, while the low T_C volatile elements likely remain in the gas phase. This was further supported by [Chambers \(2010\)](#), who claimed that the deficit of the refractory elements in the solar photosphere could account for roughly four Earth masses of terrestrial material. These studies have triggered numerous efforts to identify differences in the chemical abundances between PHSs and non-PHSs (NPHSs) using chemical-

Sources of high-energy astrophysical neutrinos

Walter Winter*

Deutsches Elektronen-Synchrotron DESY,

Platanenallee 6, 15738 Zeuthen, Germany

E-mail: walter.winter@desy.de

We discuss recent results in neutrino astronomy and their implications for the cosmic-ray acceleration in relativistic outflows, such as in Active Galactic Nuclei (AGN) jets, Gamma-Ray Bursts (GRBs), and Tidal Disruption Events (TDEs). We especially focus on challenges at the interface to particle acceleration which can be inferred from the multi-messenger context, such as the paradigm that the sources power the Ultra-High-Energy Cosmic Rays (UHECRs). We demonstrate that both AGN blazars (in the context of neutrino observations) and GRBs (as UHECR sources in the context of neutrino-non-observations) point towards acceleration spectra harder than E^{-2} , or relatively high minimal cosmic-ray injection energies, to meet the respective energy budget requirements. We furthermore speculate that neutrino flares in AGN blazars may be related to super-Eddington accretion flares, or that GRBs are powered by significantly higher kinetic energies than typically assumed in electromagnetic models. For internal shock models, the UHECR paradigm for GRBs can only be maintained in the light of neutrino stacking limits in multi-zone models. While relativistic outflows in TDEs have become recently interesting *per se* and models for the neutrino emission from jetted TDEs exist, a direct connection between TDE jets pointing in our direction and astrophysical neutrinos has not been identified yet.

High Energy Phenomena in Relativistic Outflows VIII (HEPROVIII)

23-26 October, 2023

Paris, France

*Speaker

© Copyright owned by the author(s) under the terms of the Creative Commons Attribution-NonCommercial-NoDerivatives 4.0 International License (CC BY-NC-ND 4.0).

<https://pos.sissa.it/>

Sources of high-energy astrophysical neutrinos

Walter Winter

1. Introduction

Since a diffuse astrophysical neutrino flux has been discovered by the IceCube experiment [1], several individual source contributions have been identified: neutrinos from the Active Galactic Nuclei (AGN) blazar TXS 0506+056 [2, 3], neutrinos from the active galaxy NGC 1068 [4], and neutrinos from the Galactic plane [5]. In addition, there have been a number of interesting constraints on source classes which are believed to contribute significantly to the astrophysical flux. For example, Gamma-Ray Bursts (GRBs) probably contribute less than about one percent of the diffuse flux [6]. Apart from the well established neutrino sources, a number of additional contributors with some hints for neutrino-source associations have been proposed; one example are Tidal Disruption Events (TDEs) [7–10].

Relativistic outflows are typically associated with particle acceleration leading to non-thermal primary spectra. Radiative mechanisms produce secondary electromagnetic signatures, such as synchrotron emission of electrons and inverse Compton up-scatterings of those photons by the same electrons (synchrotron self-Compton models). If protons (or nuclei) are accelerated as well, neutrinos may be produced by the interactions of protons and photons or matter, as well as additional (so-called “hadronic”) signatures on the electromagnetic spectrum are expected. One of the outstanding puzzles in astroparticle physics in the multi-messenger context is the origin of the Ultra-High-Energy Cosmic Rays (UHECRs), which are the cosmic rays at the highest energies. More specifically, if one expects significant neutrino production in the sources of the cosmic rays, astrophysical neutrinos will be a smoking gun signature for their origin.

Here we focus (in the spirit of this conference series) on source classes which potentially host relativistic outflows, and where the neutrino production might be associated with those outflows. A widely accepted neutrino source class are AGN jets, where the Lorentz factor of the outflow $\Gamma \sim 10 - 30$. AGN jets are best studied as AGN blazars, which are jets pointing in our direction, in terms of data coverage across the spectrum; electromagnetic data typically give a lot of information on the properties of the emission region and constrain its parameters. Note, however, that because of the isotropy of the Universe, we expect that AGN jets pointing in other directions have (statistically) the same properties as AGN blazars, even though they may be classified into different categories from the observational point of view. Another very interesting source class are GRBs, where we focus on the prompt emission of standard long-duration GRBs with $\Gamma \gtrsim 100$ in the context of internal shock models for the sake of simplicity. GRBs are one of the main candidate classes for the origin of the UHECRs because of their energetics, and they are also expected to produce astrophysical neutrinos [11]. The non-observation of neutrinos from GRBs [6] therefore has profound consequences for the UHECR paradigm for GRBs, as we will discuss. It has been also well established that some TDEs come with relativistic jets since the discovery of Swift J1644+57 [12]; while several likely observations of TDEs with jets have been made since then, the subject has recently gained momentum by the observation of AT2022cmc [13]; the inferred $\Gamma \sim 10 - 100$ [12, 14, 15]. The association between TDE jets and astrophysical neutrinos is somewhat more speculative, as we will see.

The purpose of this talk is *not* to discuss how the particles are accelerated, but give ideas what it needs to describe the astrophysical neutrino observations in the multi-messenger context – and what the critical issues are. For example: What kind of acceleration spectra do we need? What do

The impact of the explicit representation of convection on the climate of a tidally locked planet in global stretched-mesh simulations.

DENIS E. SERGEEV ¹ IAN A. BOUTLE ^{2,1} F. HUGO LAMBERT ³ NATHAN J. MAYNE ¹ THOMAS BENDALL ²
KRISZTIAN KOHARY ¹ ENRICO OLIVIER ⁴ AND BEN SHIPWAY²

¹*Department of Physics and Astronomy, University of Exeter, Exeter, EX4 4QL, UK*

²*Met Office, Fitzroy Road, Exeter, EX1 3PB, UK*

³*Department of Mathematics and Statistics, University of Exeter, Exeter, EX4 4QF, UK*

⁴*Research Software Engineering, University of Exeter, Exeter, EX4 4QE, UK*

ABSTRACT

Convective processes are crucial in shaping exoplanetary atmospheres but are computationally expensive to simulate directly. A novel technique of simulating moist convection on tidally locked exoplanets is to use a global 3D model with a stretched mesh. This allows us to locally refine the model resolution to 4.7 km and resolve fine-scale convective processes without relying on parameterizations. We explore the impact of mesh stretching on the climate of a slowly rotating TRAPPIST-1e-like planet, assuming it is 1:1 tidally locked. In the stretched-mesh simulation with explicit convection, the climate is 5 K colder and 25% drier than that in the simulations with parameterized convection. This is due to the increased cloud reflectivity and exacerbated by the diminished greenhouse effect due to less water vapor. At the same time, our stretched-mesh simulations reproduce the key characteristics of the global climate of tidally locked rocky exoplanets, without any noticeable numerical artifacts. Our methodology opens an exciting and computationally feasible avenue for improving our understanding of 3D mixing in exoplanetary atmospheres. Our study also demonstrates the feasibility of a global stretched mesh configuration for LFRic-Atmosphere, the next-generation Met Office climate and weather model.

Keywords: Exoplanet atmospheres (487); Planetary atmospheres (1244); Habitable planets (695); Habitable zone (696); Atmospheric circulation (112)

1. INTRODUCTION

Fine-scale atmospheric phenomena such as moist convection, are typically unresolved in exoplanet climate models because the grid in these models is too coarse. Therefore, most general circulation models (GCMs) rely on convection parameterizations (Arakawa 2004). While convection parameterizations are physically motivated, they are necessarily a simplification of the real process (Kendon et al. 2021; Rios-Berrios et al. 2022). Recent studies showed that resolving convection explicitly may impact the estimate of the global climate of terrestrial tidally locked exoplanets (Sergeev et al. 2020; Lefèvre et al. 2021; Yang et al. 2023), because of the cloud stabilizing feedback (Yang et al. 2013). However, global convection-resolving simulations are computationally challenging, especially for climate-scale runs.

Locally refined global grids offer an elegant solution. They allow one to focus on a specific area of the planet, while keeping the global coverage and allowing for interactions at different scales, e.g. between localized convection and planetary-scale water distribution. Additionally, locally refined grids avoid numerical artifacts associated with using limited-area, or regional, models (Fox-Rabinovitz et al. 2008; Uchida et al. 2016). Namely, there are no boundaries or sharp changes in resolutions between the high-resolution region and the global model. These grids also allow for the two-way interaction between the region of interest and the rest of the planet, unlike a typical regional setup as in e.g.

Modeling the Progenitor Stars of Observed IIP Supernovae

KAI-AN YOU (游凱安)^{1,2}, KE-JUNG CHEN (陳科榮)², YEN-CHEN PAN (潘彥丞)³, SUNG-HAN TSAI (蔡松翰)^{2,4} AND PO-SHENG OU (歐柏昇)^{2,4}

¹*Department of Electrical Engineering, National Tsing Hua University, No. 101, Sec. 2, Guangfu Rd., Hsinchu 30013, Taiwan*

²*Institute of Astronomy and Astrophysics, Academia Sinica, No.1, Sec. 4, Roosevelt Rd., Taipei 10617, Taiwan*

³*Graduate Institute of Astronomy, National Central University, No.300, Zhongda Rd., Taoyuan 320317, Taiwan*

⁴*Department of Physics, National Taiwan University, No.1, Sec. 4, Roosevelt Rd., Taipei 10617, Taiwan*

ABSTRACT

The luminosity of Type IIP supernovae (SNe IIP) primarily arises from the recombination of hydrogen ionized by the explosion shock and the radioactive decay of ⁵⁶Co. However, the physical connections between SNe IIP and their progenitor stars remain unclear. This paper presents a comprehensive grid of stellar evolution models and their corresponding supernova light curves (LCs) to investigate the physical properties of observed SNe IIP. The study employs the one-dimensional stellar evolution code, MESA. Our models consider the effects of stellar metallicity, mass, and rotation in the evolution of massive stars, as well as explosion energy and ⁵⁶Ni production in modeling supernovae. To elucidate the observed LCs of SNe IIP and to probe their progenitor stars, we fit the observed SNe IIP with our multi-color LCs and discuss their physical origins. Furthermore, we investigate the impact of stellar parameters on LCs. Factors such as the progenitor star's mass, rotation, metallicity, explosion energy, and ⁵⁶Ni production influence the light curve's shape and duration. We find that higher-mass stars exhibit longer plateaus due to increased photon diffusion time caused by massive ejecta, impacting the duration of the light curve. Rapid rotation affects internal stellar structures, enhancing convective mixing and mass loss, potentially affecting the plateau's brightness and duration. Higher metallicity leads to increased opacity, altering energy transport and luminosity. Higher explosion energy results in brighter but shorter plateaus due to faster ejecta. ⁵⁶Ni production affects late-time luminosity and plateau duration, with larger masses leading to slower declines.

Keywords: Stellar Evolution, Massive Stars, Supernovae, Shock Wave, Time Domain Astronomy

1. INTRODUCTION

A core-collapse supernova (CCSN) is a dramatic event that occurs when a massive star approaches the end of its life cycle (Woosley & Janka 2005; Fryer & New 2011). During the phase of CCSN, an immense amount of radiation is emitted, temporarily outshining the entire galaxy and dispersing newly formed heavy elements into the surrounding interstellar medium. This process plays a crucial role in the evolution of the cosmos. CCSNe are classified into various types based on their light curves (LCs) and spectral features (Filippenko 1997). For instance, Type II SNe, which result from the death of massive stars, are characterized by the presence of hydrogen lines in their spectra. Subtypes within Type II SNe are further defined by their LC shapes, such as Type IIP (plateau) and Type IIL (linear) (Valenti et al. 2016). However, observational studies of well-observed SNe IIP, particularly those with identified progenitor stars, are rare. By carefully examining pre-explosion images from archival data, we can potentially identify the progenitor star of observed SNe and gain insights into the demise of massive stars (Smartt 2009).

Previous studies have primarily focused on analyzing various LCs and spectra of SN, using methods like the expanding photosphere (EPM) and standard candle method (SCM) to determine distances and other physical parameters (Leonard et al. 2002). These studies have commonly identified the SN types (e.g., Type IIP events), estimated explosion dates, and assessed progenitor characteristics such as stellar mass and age. They have provided insights into the stellar evolution leading to SN explosions, contributing to our understanding of the physical processes involved in these events and refining the technique of cosmological

Fast neutrino flavor conversions in a supernova: emergence, evolution, and effects

Zewei Xiong^{1,*}, Meng-Ru Wu^{2,3,4}, Manu George², Chun-Yu Lin⁵, Noshad Khosravi Largani⁶, Tobias Fischer⁶, and Gabriel Martínez-Pinedo^{1,7}

¹*GSI Helmholtzzentrum für Schwerionenforschung, Planckstraße 1, 64291 Darmstadt, Germany*

²*Institute of Physics, Academia Sinica, Taipei 11529, Taiwan*

³*Institute of Astronomy and Astrophysics, Academia Sinica, Taipei 10617, Taiwan*

⁴*Physics Division, National Center for Theoretical Sciences, Taipei 10617, Taiwan*

⁵*National Center for High-performance Computing, Hsinchu 30076, Taiwan*

⁶*Institute of Theoretical Physics, University of Wrocław, Pl. M. Borna 9, 50-204 Wrocław, Poland*

⁷*Institut für Kernphysik (Theoriezentrum), Fachbereich Physik,*

Technische Universität Darmstadt, Schlossgartenstraße 2, 64289 Darmstadt, Germany

(Dated: March 1, 2024)

Fast flavor conversions (FFCs) of neutrinos, which can occur in core-collapse supernovae (CCSNe), are multiangle effects. They depend on the angular distribution of the neutrino's electron lepton number (ELN). In this work, we present a comprehensive study of the FFCs by solving the multi-energy and multiangle quantum kinetic equations with an extended set of collisional weak processes based on a static and spherically symmetric CCSN matter background profile. We investigate the emergence and evolution of FFCs in models featuring different ELN angular distributions, considering scenarios with two and three neutrino flavors. The spectrogram method is utilized to illustrate the small-scale spatial structure, and we show that this structure of neutrino flavor coherence and number densities in the nonlinear regime is qualitatively consistent with the dispersion relation analysis. On the coarse-grained level, we find that different asymptotic states can be achieved following the FFCs depending on the locations and shapes of the ELN distributions, despite sharing a common feature of the elimination of the ELN angular crossing. While equilibration among different neutrino flavors may be achieved immediately after the prompt FFCs, it is not a general outcome of the asymptotic state, as subsequent feedback effects from collisional neutrino-matter interactions come into play, particularly for cases where FFCs occur inside the neutrinosphere. The impacts of FFCs and the feedback effect on the net neutrino heating rates, the equilibrium electron fraction of CCSN matter, and the free-streaming neutrino energy spectra are quantitatively assessed. Other aspects including the impact of the vacuum term and the coexistence with other type of flavor instabilities are also discussed.

I. INTRODUCTION

Core-collapse supernovae (CCSNe) are cataclysmic events when massive stars reach the end of their lives. During the evolution of a CCSN, a nascent proto-neutron star (PNS) forms at the center as a prolific source of neutrinos. These neutrinos play pivotal roles on the CCSN dynamics and the evolution of chemical composition. They interact with the medium through both charged- and neutral-current weak interactions in the proximity of the PNS and deposit energy, facilitating the shock revival via reheating of material in the post-shocked layer and leading to the eventual mass ejection. Particularly, the charged-current interactions determine the proton-to-baryon ratio, denoted by the electron fraction Y_e , which is a crucial quantity for the nucleosynthesis results of CCSN explosions. A better knowledge of the flux intensities and flavor content of neutrinos is necessary to robustly model the inner dynamics of CCSNe, to predict the elemental compositions in CCSN ejecta, and to determine the neutrino signals for the detection of the next galactic supernova event (see e.g., Refs. [1, 2] for recent reviews).

The flavor oscillations of neutrinos among ν_e , ν_μ , and ν_τ in vacuum and in medium have been well studied and confirmed by various ground-based neutrino experiments [3]. When neutrino fluxes are sufficiently high in CCSNe, the forward scattering among neutrinos themselves leads to various collective phenomena of flavor instability. Particularly the fast flavor conversion (FFC) associated with the fast flavor instability (FFI; see e.g., Refs. [4–7] for reviews) attracts great interest in recent years owing to the vastly rapid conversion rate within nanoseconds and over a distance shorter than a coin. Studies based on results from the multi-dimensional CCSN simulations have shown a general occurrence of FFIs in certain regions ahead of the shock wave, near the neutrinosphere, or even deep inside the PNS [8–17].

Since the first proposal of FFI in Ref. [18], the advance of both theory and methodology throughout the past decade has improved our understanding of FFCs and guided the line of research toward the ultimate goal of implementing neutrino oscillations in CCSNe. A generic framework governing the coherent flavor evolution and collisional neutrino-matter interactions is prescribed by the neutrino quantum kinetic equation (ν QKE) [19–22]. The linear stability analysis (LSA) of the ν QKE provides a powerful tool to diagnose the existence of flavor instabilities [23–26]. It has been proved based on the

* Email: z.xiong@gsi.de

Bosonic Dark Matter Dynamics in Hybrid Neutron Stars

Zakary Buras-Stubbs^{id} and Ilídio Lopes^{id}
*Centro de Astrofísica e Gravitação - CENTRA,
Departamento de Física,
Instituto Superior Técnico - IST,
Universidade de Lisboa - UL,
Av. Rovisco Pais 1, 1049-001 Lisboa, Portugal**

This research studies the intricate interplay between dark and baryonic matter within hybrid neutron stars enriched by anisotropic bosonic dark matter halos. Our modelling, guided by the equation of state with a free parameter, reveals diverse mass-radius correlations for these astronomical objects. A pivotal result is the influence of dark matter characteristics—whether condensed or dispersed—on the observable attributes of neutron stars based on their masses. Our investigation into anisotropic models, which offer a notably authentic representation of dark matter anisotropy, reveals a unique low-density core halo profile, distinguishing it from alternative approaches. Insights gleaned from galactic clusters have further refined our understanding of the bosonic dark matter paradigm. Observational constraints derived from the dynamics of galaxy clusters have been fundamental in defining the dark matter particle mass to lie between 0.05 GeV and 0.5 GeV and the scattering length to range from 0.9 fm to 3 fm. Using terrestrial Bose-Einstein condensate experiments, we have narrowed down the properties of bosonic dark matter, especially in the often overlooked 3 to 30 GeV mass range. Our findings fortify the understanding of dark and baryonic matter synergies in hybrid neutron stars, establishing a robust foundation for future astrophysical pursuits.

I. INTRODUCTION

Dark matter, one of the most intriguing and mysterious phenomena in astrophysics, remains a subject of ongoing investigation [e.g., 1, 2]. This invisible form of matter, which does not emit, absorb, or reflect electromagnetic radiation, accounts for roughly 27% of the Universe’s total mass-energy content [e.g., 3]. The presence of dark matter has been deduced from its gravitational influence on galaxy movements, the vast cosmic structures, and the cosmic microwave background radiation [e.g., 4].

It is widely accepted that dark matter cannot be composed of fundamental particles within the Standard Model of particle physics, and it is more likely that dark matter is made up of particles that have not yet been discovered. Various hypothetical particle candidates have been proposed as potential solutions to the dark matter problem, and these particles can generally be classified into several categories based on their mass [5–8]. These categories include fuzzy dark matter or axion-like particles, axions, sterile neutrinos, and weakly interacting massive particles (WIMPs).

Our focus in this work is to investigate how the structure of neutron stars can be affected by dark matter particles within the WIMPs and axion mass ranges. In particular, we will be focusing on particles in the $10^{-2} - 10^2$ GeV range.

There are several papers in the literature that discuss the relationship between dark matter and neutron stars.

Some recent examples include [9, 10], which focus on general self-annihilating WIMP models; [11–21], which focus on specific fermionic dark matter models; [22, 23], that consider Bose-Einstein Condensate (BEC) dark matter; and [24] where both fermionic and BEC models are studied. These papers explore the possible effects of dark matter on neutron star properties and the potential for dark matter detection through observations of neutron stars. Additionally, there are several reviews that provide a more comprehensive overview of the field, such as Lattimer [25] and Del Popolo et al. [26].

Anisotropic matter exhibits different properties or behaviours depending on the direction [for a review see 27, 28]. Such behaviour can lead to pressure differences in various directions within neutron stars or other astronomical objects [e.g., 29–31]. This characteristic influences how matter interacts with surrounding objects, affecting their formation, structure, and evolution, shaping our understanding of dark matter. For instance, dark matter clouds are expected to exhibit local anisotropy, similar to any collisionless system of particles. Researchers have extensively studied these systems, especially in the context of galaxy dynamics [e.g., 32–34].

The theory of anisotropic fluids in General Relativity is well-established. Past research has demonstrated that anisotropic fluids could be geodesic in general relativity [35]. A comprehensive study of spherically symmetric dissipative anisotropic fluids has been presented, and exact static spherically symmetric anisotropic solutions of field equations have been obtained and analyzed by Herrera et al. [36], Bayin [37], and Herrera et al. [38]. Furthermore, calculations of anisotropic stars in general relativity and their mass-radius relations have been conducted Mak and Harko [39]. A detailed collection of

* zburasstubbs@tecnico.ulisboa.pt

Distribution Properties of the 6.7 GHz Methanol Masers and Their Surrounding Gases in the Milky Way

TIAN YANG,¹ XI CHEN,^{1,2} YAN-KUN ZHANG,¹ XU-JIA OUYANG,³ SHI-MIN SONG,¹ JIA-LIANG CHEN,¹ AND YING LU¹

¹*Center for Astrophysics, Guangzhou University, Guangzhou 510006, People's Republic of China*

²*Shanghai Astronomical Observatory, Chinese Academy of Sciences, 80 Nandan Road, Shanghai 200030, People's Republic of China*

³*School of Physics and Astronomy, Sun Yat-sen University, 2 Daxue Road, Tangjia, Zhuhai, Guangdong Province, People's Republic of China*

(Received March 1, 2024; Revised March 1, 2024; Accepted March 1, 2024)

Submitted to ApJS

ABSTRACT

An updated catalog consisting of 1092 6.7-GHz methanol maser sources was reported in this work. Additionally, the NH₃ (1, 1), NH₃ (2, 2), and NH₃ (3, 3) transitions were observed towards 214 star forming regions using the Shanghai Tianma radio telescope (TMRT) in order to examine the differences in physical environments, such as excitation temperature and column density of molecular clouds associated with methanol masers on the Galactic scale. Statistical results reveal that the number of 6.7 GHz methanol masers in the Perseus arm is significantly lower than that in the other three main spiral arms. In addition, the Perseus arm also has the lowest gas column density among the main spiral arms traced by the NH₃ observations. Both of these findings suggest that the Perseus arm has the lowest rate of high-mass star formation compared to the other three main spiral arms. We also observed a trend in which both the luminosity of 6.7 GHz methanol masers and the ammonia gas column density decreased as the galactocentric distances. This finding indicates that the density of material in the inner Milky Way is generally higher than that in the outer Milky Way. It further suggests that high-mass stars are more easily formed at the head of spiral arms. Furthermore, we found that the column density of ammonia gas is higher in the regions on the arms than that in the inter-arm regions, supporting that the former is more likely to be the birthplace of high-mass stars.

1. INTRODUCTION

Star formation is a fundamental and important issue in modern astronomy, closely linked to the origin and evolution of cosmic objects at all scales. In particular, the formation of high-mass stars ($M > 8 M_{\odot}$) plays a crucial role in the structure and evolution of galaxies. However, research on high-mass star formation is limited by the scarcity of observable samples of high-mass young stellar objects (HMYSOs) and their short evolutionary timescale. Furthermore, the far distance of these objects and the optical obscuration caused by molecular clouds severely hinder observations (Zinnecker & Yorke 2007; Motte et al. 2018). Despite these challenges, high-mass star forming regions (HMSFRs) can still be investigated through various observational tracers, such as interstellar molecules and masers. In particular, interstellar masers, with their extremely high spectral intensity, serve as important probes in investigating HMSFRs (Reid & Moran 1981).

Methanol masers are frequently observed toward HMSFRs within the Milky Way in radio band. They are classified into two types based on their associations with various star formation phenomena. Class I methanol masers, such as the 36.2 and 95.2 GHz methanol masers, are pumped by collisions in shock or outflow regions (Chen et al. 2011, 2013a; Leurini et al. 2016). On the contrary, Class II methanol masers which include the 6.7 and 12.2 GHz ones, are typically observed in close proximity to the HMSFRs and are pumped by infrared radiation from the HMSFRs (Cragg et al. 2005).

VLBI observations of the high-redshift X-ray bright blazar SRGE J170245.3+130104

Yuanqi Liu¹, Tao An^{1,2,3,*}, Shaoguang Guo^{1,2,3}, Yingkang Zhang^{1,3}, Ailing Wang^{1,2}, Zhijun Xu¹, Georgii Khorunzhev⁴, Yulia Sotnikova⁵, Timur Mufakharov^{5,6}, Alexander Mikhailov⁵, and Marat Mingaliev^{5,6,7}

¹ Shanghai Astronomical Observatory, Key Laboratory of Radio Astronomy, CAS, 80 Nandan Road, Shanghai 200030, China

² School of Astronomy and Space Sciences, University of Chinese Academy of Sciences, No. 19A Yuquan Road, Beijing 100049, China

³ Key Laboratory of Radio Astronomy and Technology, Chinese Academy of Sciences, A20 Datun Road, Beijing, 100101, P. R. China

⁴ Space Research Institute of RAS, Profsoyusnaya street, 84/32, 117997, Russia

⁵ Special Astrophysical Observatory of RAS, Nizhny Arkhyz, 369167, Russia

⁶ Kazan Federal University, 18 Kremlyovskaya St, Kazan 420008, Russia

⁷ Institute of Applied Astronomy RAS, St. Petersburg 191187, Russia

Received 30/01/2024; accepted 26/02/2024

ABSTRACT

Aims. The X-ray luminous and radio-loud AGN SRGE J170245.3+130104 discovered at $z \sim 5.5$ provides unique chances to probe the SMBH growth and evolution with powerful jets in the early Universe.

Methods. We present 1.35 – 5.1 GHz Very Long Baseline Array (VLBA) results on the radio continuum emission and spectrum analysis for this quasar in a low flux density state.

Results. This source is unresolved at three frequencies with the total flux densities of 8.35 ± 0.09 mJy beam⁻¹, 7.47 ± 0.08 mJy beam⁻¹, and 6.57 ± 0.02 mJy beam⁻¹ at 1.73 GHz, 2.26 GHz, and 4.87 GHz, respectively. Meanwhile, the brightness temperature is higher than 10^9 K.

Conclusions. Compared with previous radio observations with arcsec-scale resolution, nearly all the radio emission from this source concentrates in the very central milli-arcsecond (mas) scale area. We confirm this source is a bright blazar at $z > 5$. This young AGN provide us the great chances to understand the first generation of strong jets in the early Universe.

Key words. radio continuum emission – early Universe – Quasars

Use \titlerunning to supply a shorter title and/or \authorrunning to supply a shorter list of authors.

1. Introduction

The study of high-redshift active galactic nuclei (AGNs) plays a crucial role in advancing our understanding of the early Universe, particularly in exploring the formation and evolution of supermassive black holes (SMBHs). These distant AGNs provide a unique window into the nascent stages of SMBHs, shedding light on their accretion processes and immediate environment. Such studies are crucial for understanding the mechanisms that drive the early growth of these cosmic monsters.

Currently, around 600 AGNs have been discovered at redshift higher than 5 (for example, Fan et al. 2006; Willott et al. 2010; Yang et al. 2017, 2023), which is close to the end of cosmic reionization. These discoveries are essential for understanding this crucial moment in the evolution of the Universe.

Blazars are a subclass of AGN with jets aligned close to the line of sight, whose emission is relativistic beamed and Doppler boosted, providing favorable conditions for observing high-redshift AGN. Observations of jet emission from high- z blazars enable tests of relativistic jet models and physical properties (such as jet viewing angle and Lorentz factor) under extreme conditions in the early Universe and constraints on jet power and particle acceleration. Statistical studies of the number density, distribution, and evolution of blazars can yield insights into the co-evolution of black holes and galaxies in the early Universe. To date, PSO J030947.49+271757.31 at $z \sim 6.1$ (hereafter J0309+2717) is the highest redshift blazar discovered (Belladitta et al. 2020). Since very few blazars have been observed at $z > 5$, discovering and studying more high- z ($z > 5$) blazars is extremely valuable for enriching our understanding of high-redshift AGN.

* antao@shao.ac.cn

The effect of nonlocal disk processes on the volatile CHNOS budgets of planetesimal-forming material

M. Oosterloo¹, I. Kamp¹, and W. van Westrenen²

¹ Kapteyn Astronomical Institute, University of Groningen, Landleven 12, 9747 AD Groningen, The Netherlands

² Department of Earth Sciences, Vrije Universiteit Amsterdam, De Boelelaan 1085, 1081 HV Amsterdam, The Netherlands

Received: 19 December 2023; accepted: 26 February 2024

ABSTRACT

Context. The bulk abundances of CHNOS-bearing species of a planet have a profound effect on its interior structure and evolution. Therefore, it is key to investigate the behavior of the local abundances of these elements in the solid phase in the earliest stages of planet formation, where micrometer-sized dust grows into larger and larger aggregates. However, the physical and chemical processes occurring in planet-forming disks that shape these abundances are highly coupled and nonlocal.

Aims. We aim to quantify the effects of the interplay between dynamical processes (turbulent diffusion, dust settling and radial drift), collision processes (coagulation and fragmentation), and the adsorption and desorption of ices on the abundances of CHNOS in local disk solids as a function of position throughout the planet-forming region.

Methods. We used SHAMPOO (Stochastic Monomer Processor), which tracks the ice budgets of CHNOS-bearing molecules of a dust monomer as it undergoes nonlocal disk processing in a Class I disk. We used a large set of individual monomer evolutionary trajectories to make inferences about the properties of the local dust populations via a stochastic analysis of 64 000 monomers on a preexisting spatial grid.

Results. We find that spatially, monomers can travel larger distances farther out in the disk, leading to a larger spread in positions of origin for a dust population at, for example, $r = 50$ AU compared to $r = 2$ AU. However, chemically, the inner disk ($r \lesssim 10$ AU) is more nonlocal due to the closer spacing of ice lines in this disk region. Although to zeroth order the bulk ice mantle composition of icy dust grains remains similar compared to a fully local dust population, the ice mass associated with individual chemical species can change significantly. The largest differences with local dust populations were found near ice lines where the collisional timescale is comparable to the adsorption and desorption timescales. Here, aggregates may become significantly depleted in ice as a consequence of microscopic collisional mixing, a previously unknown effect where monomers are stored away in aggregate interiors through rapid cycles of coagulation and fragmentation.

Conclusions. Nonlocal ice processing in a diffusion-dominated, massive, smooth disk has the most significant impact on the inner disk ($r \lesssim 10$ AU). Furthermore, microscopic collisional mixing can have a significant effect on the amounts of ice of individual species immediately behind their respective ice lines. This suggests that ice processing is highly coupled to collisional processing in this disk region, which implies that the interiors of dust aggregates must be considered and not just their surfaces.

1. Introduction





The chemical elements carbon (C), hydrogen (H), nitrogen (N), oxygen (O), and sulfur (S) are important elements for the chemical habitability of rocky planets (Krijt et al. 2022). For example, they are the fundamental building blocks of life itself, being the main constituents of many biologically relevant molecules (Baross et al. 2020; Sasselov et al. 2020). CHNOS-bearing molecules can also affect the physical habitability of planets (e.g. Krijt et al. 2022). For example, the amount of CHNOS bearing molecules (such as CO₂, H₂O, and N₂) present in the planetary atmosphere plays a key role in determining the width of the circumstellar habitable zone where liquid water can exist on the planetary surface (Kasting et al. 1993; Kasting & Catling 2003; Kopparapu et al. 2013). The structure and evolution of the planetary interior are also strongly affected by the planetary budgets of CHNOS. Here, CHNOS abundances have important effects on the size and structure of the planetary core (e.g., Trønnes et al. 2019; Johansen et al. 2023), the physical structure and mineralogy of their mantles (e.g., Kushihiro 1969; Dasgupta & Hirschmann 2006; Hakim et al. 2019), and on the chemical composition of volcanic outgassing (Bower et al. 2022), which in turn has significant effects on the long-term evolution of the atmospheric composition (e.g., Tosi et al. 2017; Oosterloo et al.

2021).

Altogether, it is thus key to identify how much CHNOS a nascent planet receives from its host planet-forming disk. At the onset of planet formation, most solid material exists as millimeter- to centimeter-sized dust. These dust grains are subject to transport processes as a consequence of their interaction with the surrounding gas (e.g., Armitage 2010). For small grains (i.e. grains with a Stokes number $St \ll 1$) transport primarily occurs through turbulent diffusion, whereas the dynamical behavior of grains with a large Stokes number is dominated by aerodynamic drag, resulting in dust settling and radial drift (e.g., Weidenschilling 1977; Armitage 2010). This dynamical transport has been shown to allow individual dust grains to be exposed to a wide range of local physical conditions in protoplanetary disks (Ciesla 2010, 2011).

In colder disk regions, a considerable fraction of the solid-phase CHNOS mass budget in this first stages of planet formation may be incorporated as ices, with H₂O, CO, CO₂, CH₄, NH₃, H₂S, OCS, and SO₂ being major carrier molecules (Boogert et al. 2015; Krijt et al. 2020; Öberg & Bergin 2021). In addition, for carbon and oxygen, up to 50% of the total elemental mass budget can be locked away in more refractory solid material such as amorphous carbon (graphite) and silicates, respectively (Mishra & Li 2015; Öberg & Bergin 2021). Large amounts of nitrogen

BAYESIAN DISTANCES FOR QUANTIFYING TENSIONS IN COSMOLOGICAL INFERENCE AND THE SURPRISE STATISTIC

BENEDIKT SCHOSSER ^{1,*}, PEDRO RIBA MELLO ², MIGUEL QUARTIN ^{2,3,4}, AND BJÖRN MALTE SCHÄFER ^{1,‡}¹Zentrum für Astronomie der Universität Heidelberg, Astronomisches Rechen-Institut, Philosophenweg 12, 69120 Heidelberg, Germany²Instituto de Física, Universidade Federal do Rio de Janeiro, 21941-972, Rio de Janeiro, RJ, Brazil³Observatório do Valongo, Universidade Federal do Rio de Janeiro, 20080-090, Rio de Janeiro, RJ, Brazil and⁴PPGCosmo, Universidade Federal do Espírito Santo, 29075-910, Vitória, ES, Brazil

Version March 1, 2024

ABSTRACT

Tensions between cosmological parameters derived through different channels can be a genuine signature of new physics that Λ CDM as the standard model is not able to reproduce, in particular in the missing consistency between parameter estimates from measurements the early and late Universe. Or, they could be caused by yet to be understood systematics in the measurements as a more mundane explanation. Commonly, cosmological tensions are stated in terms of mismatches of the posterior parameter distributions, often assuming Gaussian statistics. More importantly, though, would be a quantification if two data sets are consistent to each other before combining them into a joint measurement, ideally isolating hints at individual data points that have a strong influence in generating the tension. For this purpose, we start with statistical divergences applied to posterior distributions following from different data sets and develop the theory of a Fisher metric between two data sets, in analogy to the Fisher metric for different parameter choices. As a topical example, we consider the tension in the Hubble-Lemaître constant H_0 from supernova and measurements of the cosmic microwave background, derive a ranking of data points in order of their influence on the tension on H_0 . For this particular example, we compute Bayesian distance measures and show that in the light of CMB data, supernovae are commonly too bright, whereas the low- ℓ CMB spectrum is too high, in agreement with intuition about the parameter sensitivity.

Keywords: Bayesian inference, tensions in cosmology, Fisher-formalism, supernova distance-redshift relation, cosmic microwave background

1. INTRODUCTION

The Bayes' theorem as the central tool of statistical inference, describes the process of updating the knowledge on the model parameters θ^μ given a data set y^i within a preselected model (for summaries and applications to cosmology, see [Fisher 1935](#); [Caticha & Giffin 2006](#); [Trotta 2017](#); [Loredo 2012](#)),

$$p(\theta|y) = \frac{\mathcal{L}(y|\theta)\pi(\theta)}{p(y)}, \quad (1)$$

by setting the posterior distribution $p(\theta|y)$ into relation with the likelihood $\mathcal{L}(y|\theta)$. The normalisation is given by the Bayes-evidence $p(y)$

$$p(y) = \int d^n\theta \mathcal{L}(y|\theta)\pi(\theta), \quad (2)$$

where the prior distribution $\pi(\theta)$ encapsulates the knowledge on the parameters θ^μ before the data set y^i has been recorded. The likelihood $\mathcal{L}(y|\theta)$ as a conditional probability describes the distribution of data points y that can be expected under a particular parameter choice θ and contains the knowledge of the physical model and the error process in the measurement. As two parameter choices θ and $\theta' = \theta + d\theta$ will differ in their prediction of the data distribution it makes sense to quantify this difference in terms of e.g. the Kullback-Leibler divergence $\Delta S(\theta, \theta + d\theta)$ ([Kullback & Leibler 1951](#); [Rényi 1960](#)),

$$s(\theta, \theta + d\theta) = \int dy \mathcal{L}(y|\theta) \ln \frac{\mathcal{L}(y|\theta)}{\mathcal{L}(y|\theta + d\theta)} \simeq \frac{1}{2} F_{\mu\nu}(\theta) d\theta^\mu d\theta^\nu, \quad (3)$$

which can be expanded with a quadratic, leading-order term, defining the Fisher metric $F_{\mu\nu}(\theta)$ ([Tegmark et al. 1997](#); [Elsner & Wandelt 2012](#); [Coe 2009](#); [Bassett et al. 2011](#); [Wolz et al. 2012](#); [Schäfer & Reischke 2016](#); [Sellentin et al. 2014](#)) as a positive

* schosser@stud.uni-heidelberg.de‡ bjoern.malte.schaefer@uni-heidelberg.de

The Reservoir of the Per-emb-2 Streamer

KOTOMI TANIGUCHI,¹ JAIME E PINEDA,² PAOLA CASELLI,² TOMOMI SHIMOIKURA,³ RACHEL K. FRIESEN,⁴
DOMINIQUE M. SEGURA-COX,^{5,2,*} AND ANIKA SCHMIEDEKE⁶

¹National Astronomical Observatory of Japan, National Institutes of Natural Sciences, 2-21-1 Osawa, Mitaka, Tokyo 181-8588, Japan

²Center for Astrochemical Studies, Max-Planck-Institut für Extraterrestrische Physik, Gießenbachstrasse 1, D-85741 Garching bei München, Germany

³Faculty of Social Information Studies, Otsuma Women's University, Sanban-cho, Chiyoda, Tokyo 102-8357, Japan

⁴Department of Astronomy & Astrophysics, University of Toronto, 50 St. George St., Toronto, ON, M5S 3H4, Canada

⁵Department of Astronomy, The University of Texas at Austin, 2500 Speedway, Austin, TX 78712, USA

⁶Green Bank Observatory, PO Box 2, Green Bank, WV 24944, USA

ABSTRACT

Streamers bring gas from outer regions to protostellar systems and could change the chemical composition around protostars and protoplanetary disks. We have carried out mapping observations of carbon-chain species (HC₃N, HC₅N, CCH, and CCS) in the 3mm and 7mm bands toward the streamer flowing to the Class 0 young stellar object (YSO) Per-emb-2 with the Nobeyama 45m radio telescope. A region with a diameter of ~ 0.04 pc is located north with a distance of $\sim 20,500$ au from the YSO. The streamer connects to this north region which is the origin of the streamer. The reservoir has high density and low temperature ($n_{\text{H}_2} \approx 1.9 \times 10^4 \text{ cm}^{-3}$, $T_{\text{kin}} = 10$ K), which are similar to those of early stage starless cores. By comparisons with the observed abundance ratios of CCS/HC₃N to the chemical simulations, the reservoir and streamer are found to be chemically young. The total mass available for the streamer is derived to be $24 - 34 M_{\odot}$. If all of the gas in the reservoir will accrete onto the Per-emb-2 protostellar system, the lifetime of the streamer has been estimated at $(1.1 - 3.2) \times 10^5$ yr, suggesting that the mass accretion via the streamer would continue until the end of the Class I stage.

Keywords: Astrochemistry (75) — Low mass stars (2050) — Star formation (1569) — Young stellar objects (1834)

1. INTRODUCTION

Streamers, velocity coherent structures funneling material around young stellar objects (YSOs), bring gas from outer regions to the disk forming regions (for a review see [Pineda et al. 2023](#)). The outer gas would have different chemical compositions from the gas close to YSOs and then these streamers could change the chemical composition at the protoplanetary disks and/or the protostellar cores. Their kinematic structures are composed of a smooth velocity gradient driven by gravity and rotation. Streamers may play essential roles during the formation of the solar system ([Arzoumanian et al.](#)

[2023](#)). Thus, it is important to reveal the physics and chemistry of these streamer structures to understand the star and planet formation including our solar system.

Many observations with interferometers have revealed the presence of streamers toward various evolutionary stage YSOs; highly embedded Class 0 phase ([Le Gouellec et al. 2019](#); [Pineda et al. 2020](#)), Class I stage ([Chou et al. 2016](#); [Valdivia-Mena et al. 2022](#)), and Class II stage ([Ginski et al. 2021](#); [Garufi et al. 2022](#)). Similar infall gas structures feeding circumbinary disks around binary systems have also been found ([Takakuwa et al. 2017](#); [Alves et al. 2019](#)). In addition, triple spiral arms connected to a triple protostellar system IRAS 042329+2436 have been found using the SO emission as seen by the Atacama Large Millimeter/submillimeter Array (ALMA, [Lee et al. 2023](#)). They compared the observational results with numerical simulations and suggested that the large triple spiral arms are produced by gravitational

Corresponding author: Kotomi Taniguchi
kotomi.taniguchi@nao.ac.jp

* NSF Astronomy and Astrophysics Postdoctoral Fellow

AB Dor: Coronal imaging and activity cycles

GURPREET SINGH^{1,2} AND J. C. PANDEY¹

¹*Aryabhata Research Institute of Observational Sciences (ARIES), Manora Peak, Nainital 263001, India*

²*Department of Physics, Deen Dayal Upadhyaya Gorakhpur University, Gorakhpur 273009, India*

ABSTRACT

Using long-term X-ray observations, we present the short-term and long-term X-ray variability analysis of the ultra-fast rotating active star AB Dor. Flaring events are common in X-ray observations of AB Dor and occupy a substantial portion of the total observation time, averaging around $57\pm 23\%$. The flare-free X-ray light curves show rotational modulation, indicating the presence of highly active regions in its corona. We have developed a light curve inversion code to image the corona of active fast rotating stars. The results of coronal imaging reveal the presence of two active regions of different brightness that are separated by $\sim 180^\circ$ in longitude. These active regions are also found to migrate along the longitude and also show variation in their brightness. Our analysis of long-term X-ray data spanning from 1979 to 2022 shows multiple periodicities. The existence of a ~ 19.2 yr cycle and its first harmonic indicates the presence of a Solar-like, long-term pattern. In comparison, the periodicities of ~ 3.6 and ~ 5.4 yr are possibly due to the presence of a flip-flop cycle in X-rays, which is also supported by similar periods findings from the optical data in the earlier studies. Further confirmation of the existence of the X-ray flip-flop cycle requires long-term observations at regular intervals in the quiescent state.

Keywords: Stellar activity (1580) — Stellar Coronae (305) — X-ray star (1823) — X-ray astronomy (1810) — Stellar imaging (1145)

1. INTRODUCTION

The variable nature of light curves of late-type active stars can be observed over the entire electromagnetic spectrum with a variability time scale ranging from a few minutes to a few decades. Both short-term variability (STV) and long-term variability (LTV) are found to be present in solar-type stars and are due to the different manifestations of magnetic activities. The STVs last a few minutes to a few days and are generally attributed to flaring activity and rotational modulation due to inhomogeneities. The LTVs last from a few yr to a few decades and are linked to the stellar activity cycles.

The STVs due to flares in X-rays have been studied and modelled in the past for a long and helped to understand the extreme physical condition of solar-type stars (e.g. Haisch et al. 1991; Reale 2007; Pandey & Singh 2008, 2012). Stellar coronae are spatially unresolved; therefore, different techniques have been developed to

extract information from the periodic STVs due to the rotational modulations of active regions in the stellar atmosphere. Doppler imaging (Brickhouse et al. 2001), extrapolating the surface magnetic maps (Hussain et al. 2007; Johnstone et al. 2010; Cohen et al. 2010, etc), and light curve inversion techniques (Siarkowski 1992; Siarkowski et al. 1996; Drake et al. 2014; Singh & Pandey 2022) are main techniques to explain such type of STVs in X-rays. These techniques have their own limitations. Doppler imaging of X-ray data requires high spectral resolution, which is inadequate for most of the stars due to instrumental and observing limitations. Inferring the coronal structures on the basis of magnetic surface maps requires simultaneous observations in optical and X-ray bands. The light-curve inversion techniques (LCITs) are a mathematically ill-posed problem where 3D information is extracted from 1D time series data. However, these techniques have gained interest with time due to the easy availability of time series data.

The study of LTVs is useful to understand the underlying dynamo mechanisms. The Sun is the only star for which the LTVs are studied in detail, and theoret-

<https://doi.org/10.15407/knit2023.06.068>

UDC 524.8

D. V. DOBRYCHEVA¹, Senior Researcher, PhD (Phys. & Math.)

M. YU. VASYLENKO¹, Junior Researcher, PhD student

I. V. KULYK¹, Senior Researcher, PhD (Phys. & Math.)

YA. V. PAVLENKO¹, Head of the Department, Doctor of Sciences

O. S. SHUBINA², Researcher at the Laboratory, PhD (Phys. & Math.)

I. V. LUK'YANYK³, Head of Department, PhD (Phys. & Math.)

P. P. KORSUN¹, Head of the Laboratory, Doctor of Sciences

¹ Main Astronomical Observatory of the National Academy of Sciences of Ukraine
27, Akademika Zabolotnoho Str., Kyiv, 03143 Ukraine

² Astronomical Institute of Slovak Academy of Sciences
Tatranská Lomnica, 059 60 Vysoké Tatry, Slovak Republic

³ Astronomical Observatory of Taras Shevchenko National University of Kyiv
3, Observatorna Str., Kyiv, 04053 Ukraine

This study introduces an approach to detecting exocomet transits in the dataset of the Transiting Exoplanet Survey Satellite (TESS), specifically within its Sector 1. Given the limited number of exocomet transits detected in the observed light curves, creating a sufficient training sample for the machine learning method was challenging. We developed a unique training sample by encapsulating simulated asymmetric transit profiles into observed light curves, thereby creating realistic data for the model training. To analyze these light curves, we employed the TSFresh software, which was a tool for extracting key features that were then used to refine our Random Forest model training.

Considering that cometary transits typically exhibit a small depth, less than 1 % of the star's brightness, we chose to limit our sample to the CDPP parameter. Our study focused on two target samples: light curves with a CDPP of less than 40 ppm and light curves with a CDPP of up to 150 ppm. Each sample was accompanied by a corresponding training set. This methodology achieved an accuracy of approximately 96 %, with both precision and recall rates exceeding 95 % and a balanced F1-score of around 96 %. This level of accuracy was effective in distinguishing between 'exocomet candidate' and 'non-candidate' classifications for light curves with a CDPP of less than 40 ppm, and our model identified 12 potential exocomet candidates. However, when applying machine learning to less accurate light curves (CDPP up to 150 ppm), we noticed a significant increase in curves that could not be confidently classified, but even in this case, our model identified 20 potential exocomet candidates.

These promising results within Sector 1 motivate us to extend our analysis across all TESS sectors to detect and study comet-like activity in the extrasolar planetary systems.

Keywords: comets, planetary systems, minor planets; eclipses, transits, planets and satellites.

Цитування: Dobrycheva D. V., Vasylenko M. Yu., Kulyk I. V., Pavlenko Ya. V., Shubina O. S., Luk'yanyk I. V., Korsun P. P. Hunting for exocomet transits in the TESS database using the Random Forest method. *Space Science and Technology*. 2023. **29**, № 6 (145). P. 68–79. <https://doi.org/10.15407/knit2023.06.068>

© Publisher PH «Akademiya» of the NAS of Ukraine, 2023. This is an open access article under the CC BY-NC-ND license (<https://creativecommons.org/licenses/by-nc-nd/4.0/>)

Multidimensional Radiation Hydrodynamics Simulations of Supernova 1987A Shock Breakout

WUN-YI CHEN,^{1,2} KE-JUNG CHEN,¹ AND MASAOMI ONO^{1,3}

¹*Institute of Astronomy and Astrophysics, Academia Sinica, Taipei 10617, Taiwan*

²*National Taiwan University, Graduate Institute of Astrophysics*

*Department of Physics/Center for Condensed Building R401, No.1, Sec. 4, Roosevelt Rd,
Taipei 10617, Taiwan*

³*Astrophysical Big Bang Laboratory (ABBL), RIKEN Cluster for Pioneering Research,
2-1 Hirosawa, Wako, Saitama 351-0198, Japan*

ABSTRACT

Shock breakout is the first electromagnetic signal from supernovae (SNe), which contains important information on the explosion energy and the size and chemical composition of the progenitor star. This paper presents the first two-dimensional (2D) multi-wavelength radiation hydrodynamics simulations of SN 1987A shock breakout by using the CASTRO code with the opacity table, OPAL, considering eight photon groups from infrared to X-ray. To investigate the impact of the pre-supernova environment of SN 1987A, we consider possible three cases of circumstellar medium (CSM) environments: only a steady wind; an eruptive mass loss; and the existence of a companion star. In sum, the resulting breakout light curve has an hour duration and its peak luminosity of $\sim 6 \times 10^{46}$ erg s⁻¹ following efficient post-breakout X-ray cooling of ~ 3.5 mag hour⁻¹. The dominant band transits to UV after around 3 hours of shock breakout and its luminosity has a decay rate of ~ 1.5 mag hour⁻¹ that agrees well with the observed shock breakout tail. The detailed features of breakout emission are sensitive to the pre-explosion environment. Our 2D simulations also demonstrate the importance of post-breakout mixing and its impacts on shock dynamics and radiation emission. The mixing driven by the shock breakout may lead to a global asymmetry of SN ejecta and affect its later supernova remnant formation.

Keywords: Supernovae — Ultraviolet astronomy — Radiation hydrodynamics

1. INTRODUCTION

The electromagnetic signals from supernovae (SNe) of massive stars begin when the explosion shock breaks out of the stellar surface. This is the so-called *shock breakout*, a luminous phenomenon that has only been detected through a few serendipitous observations (Schawinski et al. 2008; Gezari et al. 2015). The peak luminosity and duration of breakout emission can be used to probe the explosion energy, the radius of a progenitor star, and its circumstellar environment (Waxman & Katz 2017).

Previous theoretical studies of shock breakout duration and peak luminosity from blue supergiant (BSG) and red supergiant (RSG) usually assumed an adiabatic shock propagating in a spherical stellar envelope with a power-law density profile (Matzner & McKee 1999; Waxman & Katz 2017). However, modeling the realistic SN shock breakout requires a deeper understanding of the shock propagation in a clumpy stellar atmosphere and the circumstellar medium (CSM) formed before the star dies (Chevalier & Irwin 2011; González-Torà, G. et al. 2023), and the emission from the shock typically ranges from hard X-ray to UV and infrared wavelengths (Tolstov et al. 2013; Katz et al. 2010). The complex interplay of radiation-mediated shock among the structured stellar atmosphere and CSM can only be properly modeled through the multidimensional radiation hydrodynamics (RHD) (Levinson & Nakar 2020), which has been utilized to model the transport of neutrinos and photons in supernovae (Ott et al. 2008; Urobin et al. 2021; Chen et al. 2023).

Previous one-dimensional (1D) shock breakout simulations (Lovegrove et al. 2017) have provided insights into the physics of SN shock breakout. However, these simulations have limitations, as they fail to accurately model fluid instabilities, resulting in nonphysical features such as a distinct density spike (thin shell). Limited fluid instabilities in 1D simulations often concentrate a significant amount of shocked ejecta into a small region, moving at the same

LETTER TO THE EDITOR

The astrophysical parameters of chemically peculiar stars from automatic methods

E. Paunzen¹

Department of Theoretical Physics and Astrophysics, Masaryk University, Kotlářská 2, 611 37 Brno, Czech Republic
e-mail: epaunzen@physics.muni.cz

ABSTRACT

Context. The chemically peculiar (CP) stars of the upper main sequence are excellent astrophysical laboratories for investigating the diffusion, mass loss, rotational mixing, and pulsation in the presence and absence of a stable local magnetic field. For this, we need a homogeneous set of parameters, such as effective temperature (T_{eff}) and surface gravity ($\log g$), to locate the stars in the Hertzsprung-Russell diagram so that we can then estimate the mass, radius, and age.

Aims. In recent years, the results of several automatic pipelines have been published; these use various techniques and data sets, including T_{eff} and $\log g$ values for millions of stars. Because CP stars are known to have flux anomalies, these astrophysical parameters must be tested for their reliability and usefulness. If the outcome is positive, these can be used to analyse the new and faint CP stars published recently.

Methods. I compared published T_{eff} and $\log g$ values of a set of CP stars, which are mostly based on high-resolution spectroscopy, with values from four automatic pipeline approaches. In doing so, I searched for possible correlations and offsets.

Results. I present a detailed statistical analysis of a comparison between the ‘standard’ and published T_{eff} and $\log g$ values. The accuracy depends on the presence of a magnetic field and the spectral type of the CP subgroups. However, I obtain standard deviations of between 2% and 20%.

Conclusions. Considering the statistical errors, the astrophysical parameters from the literature can be used for CP stars, although caution is advised for magnetic CP stars.

Key words. stars: chemically peculiar – stars: fundamental parameters – Hertzsprung-Russell and C-M diagrams

1. Introduction

The chemically peculiar (CP) stars of the upper main sequence have been targets of astrophysical study since their discovery by the American astronomer Antonia Maury (1897). Most of the early research was devoted to detecting peculiar features in their spectra and to characterising their photometric behaviour.

According to Preston (1974), CP stars are commonly subdivided into four classes: metallic line (or Am) stars (CP1), magnetic Ap stars (CP2), HgMn stars (CP3), and He-weak stars (CP4). The CP1 stars are A- and early F-type objects and are defined by the discrepancies found in the spectral types derived from the strengths of the Ca II K line and the hydrogen and metallic lines. In comparison to the spectral types derived from the hydrogen lines, the Ca II K-line types appear too early, and the metallic-line types too late. CP1 stars do not show strong, global magnetic fields (Aurière et al. 2010) and are characterised by underabundances of calcium and scandium and overabundances of the iron peak and heavier elements. CP1 stars are primarily members of binary systems with orbital periods in the range between 2 and 10 days, and their rotational velocities are believed to have been reduced by tidal interactions, which has enabled diffusion to act (Abt 2009). The observed abundance pattern of CP1 stars is defined by the diffusion of elements and the disappearance of the outer convection zone associated with helium ionisation because of the gravitational settling of helium (Théado et al. 2005). These latter authors predict a cut-off rotational velocity for such objects (about 100 km s^{-1}), above

which meridional circulation leads to a mixing in the stellar atmosphere.

The CP2 stars are distinguished by their strong, globally organised magnetic fields that range up to several tens of kG (Bychkov et al. 2021a). In CP2 (and CP4) stars, due to additional magnetic diffusion, the chemical abundance concentrations at the magnetic poles, as well as the spectral and related photometric variabilities, are also easily understood, as are the radial velocity variations of the appearing and receding patches on the stellar surface (Alecian 2015). These inhomogeneities are responsible for the strictly periodic changes observed in the spectra and brightness of many CP2 stars, which are explained by the oblique rotator model (Stibbs 1950). Therefore, the observed periodicity of variation is the rotational period of the star.

The CP3 stars are characterised by strong lines of ionised Hg and/or Mn with overabundances by up to six orders of magnitude relative to their solar abundances (Ghazaryan et al. 2018). Several mechanisms play significant roles in our understanding of these extreme peculiarities: radiatively driven diffusion, mass loss, mixing, light-induced drift, and possibly weak magnetic fields. However, no satisfactory model exists to explain the abundance pattern (Adelman et al. 2003).

The CP4 stars are the hottest CP objects up to early B-types, where the mass-loss and stellar winds become significant (Cidale et al. 2007). Initially, the CP4 stars were defined as He-weak stars only. Later on, it was proposed that this class also includes He-strong stars (Pedersen & Thomsen 1977). However, the latter are rare and are not included in the present analysis. The He lines

ORIGINAL ARTICLE**Calculated brightness temperatures of solar structures compared with ALMA and Metsähovi measurements**Filip Matković*¹ | Roman Brajša¹ | Matej Kuhar^{2,3} | Arnold O. Benz^{2,4} | Hans -G. Ludwig⁵ | Caius L. Selhorst^{6,7} | Ivica Skokić¹ | Davor Sudar¹ | Arnold Hanslmeier⁸¹Hvar Observatory, Faculty of Geodesy, University of Zagreb, Zagreb, Croatia²Institute for Data Science, University of Applied Sciences and Arts Northwestern Switzerland, Windisch, Switzerland³Finstar, c/o Hypothekbank Lenzburg AG, Lenzburg, Switzerland⁴Institute for Particle Physics and Astrophysics, Department of Physics, ETH Zurich, Switzerland⁵Landessternwarte Königstuhl, Zentrum für Astronomie der Universität Heidelberg, Heidelberg, Germany⁶NAT - Núcleo de Astrofísica, Universidade Cidade de São Paulo, São Paulo, Brazil⁷Center for Solar-Terrestrial Research, New Jersey Institute of Technology, Newark, New Jersey, USA⁸Institute for Geophysics, Astrophysics and Meteorology, Institute of Physics, University of Graz, Graz, Austria**Correspondence***Filip Matković, Hvar Observatory, Faculty of Geodesy, University of Zagreb, Kačićeva 26, 10000 Zagreb, Croatia.
Email: fmatkovic@geof.hr**Funding Information**

Croatian Science Foundation, project ID: 7549. Austrian-Croatian Bilateral Scientific Projects. Horizon 2020 project SOLARNET, project ID: 824135. Alexander von Humboldt Foundation. Deutsche Forschungsgemeinschaft, project ID: 138713538-SFB 881. São Paulo Research Foundation (FAPESP), grant number: 2019/03301-8.

The Atacama Large Millimeter/submillimeter Array (ALMA) allows for solar observations in the wavelength range of 0.3–10 mm, giving us a new view of the chromosphere. The measured brightness temperature at various frequencies can be fitted with theoretical models of density and temperature versus height. We use the available ALMA and Metsähovi measurements of selected solar structures (quiet sun (QS), active regions (AR) devoid of sunspots, and coronal holes (CH)). The measured QS brightness temperature in the ALMA wavelength range agrees well with the predictions of the semiempirical Avrett–Tian–Landi–Curdt–Wülser (ATLCW) model, better than previous models such as the Avrett–Loeser (AL) or Fontenla–Avrett–Loeser model (FAL). We scaled the ATLCW model in density and temperature to fit the observations of the other structures. For ARs, the fitted models require 9%–13% higher electron densities and 9%–10% higher electron temperatures, consistent with expectations. The CH fitted models require electron densities 2%–40% lower than the QS level, while the predicted electron temperatures, although somewhat lower, do not deviate significantly from the QS model. Despite the limitations of the one-dimensional ATLCW model, we confirm that this model and its appropriate adaptations are sufficient for describing the basic physical properties of the solar structures.

KEYWORDS:

radio radiation, chromosphere, transition region, corona

1 | INTRODUCTION

The chromosphere is possibly the least observed and studied part of the solar atmosphere in the radio wavelength range.

Therefore, it is crucial to study this layer of the atmosphere and to construct theoretical models that best describe the (radio) observations. An important opportunity to compare the results of theoretical models with measurements and to check their

Spectroscopic survey of faint planetary-nebula nuclei III. A [WC] central star and two new PG1159 nuclei[★]

Klaus Werner¹, Helge Todt², Howard E. Bond^{3,4}, and Gregory R. Zeimann⁵

¹ Institut für Astronomie und Astrophysik, Kepler Center for Astro and Particle Physics, Eberhard Karls Universität, Sand 1, 72076 Tübingen, Germany

e-mail: werner@astro.uni-tuebingen.de

² Institut für Physik und Astronomie, Universität Potsdam, Karl-Liebknecht-Straße 24/25, 14476 Potsdam, Germany

³ Department of Astronomy & Astrophysics, Pennsylvania State University, University Park, PA 16802, USA

⁴ Space Telescope Science Institute, 3700 San Martin Dr., Baltimore, MD 21218, USA

⁵ Hobby-Eberly Telescope, University of Texas at Austin, Austin, TX 78712, USA

Received 15 January 2024 / Accepted 29 February 2024

ABSTRACT

We present spectroscopy of three hydrogen-deficient central stars of faint planetary nebulae, with effective temperatures (T_{eff}) in excess of 100 000 K. The nucleus of RaMul 2 is a Population II Wolf-Rayet star of spectral type [WC], and the central stars of Abell 25 and StDr 138 are two new members of the PG1159 class. Our spectral analyses reveal that their atmospheres have a similar chemical composition. They are dominated by helium and carbon, which was probably caused by a late helium-shell flash. Coincidentally, the three stars have similar masses of about $M = 0.53 M_{\odot}$ and, hence, form a post-AGB evolutionary sequence of an initially early-K type main-sequence star with $M = 0.8 M_{\odot}$. The central stars cover the period during which the luminosity fades from about 3000 to 250 L_{\odot} and the radius shrinks from about 0.15 to 0.03 R_{\odot} . The concurrent increase of the surface gravity during this interval from $\log g = 5.8$ to 7.2 causes the shutdown of the stellar wind from an initial mass-loss rate of $\log \dot{M}/(M_{\odot} \text{ yr}^{-1}) = -6.4$, as measured for the [WC] star. Along the contraction phase, we observe an increase of T_{eff} from 112 000 K, marked by the [WC] star, to the maximum value of 140 000 K and a subsequent cooling to 130 000 K, marked by the two PG1159 stars.

Key words. planetary nebulae: individual: Abell 25, StDr 138, RaMul 2 – stars: atmospheres – stars: evolution – white dwarfs

1. Introduction

This is the third in a series of papers presenting results from a spectroscopic survey of central stars of faint Galactic planetary nebulae (PNe). It is being carried out with the second-generation Low-Resolution Spectrograph (LRS2; Chonis et al. 2016) of the 10-m Hobby-Eberly Telescope (HET; Ramsey et al. 1998; Hill et al. 2021), located at McDonald Observatory in west Texas, USA. An overview of the survey, a description of the instrumentation and data-reduction procedures, target selection, and some initial results were presented in our first paper (Bond et al. 2023a, hereafter Paper I). Paper II in this series (Bond et al. 2023b) discussed the central star of the “PN mimic” Fr 2-30. In this third paper we present spectra of three little-studied objects that have extremely hot, hydrogen-deficient central stars. About 50 central stars have been observed to date. Future papers will discuss several more individual objects of special interest, and another publication will present results on a group of nuclei with fairly normal hydrogen-rich spectra.

The remainder of this paper is organized as follows. In Sect. 2 we introduce our program stars and their planetary nebulae, and we describe our spectroscopic observations in Sect. 3.

[★] Based on observations obtained with the Hobby-Eberly Telescope (HET), which is a joint project of the University of Texas at Austin, the Pennsylvania State University, Ludwig-Maximilians-Universität München, and Georg-August Universität Göttingen. The HET is named in honor of its principal benefactors, William P. Hobby and Robert E. Eberly.

In Sect. 4 we present our spectral analyses and their results. We summarize and discuss our findings in Sect. 5.

2. The targets

Table 1 lists celestial and Galactic coordinates, parallaxes, and magnitudes and colours for our three central stars, all taken from *Gaia* Data Release 3¹ (DR3; Gaia Collaboration et al. 2016, 2023). The following subsections give brief details of the discoveries of these faint PNe and their nuclei, and some of the nebular properties. Further information about the objects is contained in the online Hong-Kong/AAO/Strasbourg/H α Planetary Nebulae (HASH) database² (Parker et al. 2016).

2.1. Abell 25 (K 1-13)

This low-surface-brightness nebula (PN G224.3+15.3) was discovered six decades ago by Kohoutek (1963) in his inspection of prints from the Palomar Observatory Sky Survey (POSS), and is designated K 1-13. It also appears as entry number 25 in the classical list of ancient PNe found on the POSS by Abell (1966). We will use the designation Abell 25 hereafter, as this name has been used more commonly in the PN literature.

¹ <https://vizier.cds.unistra.fr/viz-bin/VizieR-3?-source=I/355/gaiadr3>

² <http://hashpn.space/>

Cosmological transition epoch from gamma-ray burst correlations

Anna Chiara Alfano,^{1,2,*} Salvatore Capozziello,^{1,2,3,†} Orlando Luongo,^{4,5,6,7,8,‡} and Marco Muccino^{4,8,9,§}

¹*Scuola Superiore Meridionale, Largo S. Marcellino 10, 80138 Napoli, Italy.*

²*Istituto Nazionale di Fisica Nucleare (INFN), Sezione di Napoli Complesso Universitario Monte S. Angelo, Via Cinthia 9 Edificio G, 80138 Napoli, Italy.*

³*Dipartimento di Fisica "E. Pancini", Università di Napoli "Federico II", Complesso Universitario Monte S. Angelo, Via Cinthia 9 Edificio G, 80126 Napoli, Italy.*

⁴*Università di Camerino, Divisione di Fisica, Via Madonna delle carceri 9, 62032 Camerino, Italy.*

⁵*SUNY Polytechnic Institute, 13502 Utica, New York, USA.*

⁶*INFN, Sezione di Perugia, Perugia, 06123, Italy.*

⁷*INAF - Osservatorio Astronomico di Brera, Milano, Italy.*

⁸*Al-Farabi Kazakh National University, Al-Farabi av. 71, 050040 Almaty, Kazakhstan.*

⁹*ICRANet, P.zza della Repubblica 10, 65122 Pescara, Italy.*

The redshift z_t and the jerk parameter j_t of the transition epoch can be constrained by using two model-independent approaches involving the direct expansion of the Hubble rate and the expansion of the deceleration parameter around $z = z_t$. To extend our analysis to high-redshifts, we employ the *Amati*, *Combo*, *Yonetoku* and *Dainotti* gamma-ray burst correlations. The *circularity problem* is prevented by calibrating these correlations through the Bézier interpolation of the updated observational Hubble data. Each gamma-ray burst data set is jointly fit with type Ia supernovae and baryonic acoustic oscillations through a Monte Carlo analysis, based on the Metropolis-Hastings algorithm, to obtain z_t , j_t and the correlation parameters. The overall results are compatible with the concordance model with some exceptions. We also focus on the behaviors of the dark energy, verifying its compatibility with a cosmological constant, and the matter density Ω_m and compare them with the expectations of the concordance paradigm.

PACS numbers: 98.70.Rz, 98.80.-k, 98.80.Es, 98.62.Py

I. INTRODUCTION

The cosmic speed up is a widely-consolidated evidence, currently supported by several observations [1–3] and firstly certified by type Ia supernovae (SNe Ia) [4, 5]. The on-set of this accelerated phase occurred as dark energy started to dominate over matter *i.e.*, in a *transition epoch* marked by a transition redshift, z_t .

The simplest model that explains this feature, the Λ CDM paradigm, is based on the dark energy in the form of a cosmological constant, Λ [6–8], and a cold dark matter contribution. Thus, while matter decelerates the expansion of the universe, the cosmological constant accelerates it acting as a repulsive gravity [9].

However, the cosmological constant hypothesis purported by the Λ CDM model suffers from a severe *fine-tuning* problem — if the physical interpretation of Λ is attributed to the vacuum energy density, then a 121 order of magnitudes discrepancy exists between predictions and observations [10, 11] — and a *coincidence* problem — the current densities of matter and Λ are strangely compatible.

To address these problems, extensions of the cosmological constant paradigm have been proposed. The simplest ones are the so-called ω CDM model, in which the

equation of state is constant [12, 13], and the Chevallier-Polarsky-Linder (CPL) parametrization [14, 15], where the equation of state is written as a function of the scale factor $a(t)$.

Alternatively, model-independent approaches have been proposed to establish whether dark energy behaves as a cosmological constant or evolves with time [16–19]. To understand this, it is essential to investigate the transition epoch resorting the cosmographic approach [20–23], based on Taylor series of the Hubble rate through the cosmographic parameters, whose number depends upon the selected order of the expansion [24–27]. When applied to the transition epoch, the key cosmographic quantities involved in the expansion are the jerk parameter at the transition $j(z_t) = j_t$ and the redshift at the transition z_t , whereas the deceleration parameter, by definition vanishes, *i.e.*, $q(z_t) = q_t = 0$.

Here, we work with the direct expansion of the Hubble rate (DHE) and the direct deceleration parameter expansion (DDPE) around $z \simeq z_t$ [28]. Then, we get constraints on the transition redshift and cosmographic parameters at the transition by adopting standard candles, SNe Ia, standard rulers, baryonic acoustic oscillations (BAO), and gamma-ray bursts (GRB), a class of distance indicators enabling the investigation of the universe at high-redshift [29–36]. However, GRB need to be calibrated in a model-independent way to avoid the well-known *circularity* problem [31] and, to this aim, we here resort to the Bézier interpolation [37–40] to model the Hubble rate and, thus, the cosmological distances. We apply this technique to four GRB correlations, namely

* a.alfano@ssmeridionale.it

† capozziello@na.infn.it

‡ orlando.luongo@unicam.it

§ marco.muccino@inf.infn.it

Induced Gravitational Wave interpretation of PTA data: complete study for general equation of state

Guillem Domènech^{a,b,*}, Shi Pi^{c,d,e,†}, Ao Wang^{c,f,‡} and Jianing Wang^{c,f,§}

^a *Institute for Theoretical Physics, Leibniz University Hannover,
Appelstraße 2, 30167 Hannover, Germany.*

^b *Max-Planck-Institut für Gravitationsphysik,
Albert-Einstein-Institut, 30167 Hannover, Germany*

^c *CAS Key Laboratory of Theoretical Physics, Institute of Theoretical Physics,
Chinese Academy of Sciences, Beijing 100190, China*

^d *School of Physical Sciences, University of Chinese Academy of Sciences, Beijing 100049, China*

^e *Kavli Institute for the Physics and Mathematics of the Universe (WPI),
The University of Tokyo, Kashiwa, Chiba 277-8583, Japan*

^f *Center for High Energy Physics, Peking University, Beijing 100871, China and*

^g *International Center for Quantum-field Measurement Systems
for Studies of the Universe and Particles (QUP, WPI),
High Energy Accelerator Research Organization (KEK),
Oho 1-1, Tsukuba, Ibaraki 305-0801, Japan*

(Dated: March 1, 2024)

We thoroughly study the induced gravitational wave interpretation of the possible gravitational wave background reported by PTA collaborations, considering the unknown equation of state w of the early universe. We perform a Bayesian analysis of the NANOGrav data using the publicly available PTARCADE code together with SIGWFAST for the numerical integration of the induced gravitational wave spectrum. We focus on two cases: a monochromatic and a log-normal primordial spectrum of fluctuations. For the log-normal spectrum, we show that, while the results are not very sensitive to w when the GW peak is close to the PTA window, radiation domination is out of the 2σ contours when only the infra-red power-law tail contributes. For the monochromatic spectrum, the 2σ bounds yield $0.1 \lesssim w \lesssim 0.9$ so that radiation domination is close to the central value. We also investigate the primordial black hole (PBH) counterpart using the peak formalism. We show that, in general terms, a larger width and stiffer equation of state alleviates the overproduction of PBHs. No PBH overproduction requires $w \gtrsim 0.42$ up to $2\text{-}\sigma$ level for the monochromatic spectrum. Furthermore, including bounds from the cosmic microwave background, we find in general that the mass range of the PBH counterpart is bounded by $10^{-5}M_{\odot} \lesssim M_{\text{PBH}} \lesssim 10^{-1}M_{\odot}$. Lastly, we find that the PTA signal can explain the microlensing events reported by OGLE for $0.42 \lesssim w \lesssim 0.50$. Our work showcases a complete treatment of induced gravitational waves and primordial black holes for general w for future data analysis.

* guillem.domenech@itp.uni-hannover.de

† shi.pi@itp.ac.cn

‡ wangao@itp.ac.cn

§ wangjianing@itp.ac.cn

High-redshift halo-galaxy connection via constrained simulations

ADI NUSSER¹

¹ *Department of Physics and the Asher Space Research Institute
Israel Institute of Technology Technion, Haifa 32000, Israel*

ABSTRACT

The evolution of halos with masses around $M_h \approx 10^{11} M_\odot$ and $M_h \approx 10^{12} M_\odot$ at redshifts $z > 9$ is examined using constrained N-body simulations. The specific mass accretion rates, \dot{M}_h/M_h , exhibit minimal mass dependence and agree with existing literature. Approximately one-third of simulations reveal an increase in \dot{M}_h around $z \approx 13$, possibly implying a dual-age stellar population. Comparing simulated halos with observed galaxies having spectroscopic redshifts, we find that for galaxies at $z \gtrsim 9$, the ratio between observed star formation rate (SFR) and \dot{M}_h is approximately 2%. This ratio remains consistent for the stellar-to-halo mass ratio (SHMR) but only for $z \gtrsim 10$. At $z \simeq 9$, the SHMR is notably lower by a factor of a few. At $z \gtrsim 10$, there is an agreement between specific star formation rates (sSFRs) and \dot{M}_h/M_h of halos. However, at $z \simeq 9$, observed sSFRs exceed simulated values by a factor of two. To explain the relatively high star formation efficiencies in high- z halos with $M_h \approx 10^{11} M_\odot$, a simplified model is proposed, assuming the applicability of the local Kennicutt-Schmidt law. The enhanced efficiency relative to low- z is mainly driven by the reduced effectiveness of stellar feedback due to deeper gravitational potential for halos of a fixed mass.

Keywords: cosmology: large-scale structure – galaxies: formation – galaxies: high redshift – galaxies: ISM – galaxies: luminosity function

1. INTRODUCTION

The standard Λ CDM cosmological model, incorporating a cosmological constant, Λ , and cold dark matter (DM), has been remarkably successful in interpreting and predicting fundamental properties of the large-scale structure of the Universe. Despite potential tensions (e.g. [Asgari et al. 2021](#); [Riess et al. 2023](#)), this success extends to temperature anisotropies of the cosmic microwave background (CMB), clustering of the distribution of galaxies, and deviations of galaxy motions from a purely Hubble flow (e.g. [Bennett et al. 2013](#); [Tegmark et al. 2004](#); [Cole et al. 2005](#); [Eisenstein et al. 2007](#); [Davis et al. 2011](#); [Carrick et al. 2015](#); [Planck Collaboration et al. 2018](#); [Lilow et al. 2021](#)). On galactic scales, predicting the properties of the galaxy population and its evolution with redshift has been less straightforward. This complexity arises from the intricate nature of baryonic physics involved in star formation processes, including gas dynamics, heating and cooling mechanisms, and

notably, the energetic feedback from supernovae (SN) and active galactic nuclei (AGNs) (e.g. [Larson 1974](#); [Dekel & Silk 1986](#); [White & Frenk 1991a](#); [Silk & Rees 1998](#); [Dekel et al. 2009b](#); [Okalidis et al. 2021](#); [Krumholz et al. 2018](#); [Nusser & Silk 2022](#)).

Prior to the era of the James Webb Space Telescope (JWST) ([Gardner et al. 2023](#)), significant efforts have been invested in fine-tuning models of galaxy formation to adequately describe observations at low and moderately high redshifts ($z \lesssim 10$) (e.g. [Finkelstein et al. 2022](#)).

Observations obtained with the JWST have significantly deepened our view of the universe, revealing galaxies as far back as a couple of hundred million years near the Big Bang. However, the JWST has also detected an unexpected excess of luminous galaxies at higher redshifts. While the initial findings from the JWST posed serious challenges for the standard Λ CDM model of structure formation, the severity of these discrepancies were largely alleviated with more precise calibration and the availability of spectroscopic redshifts (cf. [Yung et al. 2024](#), for an overview).

It should be emphasized that the star formation rates (SFRs) in high-redshift JWST galaxies are not particu-

Review

CrossMark
click for updates

Article submitted to journal

Subject Areas:

Astroparticle physics, Neutrino properties, Fundamental particles and interactions

Keywords:Neutrinos, Gamma rays,
Beyond-standard-model physics**Author for correspondence:**

Markus Ackermann

e-mail: markus.ackermann@desy.de

Klaus Helbing

e-mail: helbing@uni-wuppertal.deSearches for
beyond-standard-model
physics with astroparticle
physics instrumentsM. Ackermann¹ and K. Helbing²¹Deutsches Elektronen-Synchrotron DESY,
Platanenallee 6, 15738 Zeuthen, Germany²Dept. of Physics, University of Wuppertal, 42119
Wuppertal, Germany

Many instruments for astroparticle physics are primarily geared towards multi-messenger astrophysics, to study the origin of cosmic rays (CR) and to understand high-energy astrophysical processes. Since these instruments observe the Universe at extreme energies and in kinematic ranges not accessible at accelerators these experiments provide also unique and complementary opportunities to search for particles and physics beyond the standard model of particle physics. In particular, the reach of IceCube, Fermi and KATRIN to search for and constrain Dark Matter, Axions, heavy Big Bang relics, sterile neutrinos and Lorentz Invariance Violation (LIV) will be discussed. The contents of this article are based on material presented at the Humboldt-Kolleg "Clues to a mysterious Universe - exploring the interface of particle, gravity and quantum physics" in June 2022.

Survey of Magnetic Field Parameters Associated With Large Solar Flares

Ting Li^{1,2,3}, Yanfang Zheng⁴, Xuefeng Li⁴, Yijun Hou^{1,2,3}, Xuebao Li⁴, Yining Zhang^{1,2} & Anqin Chen⁵

ABSTRACT

Until now, how the magnetic fields in M/X-class flaring active regions (ARs) differ from C-class flaring ARs remains unclear. Here, we calculate the key magnetic field parameters within the area of high photospheric free energy density (HED region) for 323 ARs (217 C- and 106 M/X-flaring ARs), including total photospheric free magnetic energy density E_{free} , total unsigned magnetic flux Φ_{HED} , mean unsigned current helicity h_c , length of the polarity inversion lines L_{PIL} with a steep horizontal magnetic gradient, etc., and compare these with flare/coronal mass ejection (CME) properties. We first show the quantitative relations among the flare intensity, the eruptive character and Φ_{HED} . We reveal that Φ_{HED} is a measure for the GOES flux upper limit of the flares in a given region. For a given Φ_{HED} , there exists the lower limit of F_{SXR} for eruptive flares. This means that only the relatively strong flares with the large fraction of energy release compared to the total free energy are likely to generate a CME. We also find that the combinations of E_{free} - L_{PIL} and E_{free} - h_c present a good ability to distinguish between C-class and M/X-class flaring ARs. Using determined critical values of E_{free} and L_{PIL} , one predicts correctly 93 out of 106 M/X-class flaring ARs and 159/217 C-class flaring ARs. The large L_{PIL} or h_c for M/X-class flaring ARs probably implies the presence of a compact current with twisted magnetic fields winding about it.

¹CAS Key Laboratory of Solar Activity, National Astronomical Observatories, Chinese Academy of Sciences, Beijing 100101, China; liting@nao.cas.cn

²School of Astronomy and Space Science, University of Chinese Academy of Sciences, Beijing 100049, China

³National Space Science Center, Chinese Academy of Sciences, Beijing 100190, China

⁴School of computer science, Jiangsu University of Science and Technology, Zhenjiang, China; zyf062856@163.com

⁵Key Laboratory of Space Weather, National Center for Space Weather, China Meteorological Administration, Beijing 100081, China

Weak Lensing Constraints on Dark Matter-Baryon Interactions with N -Body Simulations and Machine Learning

Chi Zhang,^{1,2} Lei Zu,^{1,*} Hou-Zun Chen,³ Yue-Lin Sming Tsai,^{1,2,†} and Yi-Zhong Fan^{1,2}

¹*Key Laboratory of Dark Matter and Space Astronomy,*

Purple Mountain Observatory, Chinese Academy of Sciences, Nanjing 210023, China

²*School of Astronomy and Space Science, University of Science and Technology of China, Hefei 230026, China*

³*Institute for Astronomy, the School of Physics, Zhejiang University, Hangzhou 310027, China*

We investigate the elastic scattering cross section between dark matter and protons using the DES Year 3 weak lensing data. This scattering induces a dark acoustic oscillation structure in the matter power spectra. To address non-linear effects at low redshift, we utilize principal component analysis alongside a limited set of N -body simulations, improving the reliability of our matter power spectrum prediction. We further perform a robust Markov Chain Monte Carlo analysis to derive the upper bounds on the DM-proton elastic scattering cross-section, assuming different velocity dependencies. Our results, presented as the first Frequentist upper limits, are compared with the ones obtained by Bayesian approach. Compared with the upper limits derived from the Planck cosmic microwave background data, our findings from DES Year 3 data exhibit improvements of up to a factor of five. In addition, we forecast the future sensitivities of the China Space Station Telescope, the upcoming capabilities of this telescope could improve the current limits by approximately one order of magnitude.

I. INTRODUCTION

Dark Matter (DM) is one of the most fundamental mysteries in modern physics, even though its gravitational effects are well understood. Besides gravity, the interactions between DM and baryons are also of great interest, as explored by experiments such as PandaX [1] and XENONnT [2]. However, no signal has been detected for DM masses above about 1 GeV. Therefore, the focus of experiments has shifted to the sub-GeV mass range, for example, CDEX [3], SENSEI [4], etc.

The interaction between DM and baryons can change the matter distribution in our universe, creating a dark acoustic oscillation (DAO) feature in the matter power spectra. DAO affects the Cosmic microwave background (CMB) anisotropies and the structure formation in the early universe, and constrains the DM-proton elastic scattering cross-section [5–8]. However, the DAO suppression, similar to that of warm DM, is more sensitive to small-scale observations. For velocity independent case, one obtains a stronger limit on this cross-section ($\sigma_{\chi p} < 2.8 \times 10^{-28} \text{ cm}^3 \text{ s}^{-1}$ for DM mass around 10 MeV) from the Milky Way satellite abundance [8–11], and the tightest limit ($\sigma_{\chi p} < 1.7 \times 10^{-29} \text{ cm}^3 \text{ s}^{-1}$ for DM mass around 10 MeV) from the Lyman- α -forest [8, 12, 13]. Nevertheless, the theoretical predictions of these small-scale observations are affected by the non-linear evolution of power spectra and the baryonic feedback. A recent research have explored such baryonic feedback in the galaxies affected by the DM-baryon interactions through hydrodynamical simulation [14]. However, the systematic uncertainties of these predictions remain unclear.

Weak Gravitational Lensing (WL) is a good tool for probing the late-time Large Scale Structure (LSS) of the universe. Through statistical analyses of shape distortions in numerous galaxies induced by foreground matter fields, it can directly map the LSS of the universe. We can mask the small-scale WL data to reduce the uncertainties associated with baryonic feedback, which are more pronounced in observations of the Lyman- α -forest at the small scales. In addition, WL data is expected to be more sensitive than the CMB anisotropies. Many recent and upcoming surveys, including Dark Energy Survey (DES) [15], Kilo-Degree Survey (KiDS) [16, 17], Subaru Hyper Suprime-Cam (HSC) [18, 19], Euclid [20], the Vera C. Rubin Observatory [21], the Nancy Grace Roman Space Telescope [22], the Wide Field Survey Telescope (WFST) [23, 24], the Mephisto Telescope [25, 26] and China Space Station Telescope (CSST) [27–29], greatly improve our understanding of the matter distribution in the late universe. They, in turn, have the potential to reveal the fundamental physics of the interaction between DM and baryonic matter. In this work, we use the data from DES three-year (DES Y3) ‘3 \times 2pt’ WL observations along with the CMB and baryonic acoustic oscillation (BAO) observations data. Furthermore, we generate the mock data for CSST and present a forecast of the power of CSST.

Because the photometric galaxy surveys can cover the red-shift with the range $0 < z < 5$, the non-linear effects on the matter power spectrum are essential for the theoretical prediction of WL signal. In this study, we conducted a series of DM-only N -body simulations to accurately account for the non-linear effects on the matter power spectrum. The matter power spectrum can be modified by the elastic scattering of DM particle χ with proton p . The scattering cross-section, denoted as $\sigma_{\chi p} \equiv \sigma_n v_{\text{rel}}^n$, is parameterized by a power-law index n and the relative velocity between DM and protons v_{rel} .

* zulei@pmo.ac.cn

† smingtsai@pmo.ac.cn

Spectropolarimeter on a 2–4 m class telescope and proposed science cases

ARCHANA SOAM ¹, SIDDHARTH MAHARANA ^{1,2,3}, B-G ANDERSSON ^{4,5} AND RAMAPRAKASH, A. N.⁶

¹*Indian Institute of Astrophysics, II Block, Koramangala, Bengaluru 560034, India*

²*Institute of Astrophysics, Foundation for Research and Technology-Hellas, GR-71110 Heraklion, Greece; Department of Physics, University of Crete, GR-70013 Heraklion, Greece*

³*South African Astronomical Observatory, PO Box 9, Observatory, 7935, Cape Town, South Africa*

⁴*SOFIA Science Center/USRA, NASA Ames Research Center, M.S. N232-12, Moffett Field, CA 94035, USA*

⁵*Visiting Scholar, Institute for Scientific Research, Boston College, Kenny Cottle Hall 217, 885 Centre St., Newton, MA 02459*

⁶*Inter-University Centre for Astronomy and Astrophysics, Post Bag 4, Ganeshkhind, Pune 411 007, India*

ABSTRACT

We propose a spectropolarimeter covering a wavelength range of 3200–7000 Å [3200 Å chosen as lower limit to go to the atmospheric cut-off. It’s “needed” for some Serkowski curves and would make the instrument even more unique] for a 2-4 m class telescope. In this article, we discuss the science cases which will be covered with this proposed instrument. The technical requirements and analysis plan for each science case is also discussed. This spectropolarimeter targeting exciting galactic and extra-galactic research, will be a unique instrument on a 2-4 m facilities.

Keywords: Polarization; magnetic fields; Spectropolarimeter

1. INTRODUCTION

Interstellar magnetic fields can be mapped with the polarization of starlight caused by aligned dust grains in different lines-of-sights and in different environments. This was first observed in optical wavelengths^{11,12} and was explained to be arising from dichroic extinction by elongated dust grains aligned with the ambient magnetic field. Interstellar polarization also provides an opportunity to study the dust grain characteristics e.g. size distribution and composition.

An important science to be addressed with a spectropolarimeter is the investigation of interstellar dust. The differential extinction giving rise to the polarization curve (parameterized by the empirical, convex, “Serkowski function”³⁶

$$p(\lambda) = p_{max} \cdot \exp[-K \cdot \ln^2(\lambda/\lambda_{max})] \quad (1)$$

where p_{max} is the maximum polarization, located at λ_{max} , and “K” controls the width of the curve. As shown by (ref. 17), the Serkowski form can be understood in terms of Mie scattering off an underlying MRN²⁴ grain size distribution - if grains smaller than $\sim 0.045 \mu\text{m}$ are not aligned. The Serkowski fit to the polarization spectrum of star-light shining through this interstellar dust can therefore constrain the size of **aligned** dust grains¹⁷. Adding extinction information to the amount of polarization provides important complementary information that can break the degeneracy between the underlying grain size distribution, and the size dependent grain alignment mechanisms, and their efficiencies. Combining spectroscopy and polarimetry is a time efficient and better approach to perform such investigations in comparison to the often used technique of imaging polarimetry with use of filters.

A spectropolarimeter at a 2–4-m class telescopes is needed to address some very important science cases, especially those related to interstellar dust. Polarimeters, especially with spectroscopic capabilities are not often available on most observatories- imaging cameras and spectrographs are the most commonly available instruments for telescopes. The reason for this trend is two fold: (a) the complexities and challenges in the development and operation of accurate polarimeters and (b) often, the scientific rationale for these kind of instruments are not fully appreciated in the astronomy community.

Perturbed $f(R)$ gravity coupled with neutrinos: exploring cosmological implications

Muhammad Yarahmadi^{1*}, Amin Salehi^{1†}, Kazuharu Bamba^{2‡}

Department of Physics, Lorestan University, Khoramabad, Iran and

Faculty of Symbiotic Systems Science, Fukushima University, Fukushima 960-1296, Japan

(Dated: March 1, 2024)

We conduct a thorough examination of cosmological parameters within the context of $f(R)$ gravity coupled with neutrinos, leveraging a diverse array of observational datasets, including Cosmic Microwave Background (CMB), Cosmic Chronometers (CC), Baryon Acoustic Oscillations (BAO), and Pantheon supernova data. Our analysis unveils compelling constraints on pivotal parameters such as the sum of neutrino masses ($\sum m_\nu$), the interaction strength parameter (Γ), sound speed (c_s), Jean's wavenumbers (k_J), redshift of non-relativistic matter (z_{nr}), and the redshift of the Deceleration-Acceleration phase transition (z_{DA}). The incorporation of neutrinos within the $f(R)$ gravity framework emerges as a key factor significantly influencing cosmic evolution, intricately shaping the formation of large-scale structures and the dynamics of cosmic expansion. Additionally, a detailed analysis of bulk flow direction and amplitude across various redshifts provides valuable insights into the nature of large-scale structures. A notable aspect of our model is the nuanced integration of $f(R)$ gravity theory with neutrinos, representing a distinctive approach to unraveling cosmological phenomena. This framework, unlike previous models, explicitly considers the impact of neutrinos on gravitational interactions, the formation of large-scale structures, and the overarching dynamics of cosmic expansion within the $f(R)$ gravity paradigm. Furthermore, our study addresses the Hubble tension problem by comparing H_0 measurements within our model, offering a potential avenue for reconciling discrepancies. Our findings not only align with existing research but also contribute novel perspectives to our understanding of dark energy, gravitational interactions, and the intricate challenges posed by the Hubble tension.

PACS numbers: 98.80.-k, 04.50.Kd, 13.15.+g

I. INTRODUCTION

Despite the significant achievements of the Λ CDM model, it encounters substantial challenges that cast shadows on its explanatory power. One of the most prominent hurdles is the well-acknowledged 'cosmological continuous fine-tuning challenge,' extensively discussed by researchers such as Weinberg [1] and Astashenok [2]. Furthermore, the intricacies of fine-tuning extend to the Planck scale era, prompting inquiries into the initial conditions governing the emergence of dark energy. The 'cosmic coincidence problem' adds another layer of complexity, urging us to contemplate the intriguing similarity between the energy densities of dark energy and dark matter in the contemporary Universe. In addition to these challenges, the Λ CDM model encounters difficulties in providing a comprehensive explanation for structures at smaller scales. This is exemplified by observed phenomena such as rotation anomalies in galaxies, as discussed by researchers including Moore [4], Quinn [5], Ostriker [3], Boylan-Kolchin [6], Bullock [7], and Oh [8]. These rotation anomalies pose a significant puzzle that challenges the model's ability to fully account for the dynamics of galactic structures at lower sizes.

In essence, while the Λ CDM model has been instrumental in shaping our understanding of the large-scale structure of the Universe, the persistent challenges related to fine-tuning, cosmic coincidences, and discrepancies at smaller scales necessitate a nuanced reassessment of our cosmological paradigm. Understanding the fundamental constituents of the Universe and the nature of gravity has been a persistent quest in cosmology. Among the various approaches to address the mysteries of the cosmos, the consideration of alternative theories of gravity, such as $f(R)$ gravity, has gained prominence.

The $f(R)$ gravity framework extends the traditional General Relativity by incorporating a function $f(R)$ of the Ricci scalar R ([9–18, 61, 63]). This modification introduces new degrees of freedom and offers an alternative explanation for cosmic acceleration without the need for dark energy. The gravitational interaction in $f(R)$ gravity theories departs from the classical predictions of General Relativity, presenting a compelling arena for exploring the dynamics of the cosmos.

The key departure from General Relativity lies in the incorporation of a function of the Ricci scalar within the gravitational action. The Ricci scalar is a curvature scalar that encapsulates the intrinsic curvature of space-time at a given point. By allowing this scalar to vary as a function within the gravitational action, $f(R)$ gravity introduces a level of complexity that goes beyond the simplicity of Einstein's equations.

This modification has profound implications for our understanding of gravity on various scales, from the mi-

*Email: yarahmadimohammad10@gmail.com

†Email: salehi.a@lu.ac.ir

‡Email: bamba@sss.fukushima-u.ac.jp

Turbulence and Magnetic Fields in Star Formation

Archana Soam^{1,*}, Chakali Eswaraiyah², Amit Seta³, Lokesh Dewangan⁴, and Maheswar G.¹

¹ Indian Institute of Astrophysics, II Block, Koramangala, Bengaluru 560034, India

² Indian Institute of Science Education and Research (IISER) Tirupati, Rami Reddy Nagar, Karakambadi Road, Mangalam (P.O.), 517507, Tirupati, India

³ Research School of Astronomy and Astrophysics, Australian National University, Canberra, ACT 2611, Australia

⁴ Astronomy and Astrophysics Division, Physical Research Laboratory, 380009, Navrangpura, Ahmedabad, India

*Corresponding author. E-mail: archana.soam@iiap.res.in

Abstract. Molecular clouds are prime locations to study the process of star formation. These clouds contain filamentary structures and cores, which are crucial sites for the formation of young stars. The star-formation process has been investigated using various techniques, including polarimetry for tracing magnetic fields. In this small review-cum-short report, we put together the efforts (mainly from the Indian community) to understand the roles of turbulence and magnetic fields in star formation. These are two components of the ISM competing against gravity, which is primarily responsible for the collapse of gas to form stars. We also include attempts made using simulations of molecular clouds to study this competition. Studies on feedback and magnetic fields are combined and listed to understand the importance of the interaction between two energies in setting the current observed star formation efficiency. We have listed available and upcoming facilities with the polarization capabilities needed to trace magnetic fields. We have also stated the importance of ongoing and desired collaborations between Indian communities and facilities abroad to shed more light on the roles of turbulence and magnetic fields in the process of star formation. ———

Keywords. ISM: Clouds – Stars: Formation – ISM: Polarization – Magnetic fields

1. Introduction, findings, and global efforts

Interstellar Medium (ISM) is a dynamic medium between the stars which consists of thermal gas, dust, cosmic rays, turbulence, and magnetic fields. Stars form in cold, dense, and gravitationally unstable regions, a.k.a., molecular clouds (e.g., [Benson & Myers 1989](#)). Star formation is not the end-point process of ISM evolution; feedback effects from young stars and supernovae play a significant role in molecular cloud chemistry, evolution, and driving ISM turbulence (e.g., [Krumholz 2014](#)).

Turbulence and Magnetic fields (B-fields) are found to play important roles in the formation and evolution of these molecular clouds (see [Pattle et al. 2022](#)). B-field pervades the entire interstellar medium composed of different phases in the Galaxy ([Ferrière, 2020](#)) such as warm neutral medium (WNM), cold neutral medium (CNM), cold molecular medium (CMM), and hot ionized medium (HIM). Both recent simulations ([Seta & Federrath, 2022](#); [Gent et al., 2023](#)) and observations ([Bracco et al., 2020](#); [Borlaff et al., 2021](#)) show that the properties of B-fields differ with the phase of the ISM. In the diffuse interstellar medium (cold neutral medium;

CNM), the magnetic pressure ($\approx 10,000 \text{ K cm}^{-3}$; with B-field strength of $\approx 6 \mu\text{G}$) contributes as much as the turbulence does (see [Ferrière 2020](#) for temperature, density, and velocity information in different phases of the ISM) but dominates over thermal pressure ($\approx 4000 \text{ K cm}^{-3}$; [Jenkins & Tripp 2011](#)). How does the contribution of each pressure component change from low- to high-density (or large- to small-scale) regions of molecular clouds, and the relative importance of each component against another is a matter of investigation. B-field couples with the gas and dust ([Mestel, 1966](#)), and governs various physical processes such as (i) cloud formation and evolution, (ii) fragmentation and collapse of filaments into dense cores and protostars, and (iii) formation of outflows and circumstellar disks. B-field, rather than playing a sole role, interacts with other key agents such as gravity and turbulence in a complex fashion as shown in [Figure 1](#) and dictates the star formation process.

It is interesting to investigate the roles of turbulence and B-fields in the evolution of ISM. For that, we can use the virial theorem to discuss the relative importance of gravitational, kinematic, and magnetic energies in any region. The Venn diagram shown in [Figure 1](#) represents

Measurement of the photometric Baryon Acoustic Oscillations with self-calibrated redshift distribution

Ruiyu Song,^{1,2} Kwan Chuen Chan,^{1,2}★ Haojie Xu^{3,4,5}†, and Weilun Zheng^{1,2}

¹*School of Physics and Astronomy, Sun Yat-Sen University, 2 Daxue Road, Tangjia, Zhuhai, 519082, China*

²*CSST Science Center for the Guangdong-Hongkong-Macau Greater Bay Area, SYSU, Zhuhai, 519082, China*

³*Shanghai Astronomical Observatory, Chinese Academy of Sciences, Nandan Road 80, Shanghai 200240, China*

⁴*Department of Astronomy, Shanghai Jiao Tong University, Shanghai 200240, China*

⁵*Key Laboratory for Particle Astrophysics and Cosmology (MOE)/Shanghai Key Laboratory for Particle Physics and Cosmology, China*

Accepted XXX. Received YYY; in original form ZZZ

ABSTRACT

We use a galaxy sample derived from the DECaLS DR9 to measure the Baryonic Acoustic Oscillations (BAO). The magnitude-limited sample consists of 10.6 million galaxies in an area of 4974 deg² over the redshift range of [0.6, 1]. A key novelty of this work is that the true redshift distribution of the photo-*z* sample is derived from the self calibration method, which determines the true redshift distribution using the clustering information of the photometric data alone. Through the angular correlation function in four tomographic bins, we constrain the BAO scale dilation parameter α to be 1.025 ± 0.033 , consistent with the fiducial Planck cosmology. Alternatively, the ratio between the comoving angular diameter distance and the sound horizon, D_M/r_s is constrained to be 18.94 ± 0.61 at the effective redshift of 0.749. We corroborate our results with the true redshift distribution obtained from a weighted spectroscopic sample, finding very good agreement. We have conducted a series of tests to demonstrate the robustness of the measurement. Our work demonstrates that the self calibration method can effectively constrain the true redshift distribution in cosmological applications, especially in the context of photometric BAO measurement.

Key words: cosmology: observations - (cosmology:) large-scale structure of Universe

1 INTRODUCTION

Baryonic Acoustic Oscillations (BAO) manifest as the imprint of primordial acoustic features within the distribution of large-scale cosmic structures (Peebles & Yu 1970; Sunyaev & Zeldovich 1970). The formation physics of the BAO is linear and thoroughly understood, as exemplified by works such as Bond & Efstathiou (1984, 1987); Hu & Sugiyama (1996); Hu et al. (1997); Dodelson (2003). During the early stages of the universe, baryons and photons form a tightly coupled plasma, giving rise to the excitation of the acoustic oscillations within it. Subsequent to the cosmic microwave background decoupling, photons free stream and the acoustic patterns are preserved in the baryon distribution. With the accurate calculation of the sound horizon scale, BAO assumes a prominent role as a standard ruler in cosmology (Weinberg et al. 2013; Aubourg et al. 2015). Since its clear detection in the Sloan Digital Sky Survey by Eisenstein et al. (2005) and the 2dF Galaxy Redshift Survey by Cole et al. (2005), BAO measurements have been replicated across various spectroscopic datasets at different effective redshifts (Gaz-

tanaga et al. 2009; Percival et al. 2010; Beutler et al. 2011; Blake et al. 2012; Anderson et al. 2012; Kazin et al. 2014; Ross et al. 2015; Alam et al. 2017; Alam et al. 2021; Moon et al. 2023).

On a different note, clustering analyses of imaging datasets are yielding competitive outcomes. Despite the somewhat less precise redshifts (photo-*z*'s), imaging surveys demonstrate efficiency in capturing extensive data volumes with deep magnitude. This attribute proves particularly advantageous for BAO measurements, given its large-scale nature, necessitating substantial datasets for robust statistics. The uncertainties due to photo-*z*'s are typically as large as the BAO scales, and hence the radial BAO in photometric data cannot be reliably detected. Nonetheless, the transverse BAO can still be measured with confidence (Seo & Eisenstein 2003; Blake & Bridle 2005; Amendola et al. 2005; Benitez et al. 2009; Zhan et al. 2009; Chaves-Montero et al. 2018; Ross et al. 2017b; Chan et al. 2018; Chan et al. 2022b; Ishikawa et al. 2023). A number of photometric BAO measurements have been reported in the literature (Padmanabhan et al. 2007; Estrada et al. 2009; Hütsi 2010; Seo et al. 2012; Carnero et al. 2012; de Simoni et al. 2013; Abbott et al. 2019, 2022; Chan et al. 2022a; Abbott et al. 2024). Besides the direct BAO measurement, it is suggested that the reconstruction technique can be used to enhance the strength of the photometric

★ E-mail: chankc@mail.sysu.edu.cn (KCC)

† E-mail: haojie.xu@shao.ac.cn (HX)

Partial Tidal Disruption Events by Intermediate-mass Black Holes in Supermassive and Intermediate-mass Black Hole Binaries

Xiao-Jun Wu,^{1,2} Ye-Fei Yuan,^{3,4*} Yan Luo,^{3,4} and Wenbin Lin^{1,5†}

¹*School of Mathematics and Physics, University of South China, Hengyang, 421001, China*

²*School of Nuclear Science and Technology, University of South China, Hengyang 421001, China*

³*School of Astronomy and Space Science, University of Science and Technology of China, Hefei 230026, China*

⁴*CAS Key Laboratory for Research in Galaxies and Cosmology, University of Science and Technology of China, Hefei 230026, China*

⁵*School of Physical Science and Technology, Southwest Jiaotong University, Chengdu, 610031, China*

Accepted XXX. Received YYY; in original form ZZZ

ABSTRACT

In the centers of galaxies, stars that orbit supermassive black hole binaries (SMBHs) can undergo tidal disruptions due to the Lidov-Kozai mechanism. Nevertheless, most previous researches have predominantly focused on full tidal disruption events (FTDEs). In this study, we employ N-body simulations to investigate partial tidal disruption events (PTDEs) induced by intermediate-mass black holes (IMBHs) in SMBH-IMBH binaries, taking into account consideration the IMBH's mass, semi-major axis, and eccentricity of the outer orbit. Our findings indicate that, in comparison to FTDEs, the majority of tidal disruption events are actually PTDEs. Furthermore, we find that a significant number of stars experiencing partial disruption ultimately get captured by the IMBH, potentially leading to repeating flares. By comparing the period of the periodic eruptions observed in ASASSN-14ko, we find that PTDEs in a specific SMBH-IMBH binary system can align with the observed period if the SMBH has a mass of $10^7 M_{\odot}$, the IMBH has a mass smaller than approximately $10^5 M_{\odot}$, the eccentricity of the SMBH-IMBH binary exceeds approximately 0.5, and the semi-major axis of the SMBH-IMBH binary is larger than approximately 0.001 pc. Moreover, our model effectively accounts for the observed period derivative for ASASSN-14ko ($\dot{P} = -0.0026 \pm 0.0006$), and our results also imply that some quasi-periodic eruptions may be attributed to PTDEs occurring around SMBH-IMBH binaries.

Key words: stars: kinematics and dynamics – Galaxy: centre – Galaxy: kinematics and dynamics – transients: tidal disruption events – methods: numerical

1 INTRODUCTION

When stars approach too close towards a supermassive black hole (SMBH), they could be tidally disrupted by the SMBH, giving rise to multiband flares from X-rays to radio bands (e.g., Bade et al. 1996; Komossa & Greiner 1999; Esquej et al. 2008; Komossa et al. 2008; Bloom et al. 2011; van Velzen et al. 2011, 2016; Cenko et al. 2012; Anderson et al. 2020; Goodwin et al. 2023). This phenomenon is known as a tidal disruption event (TDE) (Rees 1988). If a star is completely destroyed during the process, it is referred to as a full TDE (FTDE), while if only a partial destruction occurs, leaving behind a remnant, it is termed a partial TDE

(PTDE). For PTDEs, the remnants can acquire a kick velocity due to the asymmetry in mass loss during the disruption process (Manukian et al. 2013). If the orbital energy of the remnants is insufficient to overcome the gravitational potential of the SMBH, they will orbit the SMBH in a bound trajectory and may undergo subsequent PTDEs or FTDEs.

There are several candidates that have been proposed as potential results of PTDEs, including HLX-1 (Lasota et al. 2011), IC 3599 (Campana et al. 2015; Grupe et al. 2015), AT 2018hyz (Gomez et al. 2020), AT2018fyk (Wewers et al. 2023), ASASSN-14ko (Payne et al. 2021), Swift J023017.0+283603 (Evans et al. 2023; Guolo et al. 2024), eRASSt J045650.3-203750 (Liu et al. 2023), and X-ray quasi-periodic eruptions (QPEs) (e.g. Miniutti et al. 2019; Giustini et al. 2020; Song et al. 2020; Arcodia et al. 2021; Chakraborty et al. 2021).

* Corresponding author. E-mail: yfyuan@ustc.edu.cn

† Corresponding author. E-mail: lwb@usc.edu.cn

Asymptotic Persistence of Langmuir modes in Kinematically Complex Plasma Flows

Ketevan Arabuli • Andria Rogava

Abstract Dynamics of Langmuir modes - Langmuir waves (LW) and shear Langmuir vortices (SLV) - in kinematically complex astrophysical plasma flows is studied. It is found that they exhibit a number of peculiar, velocity shear induced, *asymptotically persistent* phenomena: efficient energy exchange with the background flow, various kinds of instabilities, leading to their exponential growth; echoing solutions with persistent wave-vortex-wave conversions. Remarkable similarity of these phenomena with ones happening with compressible acoustic modes, revealed in (Mahajan and Rogava 1999) is pointed out. The relevance and possible importance of these phenomena for different types of astrophysical plasma flow patterns with kinematic complexity is discussed. In particular, we argue that these physical processes may account for the persistent appearance of plasma oscillations in the heliosphere and in interstellar plasma flows. In particular, we believe that kinematically complex motion of plasma may naturally lead to asymptotically persistent appearance of Langmuir modes born, grown, fed, sustained and maintained by these flows.

Keywords astrophysical plasmas; shear flows; plasma waves; heliosphere; interstellar plasma

1 Introduction

It is widely known that both the wave and the vortical modes of motion are common in many different kinds of astronomical objects. Since the visible universe is predominantly made of plasma it is obvious that the study

of both the wave and the vortical motions in plasma flows is of key importance in theoretical astrophysics. In a larger perspective, for several decades, vortex dynamics is widely recognized as a fundamental interdisciplinary scientific problem (Saffman 1993). Remarkably, there is a considerable degree of similarity between the vortices in plasmas and neutral fluids (Petviashvili 1980; Horton and Hasegawa 1994). Usually vortical motions in plasmas are associated with complicated, highly nonlinear systems. But with the gradual disclosure of so called *nonmodal* phenomena in neutral fluid shear flows (Kelvin 1887; Goldreich and Lynden-Bell 1965; Trefethen et al. 1993) it became increasingly clear that even on the linear level there exists a number of interesting shear-induced effects associated with the vortex and wave linear dynamics both in neutral fluid and plasma shear flows (Mahajan and Rogava 1999). These phenomena are characterized by intense energy exchange between the wave and the vortical modes and the background flow.

The importance of velocity shear induced phenomena in astrophysics is widely known, acknowledged and extensively discussed for several decades in a broad variety of important classes of astrophysical flows. The incomplete list of astronomical situations, where these phenomena have been considered includes: density waves in galaxies (Goldreich and Lynden-Bell 1965; Toomre 1969; Goldreich and Tremaine 1978; Fan and qing Lou 1997; Rogava et al. 1999; Poedts and Rogava 2002); transiently growing incompressible modes in accretion discs (Lominadze et al. 1988; Balbus and Hawley 1992; Tagger et al. 1992); reciprocal transformations of solar magnetohydrodynamic (MHD) waves and their role in the acceleration of the solar wind (Poedts et al. 1998; Rogava et al. 2000). It was also found out that within relativistic pulsar magnetospheric e^+e^- plasmas transformation of non-escaping longitudinal Langmuir modes into escaping electromagnetic waves

Ketevan Arabuli

KU Leuven, Leuven, Belgium

Andria Rogava

Institute for Theoretical Physics, Ilia State University, G. Tsereteli 3, 0162 Tbilisi, Georgia

Resolved Near-infrared Stellar Photometry from the Magellan Telescope for 13 Nearby Galaxies: JAGB Method Distances

ABIGAIL J. LEE,^{1,2} ANDREW J. MONSON,³ WENDY L. FREEDMAN,^{1,2} BARRY F. MADORE,^{4,1} KAYLA A. OWENS,^{1,2}
RACHAEL L. BEATON,^{5,6} CORAL ESPINOZA,^{7,1} TONGTIAN REN,⁸ AND YI REN⁹

¹*Department of Astronomy & Astrophysics, University of Chicago, 5640 South Ellis Avenue, Chicago, IL 60637*

²*Kavli Institute for Cosmological Physics, University of Chicago, 5640 South Ellis Avenue, Chicago, IL 60637*

³*Steward Observatory, The University of Arizona, 933 N. Cherry Avenue, Tucson, AZ 85721, USA*

⁴*Observatories of the Carnegie Institution for Science 813 Santa Barbara St., Pasadena, CA 91101*

⁵*Space Telescope Science Institute, Baltimore, MD, 21218, USA*

⁶*Department of Physics and Astronomy, Johns Hopkins University, Baltimore, MD 21218, USA*

⁷*Lake Forest College Physics Department, Lake Forest, IL 60045*

⁸*Jodrell Bank Centre for Astrophysics, University of Manchester, Oxford Road, Manchester, M13 9PL, UK*

⁹*College of Physics and Electronic Engineering, Qilu Normal University, Jinan 250200, China*

ABSTRACT

We present near-infrared *JHK* photometry for the resolved stellar populations in 13 nearby galaxies: NGC 6822, IC 1613, NGC 3109, Sextans B, Sextans A, NGC 300, NGC 55, NGC 7793, NGC 247, NGC 5253, Cen A, NGC 1313, and M83, acquired from the 6.5m Baade-Magellan telescope. We measure distances to each galaxy using the J-region asymptotic giant branch (JAGB) method, a new standard candle that leverages the constant luminosities of color-selected, carbon-rich AGB stars. While only single-epoch, random-phase photometry is necessary to derive JAGB distances, our photometry is time-averaged over multiple epochs, thereby decreasing the contribution of the JAGB stars' intrinsic variability to the measured dispersions in their observed luminosity functions. To cross-validate these distances, we also measure near-infrared tip of the red giant branch (TRGB) distances to these galaxies. The residuals obtained from subtracting the distance moduli from the two methods yield an RMS scatter of $\sigma_{JAGB-TRGB} = \pm 0.07$ mag. Therefore, all systematics in either the JAGB method and TRGB method (e.g., crowding, differential reddening, star formation histories) must be contained within these ± 0.07 mag bounds for this sample of galaxies because the JAGB and TRGB distance indicators are drawn from entirely distinct stellar populations, and are thus affected by these systematics independently. Finally, the composite JAGB star luminosity function formed from this diverse sample of galaxies is well-described by a Gaussian function with a modal value of $M_J = -6.20 \pm 0.003$ mag (stat), indicating the underlying JAGB star luminosity function of a well-sampled full star formation history is highly symmetric and Gaussian, based on over 6,700 JAGB stars in the composite sample.

Keywords: Observational astronomy (1145), Near-infrared astronomy (1093), Distance indicators (394), Asymptotic Giant Branch stars (2100), Carbon stars (199), Galaxy distances (590), Red giant branch (1368)

1. INTRODUCTION

Carbon stars were first serendipitously discovered more than 150 years ago by Father Secchi at the Vatican Observatory, when he noticed the similarity in the spectra between a small group of peculiarly red stars and

the light in carbon arc lights¹ (Secchi 1868). More than 100 years later, Richer (1981) laid the path for carbon stars as standard candles when he realized that the carbon star bolometric luminosity function was bright and fairly symmetric. Soon after, Cook et al. (1986) speculated the carbon star luminosity function could be used as a distance indicator after observing the similarities

Corresponding author: Abigail J. Lee
abbyl@uchicago.edu

¹ The first practical electrical lights.

Physical Pathways for JWST-Observed Supermassive Black Holes in the Early Universe

JUNEHYOUNG JEON ¹, VOLKER BROMM ^{1,2}, BOYUAN LIU ³, AND STEVEN L. FINKELSTEIN ¹

¹*Department of Astronomy, University of Texas, Austin, TX 78712, USA*

²*Weinberg Institute for Theoretical Physics, University of Texas, Austin, TX 78712, USA*

³*University of Cambridge Institute of Astronomy: Cambridge, Cambridgeshire, GB*

ABSTRACT

Observations with the *James Webb Space Telescope (JWST)* have revealed active galactic nuclei (AGN) powered by supermassive black holes with estimated masses of $10^7 - 10^8 M_{\odot}$ at redshifts $z \sim 7 - 9$. Some reside in overmassive systems with higher AGN to stellar mass ratios than locally. Understanding how massive black holes could form so early in cosmic history and affect their environment to establish the observed relations today are some of the major open questions in astrophysics and cosmology. One model to create these massive objects is through direct collapse black holes (DCBHs) that provide massive seeds ($\sim 10^5 - 10^6 M_{\odot}$), able to reach high masses in the limited time available. We use the cosmological simulation code GIZMO to study the formation and growth of DCBH seeds in the early Universe. To grow the DCBHs, we implement a gas swallowing model that is set to match the Eddington accretion rate as long as the nearby gaseous environment, affected by stellar and accretion disk feedback, provides sufficient fuel. We find that to create massive AGN in overmassive systems at high redshifts, massive seeds accreting more efficiently than the fiducial Bondi-Hoyle model are needed. We assess whether the conditions for such enhanced accretion rates are realistic by considering limits on plausible transport mechanisms. We also examine various DCBH growth histories and find that mass growth is more sustained in overdense cosmological environments, where high gas densities are achieved locally. We discuss the exciting prospect to directly probe the assembly history of the first SMBHs with upcoming, ultra-deep *JWST* surveys.

Keywords: Early universe — Galaxy formation — Supermassive black holes — Active galactic nuclei — Theoretical models

1. INTRODUCTION

How did accreting supermassive black holes (SMBHs) or active galactic nuclei (AGN) impact early cosmic history (Woods et al. 2019)? The expectation is that they were abundant in the high- z Universe, to be detected in ongoing and future surveys (Volonteri et al. 2017; Li et al. 2023; Spurzem et al. 2023; Eolyn Evans et al. 2023), unless they are obscured or too faint to be discovered (Smith et al. 2019; Gilli et al. 2022; Goulding & Greene 2022; Jeon et al. 2023). The recent influx of new observations with the *James Webb Space Telescope (JWST)* confirmed such predictions and revealed a large number of active galactic nuclei (AGN) in the early Universe (e.g. Kocevski et al. 2023; Ding et al. 2022; Larson

et al. 2023; Onoue et al. 2023; Furtak et al. 2023; Bogdán et al. 2023; Juodžbalis et al. 2023; Bosman et al. 2023; Greene et al. 2023; Kokorev et al. 2023; Fujimoto et al. 2023; Maiolino et al. 2023a).

These new observations help reveal the nature of early cosmic evolution, as AGN influence their environment and host galaxies through the large amounts of energy released. In the local Universe, we observe relationships between the AGN and host galaxy/halo properties, including the SMBH mass and stellar velocity dispersion ($M - \sigma$) (Gebhardt et al. 2000; Graham et al. 2011; Kormendy & Ho 2013), SMBH mass and galaxy luminosity (Beifiori et al. 2012), or between the masses of the SMBH and stellar component (Croton 2006; Ding et al. 2020). Such observed relations further suggest that AGN and their host galaxies co-evolve (Heckman & Best 2014). When and how these relationships were established can be investigated with the new high-redshift

METAL-Z: Measuring dust depletion in low metallicity dwarf galaxies

ALEKSANDRA HAMANOWICZ ¹, KIRILL TCHERNYSHYOV ², JULIA ROMAN-DUVAL ¹, EDWARD B. JENKINS ³,
MARC RAFELSKI ¹, KARL D. GORDON ¹, YONG ZHENG ⁴, MIRIAM GARCIA ⁵ AND JESSICA WERK ²

¹*Space Telescope Science Institute, 3700 San Martin Drive, Baltimore, MD 21218, USA*

²*Department of Astronomy, Box 351580, University of Washington, Seattle, WA 98195, USA*

³*Department of Astrophysical Sciences, Princeton University, Princeton, NJ 08544-1001, USA*

⁴*Department of Physics, Applied Physics, and Astronomy, Rensselaer Polytechnic Institute, 110 8th St, Troy, NY 12180*

⁵*Centro de Astrobiología, CSIC-INTA, Dpto. de Astrofísica, Instituto Nacional de Técnica Aeroespacial, Ctra. de Torrejón a Ajalvir, km 4, 28850 Torrejón de Ardoz (Madrid), Spain*

ABSTRACT

The cycling of metals between interstellar gas and dust is a critical aspect of the baryon cycle of galaxies, yet our understanding of this process is limited. This study focuses on understanding dust depletion effects in the low metallicity regime ($< 20\%Z_{\odot}$) typical of cosmic noon. Using medium-resolution UV spectroscopy from the COS onboard the *Hubble Space Telescope*, gas-phase abundances and depletions of iron and sulfur were derived toward 18 sightlines in local dwarf galaxies IC 1613 and Sextans A. The results show that the depletion of Fe and S is consistent with that found in the Milky Way, LMC and SMC. The depletion level of Fe increases with gas column density, indicating dust growth in the interstellar medium (ISM). The level of Fe depletion decreases with decreasing metallicity, resulting in the fraction of iron in gas ranging from 3% in the MW to 9% in IC 1613 and $\sim 19\%$ in Sextans A. The dust-to-gas and dust-to-metal ratios (D/G, D/M) for these dwarf galaxies were estimated based on the MW relations between the depletion of Fe and other elements. The study finds that D/G decreases only slightly sub-linearly with metallicity, with D/M decreasing from 0.41 ± 0.05 in the MW to 0.11 ± 0.11 at $0.10 Z_{\odot}$ (at $\log N(\text{H}) = 21 \text{ cm}^{-2}$). The trend of D/G vs. metallicity using depletion in local systems is similar to that inferred in Damped Ly- α systems from abundance ratios but lies higher than the trend inferred from FIR measurements in nearby galaxies.

Keywords: Interstellar medium (847), Interstellar dust processes (823), Galaxy chemical evolution (580), Gas-to-dust ratio (638), Interstellar abundances (832)

1. INTRODUCTION

Despite amounting to only a small fraction of the Interstellar Medium (ISM) mass, metals play a significant role in the evolution of galaxies. Formed in stellar interiors and explosions, metals gradually enrich the ISM and influence galaxies' properties and evolution through their effects on heating and cooling, radiative transfer, and chemistry. In particular, interstellar dust, the main constituents of which are carbon, oxygen, silicon, magnesium, and iron, absorbs stellar radiation in the optical and UV and re-emits it in the FIR, affecting galaxies' Spectral Energy Distribution (SED). The opacity of dust

versus wavelength, in turn, depends on the composition and size of dust grains (e.g., Gordon et al. 2003; Demyk et al. 2017a,b; Ysard et al. 2018). As a result, we need to understand the dust abundance and properties to correctly “de-redden” galaxy SEDs, infer their star formation histories and stellar populations, as well as to convert FIR emission into dust and gas masses, a common and very effective way to trace the ISM at all redshifts (Hildebrand 1983; Bolatto et al. 2011; Eales et al. 2012; Schrubba et al. 2012; Rowlands et al. 2012, 2014).

The abundance of dust and the fraction of metals locked onto dust grains is described by the dust-to-gas (D/G) and dust-to-metal (D/M) ratios ($D/G = D/M \times Z$, where Z is the metallicity of the system). These parameters are expected to vary with environment, es-

Small and Large Dust Cavities in Disks around mid-M Stars in Taurus

YANGFAN SHI (施杨帆) ^{1,2,3} FENG LONG (龙凤) ^{4,*} GREGORY J. HERCZEG (沈雷歌) ^{1,2} DANIEL HARSONO ⁵
YAO LIU ⁶ PAOLA PINILLA ⁷ ENRICO RAGUSA ^{8,9} DOUG JOHNSTONE ^{10,11} XUE-NING BAI ¹² ILARIA PASCUCCI ¹³
CARLO F. MANARA ³ GIJS D. MULDER ^{14,15} AND LUCAS A. CIEZA ¹⁶

¹Kavli Institute for Astronomy and Astrophysics, Peking University, Beijing 100871, China

²Department of Astronomy, Peking University, Beijing 100871, China

³European Southern Observatory, Karl-Schwarzschild-Str. 2, D-85748 Garching bei München, Germany

⁴Lunar and Planetary Laboratory, University of Arizona, Tucson, AZ 85721, USA

⁵Institute of Astronomy, Department of Physics, National Tsing Hua University, Hsinchu, Taiwan

⁶Purple Mountain Observatory & Key Laboratory for Radio Astronomy, Chinese Academy of Sciences, Nanjing 210023, China

⁷Mullard Space Science Laboratory, University College London, Holmbury St Mary, Dorking, Surrey RH5 6NT, UK

⁸Dipartimento di Matematica, Università degli Studi di Milano, Via Saldini 50, 20133, Milano, Italy

⁹Univ Lyon, Univ Lyon1, Ens de Lyon, CNRS, Centre de Recherche Astrophysique de Lyon UMR5574, F-69230 Saint-Genis-Laval, France

¹⁰NRC Herzberg Astronomy and Astrophysics, 5071 West Saanich Rd, Victoria, BC, V9E 2E7, Canada

¹¹Department of Physics and Astronomy, University of Victoria, Victoria, BC, V8P 5C2, Canada

¹²Institute for Advanced Study and Department of Astronomy, Tsinghua University, 100084, Beijing, China

¹³Lunar and Planetary Laboratory, the University of Arizona, Tucson, AZ 85721, USA

¹⁴Facultad de Ingeniería y Ciencias, Universidad Adolfo Ibáñez, Av. Diagonal las Torres 2640, Peñalolén, Santiago, Chile

¹⁵Millennium Institute for Astrophysics, Chile

¹⁶Instituto de Estudios Astrofísicos, Facultad de Ingeniería y Ciencias, Universidad Diego Portales, Av. Ejército 441, Santiago, Chile

ABSTRACT

High-angular resolution imaging by ALMA has revealed the near-universality and diversity of substructures in protoplanetary disks. However, disks around M-type pre-main-sequence stars are still poorly sampled, despite the prevalence of M-dwarfs in the galaxy. Here we present high-resolution (~ 50 mas, 8 au) ALMA Band 6 observations of six disks around mid-M stars in Taurus. We detect dust continuum emission in all six disks, ^{12}CO in five disks, and ^{13}CO line in two disks. The size ratios between gas and dust disks range from 1.6 to 5.1. The ratio of about 5 for 2M0436 and 2M0450 indicates efficient dust radial drift. Four disks show rings and cavities and two disks are smooth. The cavity sizes occupy a wide range: 60 au for 2M0412, and ~ 10 au for 2M0434, 2M0436 and 2M0508. Detailed visibility modeling indicates that small cavities of 1.7 and 5.7 au may hide in the two smooth disks 2M0450 and CIDA 12. We perform radiative transfer fitting of the infrared SEDs to constrain the cavity sizes, finding that micron-sized dust grains may have smaller cavities than millimeter grains. Planet-disk interactions are the preferred explanation to produce the large 60 au cavity, while other physics could be responsible for the three ~ 10 au cavities under current observations and theories. Currently, disks around mid-to-late M stars in Taurus show a higher detection frequency of cavities than earlier type stars, although a more complete sample is needed to evaluate any dependence of substructure on stellar mass.

Keywords: Protoplanetary disks (1300); Planetary-disk interactions (2204); Planetary system formation (1257)

1. INTRODUCTION


The discovery to date of over 5000 exoplanets reveals that planetary systems occupy a wide parameter space in architecture (Zhu & Dong 2021). In planetary systems around low-mass stars (e.g., lower than $0.4 M_{\odot}$), small planets occur more frequently than those around solar-mass stars (e.g.,

Mulders et al. 2015; Hardegree-Ullman et al. 2019), while giant planets around those low-mass stars are rare (but have a non-zero occurrence rate, e.g., Bryant et al. 2023).

The existence of a few giant planets around mid-to-late (later than M3) M stars has challenged the core accretion planet formation theory (e.g., Morales et al. 2019; Stefánsson et al. 2023). Planet population synthesis simulations often fail to form any giant planet around these very low-mass stars, in both the planetesimal accretion case (e.g., Miguel

* NASA Hubble Fellowship Program Sagan Fellow

Exploring the distribution and impact of bosonic dark matter in neutron stars

Davood Rafiei Karkevandi ^{1,2,*} , Mahboubeh Shahrbafe ^{3,4} , Soroush Shakeri ^{1,2} , and Stefan Typel ^{5,6} 

- ¹ Department of Physics, Isfahan University of Technology, Isfahan 84156-83111, Iran; d.rafiee@alumni.iut.ac.ir; s.shakeri@iut.ac.ir
² ICRANet-Isfahan, Isfahan University of Technology, 84156-83111, Iran.
³ Incubator of Scientific Excellence–Centre for Simulations of Superdense Fluids, University of Wroclaw; m.shahrbafe46@gmail.com
⁴ Frankfurt Institute for Advanced Studies, Ruth-Moufang-Str. 1, D-60438 Frankfurt am Main, Germany.
⁵ Technische Universität Darmstadt, Fachbereich Physik, Institut für Kernphysik, Schlossgartenstraße 9, D-64289 Darmstadt, Germany; stypel@ikp.tu-darmstadt.de
⁶ GSI Helmholtzzentrum für Schwerionenforschung GmbH, Theorie, Planckstraße 1, D-64291 Darmstadt, Germany.
* Correspondence: d.rafiee@alumni.iut.ac.ir

Abstract: The presence of dark matter (DM) within neutron stars (NSs) can be introduced by different accumulation scenarios in which DM and baryonic matter (BM) may interact only through the gravitational force. In this work, we consider asymmetric self-interacting bosonic DM which can reside as a dense core inside the NS or form an extended halo around it. It is seen that depending on the boson mass (m_χ), self-coupling constant (λ) and DM fraction (F_χ), the maximum mass, radius and tidal deformability of NSs with DM admixture will be altered significantly. The impact of DM causes some modifications in the observable features induced solely by the BM component. Here, we focus on the widely used nuclear matter equation of state (EoS) called DD2 for describing NS matter. We show that by involving DM in NSs, the corresponding observational parameters will be changed to be consistent with the latest multi-messenger observations of NSs. It is seen that for $m_\chi \gtrsim 200$ MeV and $\lambda \lesssim 2\pi$, DM admixed NSs with $4\% \lesssim F_\chi \lesssim 20\%$ are consistent with the maximum mass and tidal deformability constraints.

Keywords: Bosonic Dark matter, Neutron star, Two-fluid TOV equations, Tidal deformability

1. Introduction

Owing to the fact that DM constitutes the majority of matter in galaxies, several noteworthy ideas have been proposed about the presence of DM inside compact astrophysical objects [1–9]. Among them, NSs, due to their content of high-density matter and extreme gravitational potential, provide an interesting astronomical environment where sizeable amounts of DM may be accumulated based on various scenarios [10–14]. In this regard, the accretion of DM might occur during star evolution or over the lifetime of a NS. It is argued that high capture rates are more likely to happen towards the center of galaxies, where the density of DM is increasing [15–17]. Moreover, DM production inside NSs and supernova explosions can lead to large values of the DM fraction [5,6,18,19]. Among various models, a neutron decay anomaly by assuming a dark sector attracts considerable attention [20–22]. It is notable to say that gravitationally stable objects so-called dark stars, may be formed entirely from DM [23–26], which can be considered as a capturing center for BM or even merge with NSs resulting in the formation of a mixed compact object [5,27,28].

In recent years, multi-messenger observations of NSs, have provided a unique opportunity to probe their internal structure and the possible existence of exotic configurations including DM [29,30]. The impact of DM on NS properties has been investigated in various studies proposing a wide range of smoking guns [31–37]. Generally, the presence of DM

Citation: Rafiei Karkevandi, D.; Shahrbafe, M.; Shakeri, S.; Typel, S. Exploring the distribution and impact of bosonic dark matter in neutron stars. *Journal Not Specified* **2023**, *1*, 0. <https://doi.org/>

Received:
Revised:
Accepted:
Published:

Copyright: © 2024 by the authors. Submitted to *Journal Not Specified* for possible open access publication under the terms and conditions of the Creative Commons Attribution (CC BY) license (<https://creativecommons.org/licenses/by/4.0/>).

A Light Sail Astrobiology Precursor Mission to Enceladus and Europa

Manasvi Lingam^{a,b,*}, Adam Hibberd^c and Andreas M. Hein^{d,c}

^aDepartment of Aerospace, Physics and Space Sciences, Florida Institute of Technology, Melbourne, 32901, FL, USA

^bDepartment of Physics and Institute for Fusion Studies, The University of Texas at Austin, Austin, 78712, TX, USA

^cInitiative for Interstellar Studies (i4is), 27/29 South Lambeth Road, London, SW8 1SZ, UK

^dSnT, University of Luxembourg, 29 Avenue J.F. Kennedy, L-1855, Luxembourg

ARTICLE INFO

Keywords:

astrobiology
biosignatures
flyby missions
deep space exploration
light sails
Enceladus
Europa

ABSTRACT

Icy moons with subsurface oceans of liquid water rank among the most promising astrobiological targets in our Solar System. In this work, we assess the feasibility of deploying laser sail technology in precursor life-detection missions. We investigate such laser sail missions to Enceladus and Europa, as these two moons emit plumes that seem accessible to in situ sampling. Our study suggests that GigaWatt laser technology could accelerate a 100 kg probe to a speed of $\sim 30 \text{ km s}^{-1}$, thereupon reaching Europa on timescales of 1-4 years and Enceladus with flight times of 3-6 years. Although the ideal latitudes for the laser array vary, placing the requisite infrastructure close to either the Antarctic or Arctic Circles might represent technically viable options for an Enceladus mission. Crucially, we determine that the minimum encounter velocities with these moons (about 6 km s^{-1}) may be near-optimal for detecting biomolecular building blocks (e.g., amino acids) in the plumes by means of a mass spectrometer akin to the Surface Dust Analyzer onboard the *Europa Clipper* mission. In summary, icy moons in the Solar System are potentially well-suited for exploration via the laser sail architecture approach, especially where low encounter speeds and/or multiple missions are desirable.

1. Introduction

Resolving the fundamental question of “*Are we alone?*” has witnessed much progress in the 21st century [1, 2, 3, 4, 5, 6, 7, 8, 9]. In particular, a significant amount of attention has been devoted to the so-called icy worlds – also known as ocean worlds – in our Solar System (e.g., Enceladus, Titan, and Europa) that are empirically confirmed to harbor subsurface oceans of liquid water, which is one of the key requirements for life-as-we-know-it [10, 11, 12, 13, 14, 15, 16]. Hence, these worlds are widely perceived as promising abodes of extraterrestrial life.

Among these icy worlds, Saturn’s small moon Enceladus (with radius of $\sim 250 \text{ km}$) stands out by virtue of the wealth of data garnered by the *Cassini-Huygens* mission [17]. Enceladus not only hosts liquid water underneath its surface [18, 19, 20], but also satisfies the other major criteria for habitability [21, 22, 23], such as free energy sources [24, 25, 26, 27] and bioessential elements [28, 29, 30].¹ Furthermore, the discovery and modeling of submarine hydrothermal activity is promising [24, 35, 25], because these environments are considered viable sites for engendering prebiotic chemistry and the origin(s) of life [36, 37, 38, 39, 40, 41]. A number of theoretical [42, 43, 44, 45, 46, 47, 27] and experimental [48, 49, 50] studies indicate that Enceladus’ internal ocean might be habitable for various species of Earth-based microbes (e.g., hydrogenotrophic methanogens).

Jupiter’s moon, Europa, harbors a deep subsurface ocean that ostensibly contains more liquid water than all of Earth’s oceans combined [4, 6]. The habitability of Europa’s subsurface ocean has been extensively investigated, and while not as much empirical data is available (in comparison to Enceladus), this moon is also presumed to satisfy most of the salient requirements in this respect [e.g., 51, 52, 53, 54, 55, 56, 57, 58, 59, 60, 5, 61, 62, 27, 9]. The upcoming *Europa Clipper* mission [63, 64],² and the *JUICE* mission to a comparatively lesser extent [65, 66],³ will significantly enhance our knowledge of Europa’s subsurface ocean.

A striking feature of Enceladus is the existence of a substantial (time-varying) plume [67, 68, 69, 70], which extends up to $\sim 10^4 \text{ km}$ [71]. Likewise, there is evidence for plumes on Europa [72, 73, 74, 75, 76], although these features may be transient [77, 78, 79] and/or harder to detect [80, 81]. The access to plume samples would be valuable because they can shed light on the habitability of the subsurface ocean, as well as potentially enable the detection of molecular biosignatures (i.e., markers of life) [82, 83, 84, 85, 86, 87, 88], although unraveling the latter has attendant caveats, subtleties, and lacunae [89, 90, 91, 92, 93, 94, 95].

A variety of putative life-detection missions to Enceladus have thus been proposed in the 2020s [96, 97, 98, 99, 100],⁴ many of which have acquired greater relevance in light of the strong recommendation made by the comprehensive 2023-2032 *Decadal Strategy for Planetary Science and Astrobiology* for a flagship mission to Enceladus that would arrive at this moon in the early 2050s [102, pg. 7]. The mission concept highlighted in the Decadal Strategy was the

*Corresponding author

✉ mlingam@fit.edu (M. Lingam)

ORCID(S): 0000-0002-2685-9417 (M. Lingam); 0000-0003-1116-576X (A. Hibberd); 0000-0003-1763-6892 (A.M. Hein)

¹Previous models suggested that dissolved phosphorus might be scarce in Enceladus’ ocean [31, 32], but this prediction has been overturned by recent empirical and computational findings [33, 30, 34].

²<https://europa.nasa.gov/>

³https://www.esa.int/Science_Exploration/Space_Science/Juice

⁴Similar recommendations have been advanced for Europa, such as the *Europa Lander* mission concept [101].

The Dark Energy Survey 5-year photometrically classified type Ia supernovae without host-galaxy redshifts

A. Möller^{1,2*}, P. Wiseman³, M. Smith⁴, C. Lidman^{5,6}, T. M. Davis⁷, R. Kessler^{8,9}, M. Sako¹⁰, M. Sullivan³, L. Galbany^{11,12}, J. Lee¹⁰, R. C. Nichol¹³, B. O. Sánchez¹⁴, B. E. Tucker⁵, T. M. C. Abbott¹⁵, M. Agüena¹⁶, S. Allam¹⁷, O. Alves¹⁸, F. Andrade-Oliveira¹⁸, D. Bacon¹⁹, E. Bertin^{20,21}, D. Brooks²², A. Carnero Rosell^{16,23,24}, F. J. Castander^{11,12}, S. Desai²⁵, H. T. Diehl¹⁷, S. Everett²⁶, I. Ferrero²⁷, D. Friedel²⁸, J. Frieman^{8,17}, J. García-Bellido²⁹, E. Gaztanaga^{11,12,19}, G. Giannini^{8,30}, R. A. Gruendl^{28,31}, G. Gutierrez¹⁷, S. R. Hinton⁷, D. L. Hollowood³², K. Honscheid^{33,34}, D. J. James³⁵, K. Kuehn^{36,37}, O. Lahav²², S. Lee²⁶, J. L. Marshall³⁸, J. Mena-Fernández³⁹, F. Menanteau^{28,31}, R. Miquel^{30,40}, J. Myles⁴¹, R. L. C. Ogando⁴², A. Palmese⁴³, A. Pieres^{16,42}, A. A. Plazas Malagón^{44,45}, A. Roodman^{44,45}, E. Sanchez⁴⁶, D. Sanchez Cid⁴⁶, I. Sevilla-Noarbe⁴⁶, E. Suchyta⁴⁷, M. E. C. Swanson²⁸, G. Tarle¹⁸, D. L. Tucker¹⁷, M. Vincenzi^{3,19}, A. R. Walker¹⁵, N. Weaverdyck^{18,48}, L. N. da Costa¹⁶, M. E. S. Pereira⁴⁹

Affiliations are listed at the end of the paper

Accepted XXX. Received YYY; in original form ZZZ

ABSTRACT

Current and future Type Ia Supernova (SN Ia) surveys will need to adopt new approaches to classifying SNe and obtaining their redshifts without spectra if they wish to reach their full potential. We present here a novel approach that uses only photometry to identify SNe Ia in the 5-year Dark Energy Survey (DES) dataset using the SUPERNNOVA classifier. Our approach, which does not rely on any information from the SN host-galaxy, recovers SNe Ia that might otherwise be lost due to a lack of an identifiable host.

We select 2,298 high-quality SNe Ia from the DES 5-year dataset. More than 700 of these have no spectroscopic host redshift and are potentially new SNIa compared to the DES-SN5YR cosmology analysis. To analyse these SNe Ia, we derive their redshifts and properties using only their light-curves with a modified version of the SALT2 light-curve fitter. Compared to other DES SN Ia samples with spectroscopic redshifts, our new sample has in average higher redshift, bluer and broader light-curves, and fainter host-galaxies.

Future surveys such as LSST will also face an additional challenge, the scarcity of spectroscopic resources for follow-up. When applying our novel method to DES data, we reduce the need for follow-up by a factor of four and three for host-galaxy and live SN respectively compared to earlier approaches. Our novel method thus leads to better optimisation of spectroscopic resources for follow-up.

Key words: surveys – supernovae:general – cosmology:observations – methods:data analysis

1 INTRODUCTION

Type Ia Supernovae (SNe Ia) are crucial tools to directly measure the cosmic expansion and constrain Dark Energy models. Surveys such as the Dark Energy Survey (DES) and Zwicky Transient Facility (ZTF) have already discovered thousands of SNe Ia and other optical transients (Bellm et al. 2018; Bernstein et al. 2012). The upcoming Vera C. Rubin Observatory will provide up to 10 million

transient and variable detections every night (Rubin, LSST Science Collaboration 2009). During its 10 year Legacy Survey of Space and Time (LSST) it will detect more than a million SNe which can be used to make precise measurements of the equation-of-state parameter of Dark Energy. To constrain cosmological parameters, SNe Ia first need to be accurately classified and redshifts need to be determined.

Traditionally, classification of SNe for cosmology is done using real-time spectroscopy as in the DES 3-year analysis and Pantheon+ (Abbott et al. 2019; Brout et al. 2022). However, spectroscopic re-

* E-mail: amoller@swin.edu.au

QRIS: A Quantitative Reflectance Imaging System for the Pristine Sample of Asteroid Bennu

Ruby E. Fulford¹, Dathon R. Golish¹, Dante S. Lauretta¹, Daniella N. DellaGiustina¹, Steve Meyer¹, Nicole Lunning², Christopher Snead², Jason P. Dworkin³, Carina A. Bennett¹, Harold C. Connolly, Jr.^{1,4,5}, Taylor Johnson⁶, Anjani T. Polit¹, Pierre Haenecour¹, and Andrew J. Ryan¹

¹Lunar and Planetary Laboratory, University of Arizona, Tucson, AZ, USA

²Astromaterials Research and Exploration Science Division, NASA Johnson Space Center, Houston, TX, USA

³Solar System Division, NASA Goddard Space Flight Center, Greenbelt, MD, USA

⁴Department of Geology, Rowan University, Glassboro, NJ, USA

⁵Department of Earth and Planetary Science, American Museum of Natural History, New York, NY, USA

⁶Dust Data Management, Tucson, AZ, USA

Submitted 28 February 2024

Abstract

The Quantitative Reflectance Imaging System (QRIS) is a laboratory-based spectral imaging system constructed to image the sample of asteroid Bennu delivered to Earth by the Origins, Spectral Interpretation, Resource Identification, and Security–Regolith Explorer (OSIRIS–REx) spacecraft. The system was installed in the OSIRIS–REx cleanroom at NASA’s Johnson Space Center to collect data during preliminary examination of the Bennu sample. QRIS uses a 12-bit machine vision camera to measure reflectance over wavelength bands spanning the near ultraviolet to the near infrared. Raw data are processed by a calibration pipeline that generates a series of monochromatic, high-dynamic-range reflectance images, as well as band ratio maps, band depth maps, and 3-channel color images. The purpose of these spectral reflectance data is to help characterize lithologies in the sample and compare them to lithologies observed on Bennu by the OSIRIS–REx spacecraft. This initial assessment of lithological diversity was intended to help select the subsamples that will be used to address mission science questions about the early solar system and the origins of life and to provide important context for the selection of representative subsamples for preservation and

JWST/MIRI unveils the stellar component of the GN20 dusty galaxy overdensity at $z=4.05$

A. Crespo Gómez¹, L. Colina¹, J. Álvarez-Márquez¹, A. Bik², L. Boogaard³, G. Östlin², F. Peißker⁴, F. Walter³, A. Labiano^{5,6}, P. G. Pérez-González¹, T. R. Greve^{7,8,9}, G. Wright¹⁰, A. Alonso-Herrero⁵, K. I. Caputi¹¹, L. Costantin¹, A. Eckart⁴, M. García-Marín¹², S. Gillman^{7,8}, J. Hjorth¹³, E. Iani¹¹, D. Langeroodi¹³, J. P. Pye¹⁴, P. Rinaldi¹¹, T. Tikkanen¹⁴, P. van der Werf¹⁵, P. O. Lagage¹⁶, and E. F. van Dishoeck¹⁵

(Affiliations can be found after the references)

Received ; accepted

ABSTRACT

Dusty star-forming galaxies (DSFGs) at $z > 2$ have been commonly observed in overdense regions, where the merging processes and large halo masses induce rapid gas accretion, triggering star-formation rates (SFRs) up to $\sim 1000 M_{\odot} \text{yr}^{-1}$. Despite the importance of these DSFGs for understanding the star-formation in the early Universe, their stellar distributions traced by the near-IR emission were spatially unresolved until the arrival of the JWST. In this work we present, for the first time, a spatially-resolved morphological analysis of the rest-frame near-IR ($\sim 1.1 - 3.5 \mu\text{m}$) emission in DSFGs traced with the JWST/MIRI F560W, F770W, F1280W and F1800W filters. In particular, we study the mature stellar component for the three DSFGs and a Lyman-break galaxy (LBG) present in an overdensity at $z = 4.05$. Moreover, we use these rest-frame near-IR images along with ultraviolet (UV) and (sub)-mm ancillary photometric data to model their spectral energy distributions (SEDs) and extract their main physical properties (e.g., M_* , SFR, A_V). The sub-arcsec resolution images from the JWST have revealed that the light distributions in these galaxies present a wide range of morphologies, from disc-like to compact and clump-dominated structures. Two DSFGs and the LBG are classified as late-type galaxies (LTGs) according to non-parametric morphological indices, while the remaining DSFG is an early-type galaxy (ETG). These near-IR structures contrast with their UV emission, which is diffuse and, in GN20 and GN20.2b, off-centered by ~ 4 kpc. This result suggests that the star-formation occurs across the entire galaxy, while the UV light traces only those regions where the otherwise high internal extinction decreases significantly. The SED fitting analysis yields large SFRs ($\sim 300 - 2500 M_{\odot} \text{yr}^{-1}$), large stellar masses ($\log(M_*/M_{\odot}) = 10.30 - 11.25$) and high integrated extinction values ($A_V = 0.8 - 1.5$ mag) for our galaxies. In particular, we observe that GN20 dominates the total SFR with a value $\sim 2500 M_{\odot} \text{yr}^{-1}$ while GN20.2b has the highest stellar mass ($M_* \sim 2 \times 10^{11} M_{\odot}$). The two DSFGs classified as LTGs (GN20 and GN20.2a) have high specific SFR ($\text{sSFR} > 30 \text{Gyr}^{-1}$) placing them above the star-forming main sequence (SFMS) at $z \sim 4$ by ~ 0.5 dex, while the ETG (i.e., GN20.2b) is compatible with the high-mass end of the main sequence. When comparing with other DSFGs in overdensities at $z \sim 2 - 7$, we observe that our objects present similar SFRs, depletion times and projected separations. Nevertheless, the effective radii computed for our DSFGs ($\sim 2 - 4$ kpc) are up to two times larger than those of isolated galaxies observed in CEERS and ALMA-HUDF at similar redshifts. We interpret this difference as an effect of rapid growth induced by the dense environment.

Key words. Infrared: galaxies - Galaxies: high-redshift - Galaxies: starburst - Galaxies: individual: GN20, GN20.2a, GN20.2b, BD29079

1. Introduction

Dusty star-forming galaxies (DSFGs) are massive, compact and extremely infrared-bright galaxies which are characterised by their intense starburst episodes, with star-formation rates (SFR) larger than $200 M_{\odot} \text{yr}^{-1}$ due to their large gas and dust reservoirs (see Casey et al. 2014, for a review). These starburst galaxies, previously classified as sub-millimetre galaxies (SMGs) due to their strong emission at these wavelengths (Smail et al. 1997; Barger et al. 1998; Hughes et al. 1998; Borys et al. 2003), are key to understand the star-formation history (SFH) across the Universe (see Madau & Dickinson 2014, for a review) as they dominate the cosmic star-formation at $z \sim 4$ (Pérez-González et al. 2005; Zavala et al. 2021). Additionally, these DSFGs are also important to understand the galaxy evolution, since they are thought to be the progenitors of massive quiescent galaxies at $z \sim 2$ (Valentino et al. 2020). Although DSFGs have a redshift distribution that peaks at $z \sim 2 - 3$ (Chapman et al. 2005), a significant number of DSFGs have been found at $z > 4$ (Walter et al. 2012; Riechers et al. 2013; Strandet et al. 2017; Zavala et al. 2021, 2023). At these redshifts, DSFGs can be widely observed as part of overdensities and proto-clusters (Daddi et al. 2009;

Riechers et al. 2010; Oteo et al. 2018; Pavesi et al. 2018). The presence of DSFGs in overdense regions is thought to be the reason for their extreme SFR and short depletion times, as the higher merger probability and larger halo mass would favour the gas accretion, triggering the star formation. In fact, the connection between DSFGs and galaxy overdensities has been shown to be more abundant in the early Universe (Smolčić et al. 2017; Lewis et al. 2018; Arribas et al. 2023; Hashimoto et al. 2023). Studying in detail the physical mechanisms driving the DSFGs in overdensities will provide valuable information on the halo properties and processes (e.g., gas-cooling, dark matter mass, gas accretion, gravitational interactions), which is key to understand the galaxy formation and evolution at the early stages of the Universe.

To date, most of the spatially-resolved analyses carried out in DSFGs at $z > 4$ have been focused on their UV and (sub)-mm emission, tracing their very young stellar population and molecular and dust distributions (Carilli et al. 2010; Hodge et al. 2015; Pavesi et al. 2018; Gómez-Guijarro et al. 2019; Hodge et al. 2019). However, the available IR instruments did not allow to spatially resolve these objects, leaving the structure of the host

Optimization of cosmic filament finders and unbiased recovery of filament phase space profiles using mock filaments

Saeed Dhawalikar,¹ and Aseem Paranjape

Inter-University Centre for Astronomy & Astrophysics,
Ganeshkhind, Post Bag 4, Pune 411007, India

E-mail: saeed.dhawalikar@iucaa.in, aseem@iucaa.in

Abstract. Cosmic filaments, the most prominent features of the cosmic web, possibly hold untapped potential for cosmological inference. While it is natural to expect the structure of filaments to show universality similar to that seen in dark matter halos, the lack of agreement between different filament finders on what constitutes a filament has hampered progress on this topic. We initiate a programme to systematically investigate and uncover possible universal features in the phase space structure of cosmic filaments, by generating particle realizations of mock filaments with *a priori* known properties. Using these, we identify an important source of bias in the extraction of radial density profiles, which occurs when the local curvature κ of the spine exceeds a threshold determined by the filament thickness. This bias exists even for perfectly determined spines, thus affecting *all* filament finders. We show that this bias can be nearly eliminated by simply discarding the regions with the highest κ , with little loss of precision. An additional source of bias is the noise generated by the filament finder when identifying the spine, which depends on both the finder algorithm as well as intrinsic properties of the individual filament. We find that, to mitigate this bias, it is essential not only to smooth the estimated spine, but to *optimize* this smoothing separately for each filament. We propose a novel optimization based on minimizing the estimated filament thickness, along with Fourier space smoothing. We implement these techniques using two tools, `FilGen` which generates mock filaments and `FilAPT` which analyses and processes them. We expect these tools to be useful in calibrating the performance of filament finders, thereby enabling searches for filament universality.

Keywords: cosmic web, cosmic flows, semi-analytic modeling

¹Corresponding author.

The Role of a Neutron Component in the Photospheric Emission of Long-Duration Gamma-Ray Burst Jets

NATHAN WALKER ¹, TYLER PARSOTAN ², AND DAVIDE LAZZATI ¹

¹*Oregon State University*

*Department of Physics, 301 Weniger Hall, Oregon State University
Corvallis, OR 97331, USA*

²*Astrophysics Science Division, NASA Goddard Space Flight Center, Greenbelt, MD 20771, USA*

ABSTRACT

Long-duration gamma-ray bursts (LGRBs), thought to be produced during core-collapse supernovæ, may have a prominent neutron component in the outflow material. If present, neutrons can change how photons scatter in the outflow by reducing its opacity, thereby allowing the photons to decouple sooner than if there were no neutrons present. Understanding the details of this process could therefore allow us to probe the central engine of LGRBs, which is otherwise hidden. Here, we present results of the photospheric emission from an LGRB jet, using a combination of relativistic hydrodynamic simulations and radiative transfer post-processing using the Monte Carlo Radiation Transfer (MCRaT) code. We control the size of the neutron component in the jet material by varying the equilibrium electron fraction Y_e , and we find that the presence of neutrons in the GRB fireball affects the Band parameters α and E_0 , while the picture with the β parameter is less clear. In particular, the break energy E_0 is shifted to higher energies. Additionally, we find that increasing the size of the neutron component also increases the total radiated energy of the outflow across multiple viewing angles. Our results not only shed light on LGRBs, but are also relevant to short-duration gamma-ray bursts associated with binary neutron star mergers, due to the likelihood of a prominent neutron component in such systems.

Keywords: Gamma-ray bursts(629) — Radiative transfer simulations(1967) — Hydrodynamical simulations (767)

1. INTRODUCTION

Our understanding of Gamma-Ray Bursts (GRBs) has evolved dramatically since their discovery in the late 1960's. First detected as short transient bursts of high energy photons (Klebesadel et al. 1973), observations of afterglows (Groot et al. 1998; Costa et al. 1997) and supernova counterparts (Galama et al. 1998; Hjorth et al. 2003; Woosley & Bloom 2006; Bloom et al. 1999) have facilitated a deeper understanding of these otherwise mysterious events. Long duration gamma-ray bursts (LGRBs) are now thought to occur during core-collapse supernovæ, a process in which stars more massive than about $8M_\odot$ end their lives in a violent explosion, resulting in the formation of either a Black Hole (BH) or a Neutron Star (NS) (Woosley & Janka 2005). After the formation of either a BH or a NS, material from the preceding collapse can accrete around the compact object, providing a possible power source for an ensuing LGRB (e.g. Narayan et al. (2001)). Alternatively, a highly magnetized, fast spinning NS could power a rel-

ativistic outflow by tapping into its rotational energy (e.g., Bucciantini et al. 2012). Given the possibility of a NS as either an intermediate or a terminal stage of the supernova, there is a strong possibility of a neutron component in the accreting material, which can then be collimated into a relativistic jet and produce a LGRB.

In spite of this progress, one aspect of GRBs that still remains in contention is the nature of the prompt emission. In LGRBs, the prompt emission can last anywhere from a few seconds to a few minutes (Bloom et al. 1999; MacFadyen et al. 2001) and is characterized by bright, non-thermal spectra (Band et al. 1993). A leading model that explains this emission is the Synchrotron Shock Model (SSM). In this model, the jet expands and reaches the photosphere without producing noticeable radiation. After passing the photosphere, electrons in colliding internal shocks produce non-thermal radiation (Rees & Meszaros 1994). While this model naturally explains the characteristic non-thermal emission of GRBs and is able to fit the spectra of a number of bursts,

Primordial black holes or else?

Tidal tests on subsolar mass gravitational-wave observations

Francesco Crescimbeni,^{1,2,*} Gabriele Franciolini,^{3,†} Paolo Pani,^{1,2,‡} and Antonio Riotto^{4,5,§}

¹*Dipartimento di Fisica, Sapienza Università di Roma, Piazzale Aldo Moro 5, 00185, Roma, Italy*

²*INFN, Sezione di Roma, Piazzale Aldo Moro 2, 00185, Roma, Italy*

³*CERN, Theoretical Physics Department, Esplanade des Particules 1, Geneva 1211, Switzerland*

⁴*Département de Physique Théorique, Université de Genève, 24 quai Ansermet, CH-1211 Genève 4, Switzerland*

⁵*Gravitational Wave Science Center (GWSC), Université de Genève, CH-1211 Geneva, Switzerland*

(Dated: March 1, 2024)

The detection of a subsolar object in a compact binary merger is regarded as one of the smoking gun signatures of a population of primordial black holes (PBHs). We critically assess whether these systems could be distinguished from stellar binaries, for example composed of white dwarfs or neutron stars, which could also populate the subsolar mass range. At variance with PBHs, the gravitational-wave signal from stellar binaries is affected by tidal effects, which dramatically grow for moderately compact stars as those expected in the subsolar range. We forecast the capability of constraining tidal effects of putative subsolar neutron star binaries with current and future LIGO-Virgo-KAGRA (LVK) sensitivities as well as next-generation experiments. We show that, should LVK O4 run observe subsolar neutron-star mergers, it could measure the (large) tidal effects with high significance. In particular, for subsolar neutron-star binaries, O4 and O5 projected sensitivities would allow measuring the effect of tidal disruption on the waveform in a large portion of the parameter space, also constraining the tidal deformability at $\mathcal{O}(10\%)$ level, thus excluding a primordial origin of the binary. Viceversa, for subsolar PBH binaries, model-agnostic upper bounds on the tidal deformability can rule out neutron stars or more exotic competitors. Assuming events similar to the sub-threshold candidate SSM200308 reported in LVK O3b data are PBH binaries, O4 projected sensitivity would allow ruling out the presence of neutron-star tidal effects at $\approx 3\sigma$ C.L., thus strengthening the PBH hypothesis. Future experiments would lead to even stronger ($> 5\sigma$) conclusions on potential discoveries of this kind.

I. INTRODUCTION

The observation of a subsolar mass (SSM) object in a binary black hole (BBH) merger is considered as the most robust smoking gun of the primordial nature of a binary [1]. Exploiting this window, however, relies on our capabilities to distinguish such event from other astrophysical systems and other potential candidates from new physics [2, 3].

A signal compatible with a subsolar merger could be observed already during the ongoing O4 run of the LIGO/Virgo/Kagra (LVK) Collaboration. Previous LVK observation campaigns reported the existence of SSM candidate events with too low significance to be classified as confident detections [4], and were not included in the LVK merger catalog [5]. Subsequent work, especially Ref. [6], reported the analysis of the SSM candidate SSM200308, possibly composed by two subsolar BHs with masses $m_1 = 0.62^{+0.46}_{-0.20} M_\odot$ and $m_2 = 0.27^{+0.12}_{-0.10} M_\odot$ at a redshift of $z = 0.02^{+0.01}_{-0.01}$ (90% C.I.), showing relatively small errors on the determination of both masses even for such sub-threshold event. This is because light mergers perform a large number of cycles in the detector band.

However, the SSM nature of the event alone is not sufficient to claim the observation of a PBH binary. Since a robust detection of a subsolar BH¹ would be a breakthrough with a strong impact on cosmology, high-energy physics, and astrophysics [8–10], it is of utmost importance to exclude any possible source of confusion that might affect such a putative detection.

In this paper, we investigate whether current and future experiments would have sufficient sensitivity required to detect SSM200308-like events, and distinguish this from other astrophysical systems or more exotic competitors in the SSM range.

Although standard formation scenarios suggest that astrophysical compact objects have typically masses above M_\odot (and below a critical mass $\sim \mathcal{O}(M_\odot)$), both white dwarfs (WDs) and neutron stars (NSs) can in principle be subsolar. In typical astrophysical settings, WDs are formed with masses as low as $\approx 0.2M_\odot$ [11]. NSs are observed through X-ray observations and GWs [12–16]. All these observations point towards a population of supersolar mass NSs, although there might be selection biases, especially for X-ray sources. Smaller masses are possible for cold, dense equations of state (EoS) [17], even though very light NSs are unstable to expansion [18] and supernova theory suggests heavier lower bounds on their mass

* francesco.crescimbeni@uniroma1.it

† gabriele.franciolini@cern.ch

‡ paolo.pani@uniroma1.it

§ antonio.riotto@unige.ch

¹ Population studies suggest that, if some of the O3 events are PBHs, there will be a non-negligible probability to detect subsolar events starting from O4 [7].

CHEX-MATE: A LOFAR pilot X-ray – radio study on five radio halo clusters

M. Balboni^{1,2}, F. Gastaldello¹, A. Bonafede^{3,4}, A. Botteon⁴, I. Bartalucci¹, H. Bourdin^{10,11}, G. Brunetti⁴, R. Cassano⁴, S. De Grandi¹³, F. De Luca^{10,11}, M. Gitti^{3,4}, M. Johnston-Hollitt¹⁴, P. Mazzotta^{10,11}, M. Rossetti¹, S. Etori^{6,7}, S. Ghizzardi¹, A. Iqbal⁸, L. Lovisari¹, S. Molendi¹, E. Pointecoteau⁵, G.W. Pratt⁸, G. Riva^{1,12}, H. Rottgering⁹, M. Sereno^{6,7}, R.J. van Weeren⁹, T. Venturi⁴, I. Veronesi¹

¹ INAF - IASF Milano, via A. Corti 12, 20133 Milano, Italy

² DiSAT, Università degli Studi dell'Insubria, via Valleggio 11, I-22100 Como, Italy

³ DIFA - Università di Bologna, via Gobetti 93/2, I-40129 Bologna, Italy

⁴ INAF - IRA, Via Gobetti 101, I-40129 Bologna, Italy

⁵ IRAP, Université de Toulouse, CNRS, CNES, UT3-UPS, (Toulouse), France

⁶ INAF, Osservatorio di Astrofisica e Scienza dello Spazio, via Piero Gobetti 93/3, 40129 Bologna, Italy

⁷ INFN, Sezione di Bologna, viale Berti Pichat 6/2, 40127 Bologna, Italy

⁸ Université Paris-Saclay, Université Paris Cité, CEA, CNRS, AIM, 91191, Gif-sur-Yvette, France

⁹ Leiden Observatory, Leiden University, PO Box 9513, 2300 RA Leiden, The Netherlands

¹⁰ INFN, Sezione di Roma 2, Università degli studi di Roma Tor Vergata, Via della Ricerca Scientifica, 1, Roma, Italy

¹¹ Università degli studi di Roma 'Tor Vergata', Via della ricerca scientifica, 1, 00133 Roma, Italy

¹² Dipartimento di Fisica, Università degli Studi di Milano, Via G. Celoria 16, 20133 Milano, Italy

¹³ INAF - Osservatorio Astronomico di Brera, via E. Bianchi 46, I-23807 Merate (LC), Italy

¹⁴ Curtin Institute for Data Science, Curtin University, GPO Box U1987, Perth, WA 6845, Australia

March 1, 2024

ABSTRACT

The connection between the thermal and non-thermal properties in galaxy clusters hosting radio halos seems fairly well established. However, a comprehensive analysis of such a connection has been made only for integrated quantities (e.g. $L_X - P_{radio}$ relation). In recent years new-generation radio telescopes have enabled the unprecedented possibility to study the non-thermal properties of galaxy clusters on a spatially resolved basis. Here, we perform a pilot study to investigate the mentioned properties on five targets, by combining X-ray data from the CHEX-MATE project with the second data release from the LOFAR Two meter Sky survey. We find a strong correlation ($r_s \sim 0.7$) with a slope less than unity between the radio and X-ray surface brightness. We also report differences in the spatially resolved properties of the radio emission in clusters which show different levels of dynamical disturbance. In particular, less perturbed clusters (according to X-ray parameters) show peaked radio profiles in the centre, with a flattening in the outer regions, while the three dynamically disturbed clusters have steeper profiles in the outer regions. We fit a model to the radio emission in the context of turbulent re-acceleration with a constant ratio between thermal and non-thermal particles energy density and a magnetic field profile linked to the thermal gas density as $B(r) \propto n_{th}^{0.5}$. We found that this simple model cannot reproduce the behaviour of the observed radio emission.

Key words. galaxy clusters – radio – X-ray

1. Introduction

Galaxy clusters are excellent laboratories for studying non-thermal phenomena, such as particle acceleration processes on large scales. In the last decades, a growing number of studies evidenced the presence of radio synchrotron emission in many of these objects (e.g. van Weeren et al. 2019, for a review). In particular, the most puzzling cases of radio emission are the extended radio sources (e.g. radio relics, mini-halos, giant halos). Giant radio halos are among the most extended cases of such emission. They are diffuse sources characterised by a steep spectral index ($\alpha < -1$, where $S_\nu \propto \nu^\alpha$) most frequently found in massive merging clusters.

Historically, two main scenarios have been proposed to explain radio halo origin: turbulent re-acceleration and hadronic models. In the former, relativistic electrons are re-accelerated via a Fermi-II like process by the turbulence injected in the

Intra-Cluster Medium (ICM) by cluster-cluster merger events (Brunetti et al. 2001; Petrosian 2001). In the latter case, instead, synchrotron emitting electrons are produced as *secondary* particles, i.e. as a decay product of heavy nuclei/particle collisions. These secondary models exploit cosmic ray protons (CRp) long lifetime over which they can diffuse on \sim Mpc scales and then, through collisions with ICM heavy nuclei, produce Cosmic Ray electrons (CRE) throughout all the cluster environment (e.g. Dennison 1980; Blasi & Colafrancesco 1999; Pfrommer & Enßlin 2004). Such CRp can be produced mainly by AGN activity but also by accretion shocks and galactic outflows (Brunetti & Jones 2014).

The non-detection of gamma rays from π^0 decay from clusters (Ackermann et al. 2016; Brunetti et al. 2017; Adam et al. 2021), the connection of radio halos with mergers (Cassano et al. 2010, 2023; Cuciti et al. 2021) and the spectral properties of halos

CHEX-MATE: Robust reconstruction of temperature profiles in galaxy clusters with XMM-Newton

M. Rossetti¹, D. Eckert², F. Gastaldello¹, E. Rasia^{3,4}, G.W. Pratt⁵, S. Ettori^{6,7}, S. Molendi¹, M. Arnaud⁵, M. Balboni^{1,8}, I. Bartalucci¹, R.M. Batalha⁵, S. Borgani^{3,4,9}, H. Bourdin^{10,11}, S. De Grandi¹², F. De Luca^{10,11}, M. De Petris¹³, W. Forman¹⁴, M. Gaspari¹⁵, S. Ghizzardi¹, A. Iqbal⁵, S. Kay¹⁶, L. Lovisari^{1,14}, B.J. Maughan¹⁷, P. Mazzotta^{10,11}, E. Pointecouteau¹⁸, G. Riva^{1,19}, J. Sayers²⁰, and M. Sereno^{6,7}

(Affiliations can be found after the references)

March 1, 2024

ABSTRACT

The “Cluster HEritage project with XMM-Newton: Mass Assembly and Thermodynamics at the Endpoint of structure formation” (CHEX-MATE) is a multi-year Heritage program, to obtain homogeneous XMM-Newton observations of a representative sample of 118 galaxy clusters. The observations are tuned to reconstruct the distribution of the main thermodynamic quantities of the ICM up to R_{500} and to obtain individual mass measurements, via the hydrostatic-equilibrium equation, with a precision of 15-20%. Temperature profiles are a necessary ingredient for the scientific goals of the project and it is thus crucial to derive the best possible temperature measurements from our data. This is why we have built a new pipeline for spectral extraction and analysis of XMM-Newton data, based on a new physically motivated background model and on a Bayesian approach with Markov Chain Monte Carlo (MCMC) methods, that we present in this paper for the first time. We applied this new method to a subset of 30 galaxy clusters representative of the CHEX-MATE sample and show that we can obtain reliable temperature measurements up to regions where the source intensity is as low as 20% of the background, keeping systematic errors below 10%. We compare the median profile of our sample and the best fit slope at large radii with literature results and we find a good agreement with other measurements based on XMM-Newton data. Conversely, when we exclude from our analysis the most contaminated regions, where the source intensity is below 20% of the background, we find significantly flatter profiles, in agreement with predictions from numerical simulations and independent measurements with a combination of Sunyaev-Zeldovich and X-ray imaging data.

Key words. Galaxies:clusters:general, X-rays: galaxies: clusters

1. Introduction

Galaxy clusters represent the endpoint of structure formation in the Universe: they are the most massive virialized structures to have formed thus far and are located at the nodes of the cosmic web, continuously accreting matter from the filaments. The intra-cluster medium (ICM) constitutes their main baryonic component and is heated to X-ray emitting temperatures ($10^7 - 10^8$ K) during the formation and accretion processes, driven by dark matter. As such, the ICM carries important information on the physical processes of structure formation and on the global cluster properties: ICM thermodynamic properties correlate well with the total gravitational mass and properly scaled radial profiles of thermodynamic quantities are nearly universal, reflecting the properties of the underlying dark matter structure (Kaiser 1986). Deviations from these relations do exist and are a clear signpost of important effects such as cooling, non-gravitational feedback from Active Galactic Nuclei (AGN) or supernovae, bulk motions and turbulence induced by accretion processes (see Lovisari & Maughan 2022 for a recent review, Gaspari et al. 2014; Bulbul et al. 2019; Sereno et al. 2020; Poon et al. 2023).

The ICM temperature is one of the key observable quantities that can be derived from X-ray observations of galaxy clusters, along with density and metal abundance. It is derived from the analysis of X-ray spectra, mainly through the position of the *Bremsstrahlung* exponential cut-off. In the last 30 years, the previous and present generation of X-ray satellites have allowed spatially resolved spectral measurements, mapping the distribu-

tion of ICM temperatures from the cores to the external regions. Temperature profiles in radial annuli are a necessary ingredient to derive the radial distributions of thermodynamic quantities, such as pressure and entropy, and to reconstruct the total mass, through the hydrostatic equilibrium equation. Early temperature profiles with *ASCA* and *BeppoSAX* (e.g. Fabian et al. 1994; De Grandi & Molendi 2002) unambiguously demonstrated that some clusters do show a temperature decline in their inner regions, consistent with a short cooling time of the high-density central regions and the prediction of the cooling flow model (Fabian et al. 1984; Fabian 1994). With the fall of this model, after high resolution spectra with XMM-Newton RGS showed that the gas does not cool below a critical value (e.g. Peterson et al. 2001, 2003), these systems were dubbed Cool Cores (CC, Molendi & Pizzolato 2001) and showed to be typically associated with clusters in a relaxed dynamical state. Conversely, in the external regions, *ASCA* and *BeppoSAX* observations, lead to controversial results on the presence of a temperature gradient (e.g. Markevitch et al. 1998; Irwin et al. 1999; White 2000; De Grandi & Molendi 2002). This is due to technical challenges in measuring temperature profiles in the external regions of galaxy clusters, where the intensity of the source is low with respect to contamination from other brighter cluster regions because of the large Point Spread Function (PSF) and of several background components (see Ettori & Molendi 2011 for a review). The former issue has been resolved with the advent of the current generation of X-ray telescopes XMM-Newton and *Chandra*, which unambiguously showed a declining trend of the temperature profiles with radius

Design of the 50-meter Atacama Large Aperture Submm Telescope

A next-generation high throughput single dish facility for submillimeter astronomy

Tony Mroczkowski^{1*}, Patricio A. Gallardo², Martin Timpe³, Aleksej Kiselev³, Manuel Groh³, Hans Kaercher⁴, Matthias Reichert³, Claudia Cicone⁵, Roberto Puddu⁶, Pierre Dubois-dit-Bonclaud³, Daniel Bok³, Erik Dahl³, Mike Macintosh⁷, Simon Dicker⁸, Isabelle Violen⁹, Sabrina Sartori⁹, Guillermo Andrés Valenzuela Venegas⁹, Marianne Zeyringer⁹, Michael Niemack^{10,11}, Sergio Poppi¹², Rodrigo Olguin¹³, Evanthia Hatziminaoglou^{1,14,15}, Carlos De Breuck¹, Pamela Klaassen⁷, Francisco Montenegro-Montes^{1,16}, Thomas Zimmerer³

¹ European Southern Observatory, Karl-Schwarzschild-Str. 2, Garching 85748, Germany
e-mail: tonym@eso.org

² Kavli Institute for Cosmological Physics, University of Chicago, Chicago, IL, 60637, USA

³ OHB Digital Connect, Weberstraße 21, D-55130 Mainz, Germany

⁴ Independent Consultant, Kirchgasse 4, D-61184 Karben, Germany

⁵ Institute of Theoretical Astrophysics, University of Oslo, P.O. Box 1029, Blindern, 0315 Oslo, Norway

⁶ Instituto de Astrofísica and Centro de Astro-Ingeniería, Facultad de Física, Pontificia Universidad Católica de Chile, Santiago, Chile

⁷ UK Astronomy Technology Centre, Royal Observatory Edinburgh, Blackford Hill, Edinburgh EH9 3HJ, UK

⁸ Department of Physics and Astronomy, University of Pennsylvania, 209 South 33rd Street, Philadelphia, PA, 19104, USA

⁹ Department of Technology Systems, University of Oslo, Gunnar Randars Vei 19, 2007 Kjeller, Norway

¹⁰ Department of Physics, Cornell University, Ithaca, NY 14853, USA

¹¹ Department of Astronomy, Cornell University, Ithaca, NY 14853, USA

¹² INAF - Osservatorio Astronomico di Cagliari, 09047 Selargius, Italy

¹³ European Southern Observatory, Alonso de Cordova 3107, Vitacura, Santiago, Chile

¹⁴ Instituto de Astrofísica de Canarias (IAC), E-38205 La Laguna, Tenerife, Spain

¹⁵ Universidad de La Laguna, Dpto. Astrofísica, E-38206 La Laguna, Tenerife, Spain

¹⁶ Departamento de Física de la Tierra y de la Atmósfera e Instituto de Física de Partículas y del Cosmos (IPARCOS). Universidad Complutense de Madrid, Av. Complutense, s/n, 28040 Madrid, Spain

Received February 29, 2024; accepted month XX, 2024

ABSTRACT

Submillimeter and millimeter wavelengths can reveal a vast range of objects and phenomena that are either too cold, too distant, or too hot and energetic to be measured at visible wavelengths. For decades the astronomical community has highlighted the need for a large, high-throughput submm single dish that can map statistically significant portions of the sky with sufficient surface brightness sensitivity and angular and spectral resolution to probe truly representative source populations. The Atacama Large Aperture Submillimeter Telescope (AtLAST), with its 50-m aperture and 2° maximal field of view, aims to be such a facility. We present here the full design concept for AtLAST, developed through an EU-funded project. Our design approach begins with a long lineage of submm telescopes, relies on calculations and simulations to realize the optics, and uses finite element analysis to optimize the mechanical structure and subsystems. The result is an innovative rocking chair design with six instrument bays, two of which are mounted on Nasmyth platforms. AtLAST will be capable of 3° s^{-1} scanning and 1° s^{-2} acceleration, and will feature a surface accuracy of $\leq 20 \mu\text{m}$ half wavefront error allowing observations up to $\approx 950 \text{ GHz}$. Further, AtLAST will be a sustainable, visionary facility that will allow upgrades for decades to come. The demanding design requirements for AtLAST, set by transformative science goals, were met by combining novel concepts with lessons learned from past experience. While some aspects require further testing, prototyping, and field demonstrations, we estimate that the design will be construction-ready this decade.

Key words. Telescopes – Astronomical instrumentation, methods and techniques – Instrumentation: high angular resolution – Submillimeter: general

1. Introduction

The desire to understand the Universe and how we came to be—our *cosmic origins*—has been the driving force behind enormous scientific and technological progress in the field of astrophysics,

leading to advances that have benefited society as a whole.¹

¹ We note that by using the phrase *cosmic origins*, we do not mean to imply any formal association with any other ongoing effort, though synergies exist. While recent usage has included NASA's Cosmic Origins Program (officially founded in 2011; see <https://cor.gsfc.nasa.gov/news/news.php>) and the film

* contact e-mail: tonym@eso.org

The frequency of metal-enrichment of cool helium-atmosphere white dwarfs using the DESI Early Data Release

Christopher J. Manser,^{1,2*} Boris T. Gänsicke,² Paula Izquierdo,² Andrew Swan,² Joan Najita,³ C. Rockosi,^{4,5,6} Andreia Carrillo,^{7,8} Bokyoung Kim,⁹ Siyi Xu,¹⁰ Arjun Dey,³ J. Aguilar,¹¹ S. Ahlen,¹² R. Blum,³ D. Brooks,¹³ T. Claybaugh,¹¹ K. Dawson,¹⁴ A. de la Macorra,¹⁵ P. Doel,¹³ E. Gaztañaga,^{16,17,18} S. Gontcho A Gontcho,¹¹ K. Honscheid,^{19,20,21} R. Kehoe,²² A. Kremin,¹¹ M. Landriau,¹¹ L. Le Guillou,²³ Michael E. Levi,¹¹ T. S. Li,²⁴ A. Meisner,³ R. Miquel,^{25,26} J. Nie,²⁷ M. Rezaie,²⁸ G. Rossi,²⁹ E. Sanchez,³⁰ M. Schubnell,^{31,32} G. Tarlé,³² B. A. Weaver,³ Z. Zhou,²⁶ H. Zou²⁶

¹ *Astrophysics Group, Department of Physics, Imperial College London, Prince Consort Rd, London, SW7 2AZ, UK*

² *Department of Physics, University of Warwick, Coventry CV4 7AL, UK*

³ *NSF's NOIRLab, 950 N. Cherry Avenue, Tucson, AZ 85719, USA*

⁴ *Department of Astronomy and Astrophysics, University of California, Santa Cruz, 1156 High Street, Santa Cruz, CA 95065, USA*

⁵ *Department of Astronomy and Astrophysics, UCO/Lick Observatory, University of California, 1156 High Street, Santa Cruz, CA 95064, USA*

⁶ *University of California Observatories, 1156 High Street, Santa Cruz, CA 95065, USA*

⁷ *Institute for Computational Cosmology, Department of Physics, Durham University, Durham DH1 3LE, U.K*

⁸ *Centre for Extragalactic Astronomy, Department of Physics, University of Durham, South Road, Durham DH1 3LE, UK*

⁹ *Institute for Astronomy, University of Edinburgh, Royal Observatory, Blackford Hill, Edinburgh EH9 3HJ, UK*

¹⁰ *Gemini Observatory/NSF's NOIRLab, 670 N. Aohoku Place, Hilo, Hawaii, 96720, USA*

¹¹ *Lawrence Berkeley National Laboratory, 1 Cyclotron Road, Berkeley, CA 94720, USA*

¹² *Physics Dept., Boston University, 590 Commonwealth Avenue, Boston, MA 02215, USA*

¹³ *Department of Physics & Astronomy, University College London, Gower Street, London, WC1E 6BT, UK*

¹⁴ *Department of Physics and Astronomy, The University of Utah, 115 South 1400 East, Salt Lake City, UT 84112, USA*

¹⁵ *Instituto de Física, Universidad Nacional Autónoma de México, Cd. de México C.P. 04510, México*

¹⁶ *Institut d'Estudis Espacials de Catalunya (IEEC), 08034 Barcelona, Spain*

¹⁷ *Institute of Cosmology & Gravitation, University of Portsmouth, Dennis Sciana Building, Portsmouth, PO1 3FX, UK*

¹⁸ *Institute of Space Sciences, ICE-CSIC, Campus UAB, Carrer de Can Magrans s/n, 08913 Bellaterra, Barcelona, Spain*

¹⁹ *Center for Cosmology and AstroParticle Physics, The Ohio State University, 191 West Woodruff Avenue, Columbus, OH 43210, USA*

²⁰ *Department of Physics, The Ohio State University, 191 West Woodruff Avenue, Columbus, OH 43210, USA*

²¹ *The Ohio State University, Columbus, 43210 OH, USA*

²² *Department of Physics, Southern Methodist University, 3215 Daniel Avenue, Dallas, TX 75275, USA*

²³ *Sorbonne Université, CNRS/IN2P3, Laboratoire de Physique Nucléaire et de Hautes Energies (LPNHE), FR-75005 Paris, France*

²⁴ *Department of Astronomy & Astrophysics, University of Toronto, Toronto, ON M5S 3H4, Canada*

²⁵ *Institució Catalana de Recerca i Estudis Avançats, Passeig de Lluís Companys, 23, 08010 Barcelona, Spain*

²⁶ *Institut de Física d'Altes Energies (IFAE), The Barcelona Institute of Science and Technology, Campus UAB, 08193 Bellaterra Barcelona, Spain*

²⁷ *National Astronomical Observatories, Chinese Academy of Sciences, A20 Datun Rd., Chaoyang District, Beijing, 100012, P.R. China*

²⁸ *Department of Physics, Kansas State University, 116 Cardwell Hall, Manhattan, KS 66506, USA*

²⁹ *Department of Physics and Astronomy, Sejong University, Seoul, 143-747, Korea*

³⁰ *CIEMAT, Avenida Complutense 40, E-28040 Madrid, Spain*

³¹ *Department of Physics, University of Michigan, Ann Arbor, MI 48109, USA*

³² *University of Michigan, Ann Arbor, MI 48109, USA*

Accepted XXX. Received YYY; in original form ZZZ

ABSTRACT

There is overwhelming evidence that white dwarfs host planetary systems; revealed by the presence, disruption, and accretion of planetary bodies. A lower limit on the frequency of white dwarfs that host planetary material has been estimated to be $\approx 25 - 50$ per cent; inferred from the ongoing or recent accretion of metals onto both hydrogen-atmosphere and warm helium-atmosphere white dwarfs. Now with the unbiased sample of white dwarfs observed by the Dark Energy Spectroscopic Instrument (DESI) survey in their Early Data Release (EDR), we have determined the frequency of metal-enrichment around cool-helium atmosphere white dwarfs as 21 ± 3 per cent using a sample of 234 systems. This value is in good agreement with values determined from previous studies. With the current samples we cannot distinguish whether the frequency of planetary accretion varies with system age or host-star mass, but the DESI data release 1 will contain roughly an order of magnitude more white dwarfs than DESI EDR and will allow these parameters to be investigated.

Key words: white dwarfs – surveys – planetary systems – exoplanets

[Ne v] emission from a faint epoch of reionization-era galaxy: evidence for a narrow-line intermediate mass black hole

J. Chisholm^{1*}, D. A. Berg¹, R. Endsley¹, S. Gazagnes¹, C. T. Richardson², E. Lambrides^{3,4}, J. Greene⁵, S. Finkelstein¹, S. Flury^{6,7}, N. G. Guseva⁸, A. Henry⁹, T. A. Hutchison^{3,4}, Y. I. Izotov⁸, R. Marques-Chaves¹⁰, P. Oesch¹⁰, C. Papovich¹¹, A. Saldana-Lopez¹², D. Schaerer^{10,13}, M. G. Stephenson¹

¹Department of Astronomy, University of Texas at Austin, 2515 Speedway, Austin, Texas 78712, USA

²Elon University, 100 Campus Drive, Elon, NC 27244

³Astrophysics Science Division, Code 662, NASA Goddard Space Flight Center, 8800 Greenbelt Rd, Greenbelt, MD 20771, USA

⁴NASA Postdoctoral Fellow

⁵Department of Astrophysical Sciences, Princeton University, 4 Ivy Lane, Princeton, NJ08544, USA

⁶Department of Astronomy, University of Massachusetts Amherst, Amherst, MA 01002, United States

⁷NASA FINESST Fellow

⁸Bogolyubov Institute for Theoretical Physics, National Academy of Sciences of Ukraine, 14-b Metrolohichna str., Kyiv, 03143, Ukraine

⁹Space Telescope Science Institute, 3700 San Martin Drive Baltimore, MD 21218, United States

¹⁰Geneva Observatory, Department of Astronomy, University of Geneva, Chemin Pegasi 51, CH-1290 Versoix, Switzerland

¹¹Department of Physics and Astronomy, Texas A&M University, College Station, TX, 77843-4242 USA

¹²Department of Astronomy, Stockholm University, Oscar Klein Centre, AlbaNova University Centre, 106 91 Stockholm, Sweden

¹³CNRS, IRAP, 14 Avenue E. Belin, 31400 Toulouse, France

Accepted XXX. Received YYY; in original form ZZZ

ABSTRACT

Here we present high spectral resolution *JWST* NIRSpec observations of GN 42437, a low-mass ($\log(M_*/M_\odot) = 7.9$), compact ($r_e < 500$ pc), extreme starburst galaxy at $z = 5.59$ with 13 emission line detections. GN 42437 has a low-metallicity (5–10% Z_\odot) and its rest-frame $H\alpha$ equivalent width suggests nearly all of the observed stellar mass formed within the last 3 Myr. GN 42437 has an extraordinary 7σ significant [Ne v] 3427 Å detection. The [Ne v] line has a rest-frame equivalent width of 11 ± 2 Å, $[\text{Ne v}]/H\alpha = 0.04 \pm 0.007$, $[\text{Ne v}]/[\text{Ne III}] 3870\text{Å} = 0.26 \pm 0.04$, and $[\text{Ne v}]/\text{He II } 4687\text{Å} = 1.2 \pm 0.5$. Ionization from massive stars, shocks, or high-mass X-ray binaries cannot simultaneously produce these [Ne v] and other low-ionization line ratios. Reproducing the complete nebular structure requires both massive stars and accretion onto a black hole. We do not detect broad lines nor do the traditional diagnostics indicate that GN42437 has an accreting black hole. Thus, the very-high-ionization emission lines powerfully diagnose faint narrow-line black holes at high-redshift. We approximate the black hole mass in a variety of ways as $\log(M_{\text{BH}}/M_\odot) \sim 5 - 7$. This black hole mass is consistent with local relations between the black hole mass and the observed velocity dispersion, but significantly more massive than the stellar mass would predict. Very-high-ionization emission lines may reveal samples to probe the formation and growth of the first black holes in the universe.

Key words: galaxies: high-redshift – galaxies: evolution – galaxies: formation

1 INTRODUCTION

JWST observations have discovered a rich and ubiquitous population of super massive black holes (SMBH) in fainter galaxies at higher redshifts than previously known (Brinchmann 2023; Furtak et al. 2023; Goulding et al. 2023; Greene et al. 2023; Harikane et al. 2023; Kocevski et al. 2023; Kokorev et al. 2023; Labbé et al. 2023; Larson et al. 2023; Maiolino et al. 2023; Matthee et al. 2023; Onoue et al. 2023; Scholtz et al. 2023; Übler et al. 2023; Kokorev et al. 2024; Lambrides et al. 2024). These recently detected black holes have masses that range up to $\sim 10^8 M_\odot$ only a few 100 Myr after the Big Bang. Energy and momentum from these intrinsically luminous

sources may impact the formation and evolution of their host galaxies (Gebhardt et al. 2000; Ferrarese & Merritt 2000). Fully accounting for the energy and momentum that accretion onto early black holes injects into the gas within galaxies requires revealing the population demographics of black holes in the early universe.

Combined with observations of UV-bright quasars (Becker et al. 2001; Fan et al. 2006; Willott et al. 2010; Jiang et al. 2016; Bañados et al. 2018; Matsuoka et al. 2018, 2019; Eilers et al. 2023; Yang et al. 2023), these observations have firmly established the existence of SMBHs at $z > 5$, but theory still debates how these SMBHs formed. The age of the universe is just 1 Gyr at $z = 5.5$. If black holes start as stellar mass black holes ($\sim 10 - 100 M_\odot$), Eddington-limited accretion just barely grows the black hole to $10^8 M_\odot$ in the age of the universe (Haiman & Loeb 2001; Bromm & Larson 2004).

* E-mail: chisholm@austin.utexas.edu

Chemical Diagnostics to Unveil Environments Enriched by First Stars

IRENE VANNI,^{1,2} STEFANIA SALVADORI,^{1,2} VALENTINA D'ODORICO,^{3,4,5} GEORGE D. BECKER,⁶ AND GUIDO CUPANI³

¹*Dipartimento di Fisica e Astrofisica, Università degli Studi di Firenze, Via G. Sansone 1, I-50019 Sesto Fiorentino, Italy*

²*INAF/Osservatorio Astrofisico di Arcetri, Largo E. Fermi 5, I-50125 Firenze, Italy*

³*INAF/Osservatorio Astronomico di Trieste, Via G. Tiepolo 11, I-34143, Trieste, Italy*

⁴*Scuola Normale Superiore, Piazza dei Cavalieri 7, I-56126, Pisa, Italy*

⁵*IFPU - Institute for Fundamental Physics of the Universe, via Beirut 2, I-34151 Trieste, Italy*

⁶*Department of Physics & Astronomy, University of California, Riverside, CA-92521, USA*

Abstract

Unveiling the chemical fingerprints of the first (Pop III) stars is crucial for indirectly studying their properties and probing their massive nature. In particular, very massive Pop III stars explode as energetic Pair-Instability Supernovae (PISNe), so their chemical products might escape in the diffuse medium around galaxies, opening the possibility to observe their fingerprints in distant gas clouds. Recently, three $z > 6.3$ absorbers with abundances consistent with an enrichment from PISNe have been observed with JWST. In this Letter, we present novel chemical diagnostics to uncover environments mainly imprinted by PISNe. Furthermore, we revise the JWST low-resolution measurements by analysing the publicly available high-resolution X-Shooter spectra for two of these systems. Our results reconcile the chemical abundances of these absorbers with those from literature, which are found to be consistent with an enrichment dominated ($> 50\%$ metals) by normal Pop II SNe. We show the power of our novel diagnostics in isolating environments uniquely enriched by PISNe from those mainly polluted by other Pop III and Pop II SNe. When the subsequent enrichment from Pop II SNe is included, however, we find that the abundances of PISN-dominated environments partially overlap with those predominantly enriched by other Pop III and Pop II SNe. We dub these areas *confusion regions*. Yet, the odd-even abundance ratios [Mg,Si/Al] are extremely effective in pinpointing PISN-dominated environments and allowed us to uncover, for the first time, an absorber consistent with a PISN enrichment for all the *six* measured elements.

1. INTRODUCTION

Understanding the properties of the first (Pop III) stars and their impact on subsequent galaxy formation is a fundamental problem (e.g. Klessen & Glover 2023). Discovering the chemical fingerprints of Pop III stars exploding as supernovae (SNe) is crucial to achieve this goal (e.g. Koutsouridou et al. 2023). Indeed, cosmological simulations show that Pop III stars were more massive than present-day stars (e.g. Hirano et al. 2014; Susa et al. 2014), an idea also supported by the persistent lack of metal-free stars (e.g. Rossi et al. 2021). Thus, most Pop III stars might have rapidly disappeared as SNe, promptly enriching the pristine gas with their newly formed chemical products.

Pop III SNe with various progenitor masses and explosion energies synthesize different heavy elements (e.g. Heger & Woosley 2010; Kobayashi 2012) thus producing distinctive chemical fingerprints (see Vanni et al. 2023a). These unique signatures can be observed in distant gaseous absorbers directly enriched by these pristine sources (Saccardi et al. 2023), or in long-lived metal-poor stars born in Pop III enriched environments (e.g. Frebel et al. 2019; Skúladóttir et al. 2021). Stellar evolution calculations for the chemical products of very massive pair instability SNe (PISNe, $M_* = 140 - 260M_\odot$) are extremely robust and predict unique abundance patterns, featuring a strong odd-even effect (Heger & Woosley 2002; Takahashi 2018).

Many efforts have been dedicated to seek out these unique PISN fingerprints (see Salvadori et al. 2019; Aguado et al. 2023; Caffau et al. 2023) and finally one possible pure PISN descendant has been found in the LAMOST survey (Xing et al. 2023). If predominantly

Constraining the hadronic properties of star-forming galaxies above 1 GeV with 15-years Fermi-LAT data

A. Ambrosone^{1,2}, M. Chianese^{3,4}, and A. Marinelli^{3,4,5}

¹ Gran Sasso Science Institute (GSSI), Viale Francesco Crispi 7, 67100 L'Aquila, Italy

² INFN-Laboratori Nazionali del Gran Sasso(LNGS), via G. Acitelli 22, 67100 Assergi (AQ), Italy

³ Dipartimento di Fisica “Ettore Pancini”, Università degli studi di Napoli “Federico II”, Complesso Univ. Monte S. Angelo, I-80126 Napoli, Italy

⁴ INFN - Sezione di Napoli, Complesso Univ. Monte S. Angelo, I-80126 Napoli, Italy

⁵ INAF - Osservatorio Astronomico di Capodimonte, Salita Moiarriello 16, I-80131 Naples, Italy

Received XXXX; accepted XXXX

ABSTRACT

Context. Star-forming and starburst galaxies (SFGs and SBGs) are considered to be powerful emitters of non-thermal γ -rays and neutrinos, due to their intense phases of star-formation activity, which should confine high-energy Cosmic-Rays (CRs) inside their environments. On this regard, the Fermi-LAT collaboration has found a correlation between the γ -ray and infrared luminosities for a sample of local sources. Yet, the physics behind these non-thermal emission is still under debate.

Aims. We aim at refining the correlation between γ -rays and star formation rate (SFR) exploiting 15 years of public Fermi-LAT data, thus probing the calorimetric fraction F_{cal} of high-energy protons in SFGs and SBGs. Further, we aim at extrapolating this information to their diffuse γ -ray and neutrino emissions constraining their contribution to the extra-galactic gamma-ray background (EGB) and the diffuse neutrino flux.

Methods. Using the publicly-available `fermitools`, we analyse 15.3 years of γ -ray between 1 – 1000 GeV data for 70 sources, 56 of which were not previously detected. We relate this emission to a physically-motivated model for SBGs in order to constrain F_{cal} for each source and then study its correlation with the star formation rate of the sources.

Results. Firstly, we find at 4σ level an indication of γ -ray emission for other two SBGs, namely M 83 and NGC 1365. By contrast, we find that, with the new description of background, the significance for the γ -ray emission of the previously detected M 33 reduces at 4σ . We also find that the physically-motivated model for F_{cal} correctly describes the γ -ray observations, and it is crucial to assess the systematic uncertainty on the star formation rate. Finally, undiscovered sources strongly constraints F_{cal} at 95% CL, providing fundamental information when we interpret the results as common properties of SFGs and SBGs. Hence, we find that these sources might contribute $(20 \pm 5)\%$ to the EGB, while the corresponding diffuse neutrino flux strongly depends on the spectral index distribution along the source class.

Key words. Galaxies:starbursts – galaxies:star formation – gamma rays:galaxies

1. Introduction

Star-forming and starburst galaxies (SFGs and SBGs) are galaxies in a phase of intense star formation, leading to high gas density and to an enhanced rate of supernovae (SN) explosions Peretti et al. (2019). This activity is expected to be directly correlated to γ -rays and neutrinos, via proton-proton (pp) collisions between high-energy Cosmic-Rays (CRs) accelerated by supernovae remnants (SNRs) and the gas (Peretti et al. 2019, 2020; Ambrosone et al. 2021a,b; Kornecki et al. 2020; Kornecki et al. 2022). The Fermi-LAT collaboration has indeed detected a sample of 14 SFGs which feature a correlation between the γ -ray luminosity from 100 MeV to 100 GeV ($L_{[0.1-100]\text{GeV}}$) and the infrared luminosity ($L_{8-1000\mu\text{m}}$) (Ackermann et al. 2012). These detections have also been updated by several authors, such as (Rojas-Bravo & Araya 2016; Ajello et al. 2020; Xiang et al. 2023).

These results are typically interpreted as an evidence for the existence of common properties shared by the entire population of SFGs and SBGs (Kornecki et al. 2022). For instance, the fact that these sources present hard power-law spectra $E^{-\gamma}$, with $\gamma \sim 2.2 - 2.3$, might indicate that the physics of CRs is

dominated by energy-independent mechanisms, such as the pp inelastic timescale or advection (Lacki & Beck 2013). However, some works (Krumholz et al. 2020; Roth et al. 2021, 2023) have recently proposed that CR transport inside these source might be dominated by diffusion for $E_{\text{CR}} \geq 100 \text{ GeV}$, leading to a suppression of the γ -ray and neutrino production rates at higher energies. Physically, this means that the calorimetric fraction F_{cal} – i.e. the fraction of high-energy CRs which actually lose energy inside SFGs and SBGs producing γ -rays and neutrinos – might be smaller than previously predicted and also energy-dependent. In order to discriminate these two scenarios, however, new and more precise measurements (especially in the TeV energy range) are required (Ambrosone et al. 2022).

In this paper, we provide new constraints on the calorimetric fraction of SFGs and SBGs by analysing a catalogue of 70 sources introduced by Ackermann et al. (2012), using ~ 15.3 years of Fermi-LAT data¹ and the publicly-available

¹ Fermi-LAT data can be freely downloaded at <https://fermi.gsfc.nasa.gov/ssc/data/access/>

El Gordo needs *El Anzuelo*: Probing the structure of cluster members with multi-band extended arcs in JWST data

A. Galan^{1,2,*}, G. B. Caminha^{1,2}, J. Knollmüller^{1,3,4}, J. Roth^{5,2,6} and S. H. Suyu^{1,2}

¹ Technical University of Munich, TUM School of Natural Sciences, Department of Physics, James-Frank-Str 1, 85748 Garching, Germany

² Max-Planck-Institut für Astrophysik, Karl-Schwarzschild-Str. 1, 85748 Garching, Germany

³ ORIGINS Excellence Cluster, Boltzmannstr. 2, 85748 Garching, Germany

⁴ Radboud University, Heyendaalseweg 135, 6525 AJ Nijmegen, Netherlands

⁵ Technische Universität München (TUM), Boltzmannstr. 3, 85748 Garching, Germany

⁶ Ludwig-Maximilians-Universität, Geschwister-Scholl-Platz 1, 80539 Munich, Germany

March 1, 2024

ABSTRACT

Gravitational lensing by galaxy clusters involves hundreds of galaxies over a large redshift range and increases the likelihood of rare phenomena (supernovae, microlensing, dark substructures, etc.). Characterizing the mass and light distributions of foreground and background objects often requires a combination of high-resolution data and advanced modeling techniques. We present the detailed analysis of *El Anzuelo*, a prominent quintuply imaged dusty star forming galaxy ($z_s = 2.29$), mainly lensed by three members of the massive galaxy cluster ACT-CL J0102–4915, also known as *El Gordo* ($z_d = 0.87$). We leverage JWST/NIRCam data containing previously unseen lensing features using a Bayesian, multi-wavelength, differentiable and GPU-accelerated modeling framework that combines HERCULENS (lens modeling) and NIFTY (field model and inference) software packages. For one of the deflectors, we complement lensing constraints with stellar kinematics measured from VLT/MUSE data. In our lens model, we explicitly include the mass distribution of the cluster, locally corrected by a constant shear field. We find that the two main deflectors (L1 and L2) have logarithmic mass density slopes steeper than isothermal, with $\gamma_{L1} = 2.23 \pm 0.05$ and $\gamma_{L2} = 2.21 \pm 0.04$. We argue that such steep density profiles can arise due to tidally truncated mass distributions, which we probe thanks to the cluster lensing boost and the strong asymmetry of the lensing configuration. Moreover, our three-dimensional source model captures most of the surface brightness of the lensed galaxy, revealing a clump of at most 400 parsecs at the source redshift, visible at wavelengths $\lambda_{\text{rest}} \gtrsim 0.6 \mu\text{m}$. Finally, we caution on using point-like features within extended arcs to constrain galaxy-scale lens models before securing them with extended arc modeling.

Key words. Galaxies: clusters: general - Galaxies: clusters: individual: ACT-CL J0102–4915 - Galaxies: evolution - Infrared: galaxies - Gravitational lensing: strong - Methods: data analysis

1. Introduction

1.1. Strong gravitational lensing in galaxy clusters

Extending over megaparsec scales and reaching up to quadrillion solar masses, massive galaxy clusters are direct tracers of the cosmic web and its evolution through cosmic time. Galaxy clusters emerge as information-rich targets for jointly studying rare phenomena such as microlensing and caustic-crossing events (e.g., Dai et al. 2020; Williams et al. 2024), distant supernovae (e.g., Rodney et al. 2021; Frye et al. 2024), and probing the cosmological evolution of the Universe (e.g., Abbott et al. 2020; Bocquet et al. 2024). The most massive clusters are made of several hundreds of co-evolving galaxies, showcasing in a single scene the many different stages of galaxy evolution predominantly in the redshift range $z \sim 0 - 1$ (e.g., Wen et al. 2012; Hilton et al. 2021; Klein et al. 2023; Bulbul et al. 2024), probing the transition from a matter-dominated Universe to one driven by dark energy. Additionally, these clusters act as vast permeable screens standing between our telescopes and a plethora of more distant objects, enabling their detection up to redshifts $z \sim 13$ (e.g., Adams et al. 2023; Wang et al. 2023, 2024) and probing

the epoch of reionization. Galaxy clusters do not only magnify these distant objects but also distort and duplicate their images, which can take the form of giant arcs extending over several arcseconds (Bayliss et al. 2011; Cava et al. 2018; Welch et al. 2022). This striking phenomenon, called strong gravitational lensing, is a direct consequence of the extensive gravitational potential of foreground galaxy clusters and their alignment with populations of background sources. A notable property of strong gravitational lensing in clusters is the extreme time delays between the multiple images of time-varying sources, which are used to geometrically measure absolute distances and cosmological parameters (e.g., Caminha et al. 2022; Kelly et al. 2023; Grillo et al. 2024), for which gains in precision are expected specifically with galaxy clusters (Acebron et al. 2023; Bergamini et al. 2024).

Strong gravitational lensing in galaxy clusters is a natural and direct tool to characterize both visible and invisible massive structures of galaxies and their surroundings, which is key to deepen our understanding of their formation and evolution. The high multiplicity of lensed background sources can be used to constrain physical quantities describing individual galaxy members as well as their host dark matter halo through a process

* Corresponding author (aymeric.galan@gmail.com).

Mass scaling relations for dark halos from an analytic universal outer density profile

Giorgos Korkidis^{1,2}, and Vasiliki Pavlidou^{1,2}

¹ Department of Physics and Institute for Theoretical and Computational Physics, University of Crete, GR-70013 Heraklio, Greece
email:gkorkidis@physics.uoc.gr;pavlidou@physics.uoc.gr

² Institute of Astrophysics, Foundation for Research and Technology – Hellas, Vassilika Vouton, GR-70013 Heraklio, Greece

ABSTRACT

Context. The average matter density within the turnaround scale, which demarcates where galaxies shift from clustering around a structure to joining the expansion of the Universe, is an important cosmological probe. However, a measurement of the mass enclosed by the turnaround radius is difficult. Analyses of the turnaround scale in simulated galaxy clusters place the turnaround radius at about three times the virial radius in a Λ CDM universe and at a (present-day) density contrast with the background matter density of the Universe of $\delta \sim 11$. Assessing the mass at such extended distances from a cluster’s center is a challenge for current mass measurement techniques. Consequently, there is a need to develop and validate new mass-scaling relations, to connect observable masses at cluster interiors with masses at greater distances.

Aims. Our research aims to establish an analytical framework for the most probable mass profile of galaxy clusters, leading to novel mass scaling relations, allowing us to estimate masses at larger scales. We derive such analytical mass profiles and compare them with those from cosmological simulations.

Methods. We use excursion set theory, which provides a statistical framework for the density and local environment of dark matter halos, and complement it with the spherical collapse model to follow the non-linear growth of these halos.

Results. The profile we developed analytically shows a good agreement (better than 30%, and dependent on halo mass) with the mass profiles of simulated galaxy clusters. Mass scaling relations are obtained from the analytical profile with offset better than 15% from the simulated ones. This level of precision highlights the potential of our model for probing structure formation dynamics at the outskirts of galaxy clusters.

Key words. large-scale structure of Universe – Methods: analytical, numerical – Galaxies: clusters: general

1. Introduction

Galaxy clusters, the largest gravitationally bound structures in the universe, have long been recognized as valuable cosmological laboratories. Over the past three decades, significant advancements have been made in understanding their composition, dynamics, and integral role within the cosmic web. The well-studied interiors of these clusters, particularly their relaxed regions, have laid the foundations for our concordance model of hierarchical structure formation. This progress has now extended beyond the traditionally studied virialization regime to include the kinetically driven splashback regions (Diemer & Kravtsov 2014; Adhikari et al. 2014; More et al. 2015, 2016; O’Neil et al. 2021). However, the potential of the outer regions of galaxy clusters, extending outside the splashback radius, into the infalling region and beyond, remains largely untapped. These outer reaches hold substantial promise for deepening our understanding of structure formation and cosmology.

Recently, the turnaround scale has gathered significant attention in cosmological studies (Pavlidou & Tomaras 2014; Lee & Li 2017; Fong et al. 2022; Lopes et al. 2019; Capozziello et al. 2019). This scale represents the point at which galaxies transition from infall towards the central cluster to expansion with the background Universe. In previous work (Pavlidou et al. 2020), we identified the turnaround scale as a novel cosmological probe. We showed that the present average matter density on this scale (the *turnaround density* ρ_{ta}) probes the

overall matter content of the universe, and that its evolution with time is influenced by the existence of a cosmological constant. The turnaround scale has thus the potential to provide new constraints on cosmological parameters, complementary to the ones obtained from the Cosmic Microwave Background (CMB)(e.g., Komatsu et al. 2011), Baryon Acoustic Oscillations (BAO)(e.g., Eisenstein et al. 2005), and Type Ia Supernovae (e.g., Amanullah et al. 2010).

Our subsequent studies (Korkidis et al. 2020, 2023) confirmed the utility of ρ_{ta} for testing cosmological models using N-body cosmological simulations. However, measuring the turnaround density in actual observations using current astronomical surveys presents significant challenges. The radius where galaxies join the Hubble flow has thus far been measured for only a few nearby superclusters (Karachentsev & Nasonova 2010; Nasonova et al. 2011; Lee 2018). Accurately measuring the total mass of galaxies at these scales presents an even more formidable challenge. Several issues complicate such observations on a cluster-by-cluster basis, making the associated errors unsuitable for precise cosmological analysis: (a) Accurate measurement of the mass at the turnaround scale would necessitate extensive spectroscopic and gravitational lensing surveys, mapping the galaxy distribution on very large scales around clusters. (b) In the context of the cold dark matter (CDM) model of structure formation, it is well-acknowledged that most of the mass surrounding galaxies is dark and, for such small objects as galactic halos, largely inaccessible; (c) Foreground and background

A toy model for gas sloshing in galaxy clusters

E. Roediger,^{1*} I. Vaezzadeh^{2,1}, and P. Nulsen^{3,4}

¹*E.A. Milne Centre, University of Hull, Cottingham Road, HU6 7RX, U.K.*

²*I. Physikalisches Institut, Universität zu Köln, Zùlpicher Str. 77, D-50937 Köln, Germany*

³*Center for Astrophysics|Harvard & Smithsonian, 60 Garden St., Cambridge, MA 02138, USA*

⁴*International Centre for Radio Astronomy Research, University of Western Australia, 35 Stirling Hwy, Crawley, WA 6009, Australia*

Accepted XXX. Received YYY; in original form ZZZ

ABSTRACT

We apply a toy model based on ‘pendulum waves’ to gas sloshing in galaxy clusters. Starting with a galaxy cluster potential filled with a hydrostatic intra-cluster medium (ICM), we perturb all ICM by an initial small, unidirectional velocity, i.e., an instantaneous kick. Consequently, each parcel of ICM will oscillate due to buoyancy with its local Brunt-Väisälä (BV) period, which we show to be approximately proportional to the cluster radius. The oscillation of gas parcels at different radii with different periods leads to a characteristic, outwards-moving coherent pattern of local compressions and rarefactions; the former form the sloshing cold fronts (SCFs). Our model predicts that SCFs (i) appear in the cluster centre first, (ii) move outwards on several Gyr timescales, (iii) form a staggered pattern on opposite sides of a given cluster, (iv) each move outwards with approximately constant speed; and that (v) inner SCFs form discontinuities more easily than outer ones. These features are well known from idealised (magneto)-hydrodynamic simulations of cluster sloshing. We perform comparison hydrodynamic+N-body simulations where sloshing is triggered either by an instantaneous kick or a minor merger. Sloshing in these simulations qualitatively behaves as predicted by the toy model. However, the toy model somewhat over-predicts the speed of sloshing fronts, and does not predict that inner SCFs emerge with a delay compared to outer ones. In light of this, we identify the outermost cold front, which may be a ‘failed’ SCF, as the best tracer of the age of the merger that set a cluster sloshing.

Key words: Galaxies: clusters: intracluster medium — Galaxies: clusters: general — Physical Data and Processes: hydrodynamics

1 INTRODUCTION

Mergers between galaxy clusters leave observable features in the X-ray emitting intracluster medium (ICM) of a galaxy cluster. These features include shocks and cold fronts (Markevitch & Vikhlinin 2007). Cold fronts differ from shocks in that the pressure is continuous across a cold front, so that the denser side of the discontinuity is colder than the more diffuse side.

Here we focus on sloshing cold fronts (SCFs), which arise when the ICM of a cluster is perturbed by, e.g., a minor merger as first proposed by Tittley & Henriksen (2005); Ascasibar & Markevitch (2006). They showed that the gravitational disturbance caused by a subcluster passing through the primary cluster is sufficient to cause the ICM of the primary cluster to ‘slosh’ about the gravitational potential minimum, leading to the familiar arc-shaped ‘edges’ in X-ray surface brightness, wrapped around the cluster core. SCFs have been observed in many galaxy clusters (for a review see ZuHone et al. 2016) and are thought to be ubiquitous in cool-core (CC) clusters (Markevitch et al. 2003; Ghizzardi et al. 2010).

The development and evolution of SCFs has been well-studied using hydrodynamic simulations both in the interest of constructing cluster merger histories (Roediger et al. 2011; Roediger & ZuHone

2012; Su et al. 2017; Sheardown et al. 2018; Vaezzadeh et al. 2022) and constraining transport processes within the ICM (ZuHone 2011; Roediger et al. 2013b; ZuHone et al. 2013, 2015; Brzycki & ZuHone 2019). Keshet et al. (2023) describe a spiral structure as a quasi-stationary solution for the ICM.

The positive entropy gradient in the ICM leads to the ICM being stable against convection, i.e. after a perturbation a parcel of ICM oscillates rather than keeping rising or sinking. The frequency of such a radial oscillation is known as the Brunt-Väisälä frequency (Cox 1980), and can be written as:

$$\omega_{\text{BV}}(r) = \Omega_{\text{K}} \sqrt{\frac{1}{\gamma} \frac{d \ln K(r)}{d \ln r}} \quad (1)$$

where $\Omega_{\text{K}} = \sqrt{\frac{GM}{r^3}}$ is the Keplerian frequency, $\gamma = 5/3$ is the ratio of specific heats and $K = kTn^{-2/3}$ the entropy index. Churazov et al. (2003) and Su et al. (2017) have used the BV period,

$$T_{\text{BV}} = 2\pi/\omega_{\text{BV}} \quad (2)$$

as an estimate of the sloshing timescale.

In this paper we present a toy model that links local oscillations of ICM parcels with their BV period to the global motion of SCFs, following in broad terms the scenario outlined in Churazov et al. (2003). In essence, our toy model draws an analogy between sloshing fronts

* E-mail: e.roediger@hull.ac.uk (ER)

ALMA view of the L1448-mm protostellar system on disk scales: CH₃OH and H¹³CN as new disk wind tracers

P. Nazari¹, B. Tabone², A. Ahmadi¹, S. Cabrit^{3,4}, E. F. van Dishoeck^{1,5}, C. Codella^{6,4}, J. Ferreira⁴, L. Podio⁶, Ł. Tychoniec⁷, and M. L. van Gelder¹

¹ Leiden Observatory, Leiden University, P.O. Box 9513, 2300 RA Leiden, the Netherlands
e-mail: nazari@strw.leidenuniv.nl

² Université Paris-Saclay, CNRS, Institut d'Astrophysique Spatiale, 91405 Orsay, France

³ Observatoire de Paris, PSL University, Sorbonne Université, CNRS UMR 8112, LERMA, 61 Avenue de l'Observatoire, 75014 Paris, France

⁴ Univ. Grenoble Alpes, CNRS, IPAG, 38000 Grenoble, France

⁵ Max Planck Institut für Extraterrestrische Physik (MPE), Giessenbachstrasse 1, 85748 Garching, Germany

⁶ INAF, Osservatorio Astrofisico di Arcetri, Largo E. Fermi 5, I-50125 Firenze, Italy

⁷ European Southern Observatory, Karl-Schwarzschild-Strasse 2, 85748 Garching, Germany

Received 20 November 2023 / Accepted 19 February 2024

ABSTRACT

Protostellar disks are known to accrete, however, the exact mechanism that extracts the angular momentum and drives accretion in the low-ionization "dead" region of the disk is under debate. In recent years, magneto-hydrodynamic (MHD) disk winds have become a popular solution. Yet, observations of these winds require both high spatial resolution (~ 10 au) and high sensitivity, which has resulted in only a handful of MHD disk wind candidates so far. In this work we present high angular resolution (~ 30 au) ALMA observations of the emblematic L1448-mm protostellar system and find suggestive evidence for an MHD disk wind. The disk seen in dust continuum (~ 0.9 mm) has a radius of ~ 23 au. Rotating infall signatures in H¹³CO⁺ indicate a central mass of $0.4 \pm 0.1 M_{\odot}$ and a centrifugal radius similar to the dust disk radius. Above the disk, we unveil rotation signatures in the outflow traced by H¹³CN, CH₃OH, and SO lines and find a kinematical structure consistent with theoretical predictions for MHD disk winds. This is the first detection of an MHD disk wind candidate in H¹³CN and CH₃OH. The wind launching region estimated from cold MHD wind theory extends out to the disk edge. The magnetic lever arm parameter would be $\lambda_{\phi} \simeq 1.7$, in line with recent non-ideal MHD disk models. The estimated mass-loss rate is ~ 4 times the protostellar accretion rate ($\dot{M}_{\text{acc}} \simeq 2 \times 10^{-6} M_{\odot}/\text{yr}$) and suggests that the rotating wind could carry enough angular momentum to drive disk accretion.

Key words. Stars: protostars – ISM: molecules – Stars: winds, outflows – Techniques: interferometric

1. Introduction

Star formation starts with a cloud of gas and dust which collapses as it rotates. Because of conservation of angular momentum, the envelope flattens and a disk forms. If angular momentum is not transported away, the disk cannot accrete and the star cannot grow (Hartmann et al. 2016). Therefore, angular momentum needs to be extracted from the disk by either turbulent stresses (Shakura & Sunyaev 1973; Lynden-Bell & Pringle 1974; Balbus & Hawley 1998) or magnetized disk winds (Blandford & Payne 1982; Ferreira 1997). Magneto-hydrodynamic (MHD) disk winds are expected to be a natural result of the vertical magnetic field in the disk inherited from the collapse (Ferreira 1997; Tomida et al. 2010; Bai & Stone 2013). These winds have become particularly popular in recent years as a viable solution to the angular momentum problem in disk regions $\simeq 1 - 50$ au, where ionization is too low to sustain MHD turbulence (see PPVII reviews by Pascucci et al. 2023; Manara et al. 2023; Lesur et al. 2023), and to explain disk demographics (Tabone et al. 2022).

Yet, only a handful of spatially resolved observations of such disk wind candidates are available (Launhardt et al. 2009; Bjerkeli et al. 2016; Hirota et al. 2017; Tabone et al. 2017; Lee

et al. 2018; de Valon et al. 2020, 2022). The high sensitivity, angular and spectral resolution of the Atacama Large Millimeter/submillimeter Array (ALMA) are particularly needed to resolve the rotating signatures of disk winds and provide clues on their launch point (Tabone et al. 2020). Therefore, it is still an open question as to whether MHD disk winds are ubiquitous. It is not yet clear whether the low-velocity, wide-angle molecular outflow often surrounding the base of the high-velocity jet is simply a result of envelope entrainment by the central jet or if it mainly originates as an MHD wind launched from an extended region of the disk (see de Valon et al. 2022; Pascucci et al. 2023 for in-depth discussions).

In this paper we present high angular resolution ($\sim 0.1'' = 30$ au) and high sensitivity ALMA observations to characterize the disk of the emblematic L1448-mm protostellar system, analyze the base of its outflow, and present first evidence for its MHD disk wind. L1448-mm (also known as L1448-C and Peremb 26) is a well-known Class 0 source located in the Perseus star-forming region ($d \simeq \sim 300$ pc; Ortiz-León et al. 2018), first betrayed by its spectacular outflow and jet (Bachiller et al. 1990, 1991), and with a luminosity of $\sim 9 L_{\odot}$ (André et al. 2010; van't Hoff et al. 2022). Over the past 35 years, its dust continuum has been extensively studied at millimeter and centimeter wave-

Probing the dust grain alignment mechanisms in spiral galaxies with M 51 as the case study

ENRIQUE LOPEZ-RODRIGUEZ¹ AND LE NGOC TRAM²

¹*Kavli Institute for Particle Astrophysics & Cosmology (KIPAC), Stanford University, Stanford, CA 94305, USA*

²*Max-Planck-Institut für Radioastronomie, Auf dem Hügel 69, 53121 Bonn, German*

ABSTRACT

Magnetic fields (B-fields) in galaxies have recently been traced using far-infrared and sub-mm polarimetric observations with SOFIA, JCMT, and ALMA. The main assumption is that dust grains are magnetically aligned with the local B-field in the interstellar medium (ISM). However, the range of physical conditions of the ISM, dust grain sizes, and B-field strengths in galaxies where this assumption is valid has not been characterized yet. Here, we use the well-studied spiral galaxy M 51 as a case study. We find that the timescale for the alignment mechanism arising from magnetically aligned dust grains (B-RAT) dominates over other alignment mechanisms, including radiative precession (k-RAT), and mechanical alignment (v-MAT), as well as to the randomization effect (gas damping). We estimate the sizes of the aligned dust grain to be in the range of $0.009 - 0.182 \mu\text{m}$ and $0.019 - 0.452 \mu\text{m}$ for arms and inter-arms, respectively. We show that the difference in the polarization fraction between arms and interarms can arise from the enhancement of small dust grain sizes in the arms as an effect of the grain alignment disruption (RAT-D). We argue that the RAT-D mechanism needs to have additional effects, e.g., intrinsic variations of the B-field structure and turbulence, in the galaxy's components to fully explain the polarization fraction variations within the arms and inter-arms.

Keywords: galaxies: spiral – galaxies: individual (M 51) – galaxies: ISM – ISM: dust, extinction – starlight polarization

1. INTRODUCTION

Far-infrared (FIR; $50 - 220 \mu\text{m}$) and sub-mm ($850 - 1200 \mu\text{m}$) imaging polarimetric observations have opened a new window to explore extragalactic magnetism (e.g., Lopez-Rodriguez et al. 2018; Jones et al. 2019; Lopez-Rodriguez et al. 2020; Jones et al. 2020; Lopez-Rodriguez 2021; Lopez-Rodriguez et al. 2021; Borlaff et al. 2021; Pattle et al. 2021a; Lopez-Rodriguez et al. 2022; Borlaff et al. 2023; Lopez-Rodriguez 2023). All observed nearby (≤ 20 Mpc) galaxies (e.g., spirals, mergers, starbursts, active galactic nuclei) show kpc-scale ordered magnetic fields (B-fields) cospatial with the dense and cold phase of the interstellar medium (ISM) and star-forming regions. These observations were performed using the High-Angular Wideband Camera Plus (HAWC+) on board the 2.7-m Stratospheric Observatory for Infrared Astronomy (SOFIA), POL-2 on the James Clerk Maxwell Telescope (JCMT), and the Atacama Large Millimeter/submillimeter Array (ALMA). The angular resolutions of single-dish telescopes are in the range of $5 - 18''$, which corresponds to spatial scales of ~ 300 pc for a typical nearby galaxy at ~ 10 Mpc and at an angular resolution of $10''$ (Lopez-Rodriguez et al. 2022), while ALMA has performed polarimetric observations of resolution of ~ 5 pc in the starburst galaxy NGC 253 at a distance of 3.50 Mpc (Lopez-Rodriguez 2023). Furthermore, recent ALMA polarimetric observations have measured B-fields of ~ 5 kpc scale in a gravitationally lensed dusty star-forming galaxy

at redshift $z = 2.6$ by means of polarized thermal emission in the rest frame of $\sim 350 \mu\text{m}$ (Geach et al. 2023). These measurements rely on that the dust grains are magnetically aligned with the local B-field (e.g., Andersson et al. 2015), and that the measured B-field orientation is a density-weighted average of a non-trivial B-field structure within the several hundred pc size given by the angular resolution (Martin-Alvarez et al. 2023). Thus, several fundamental questions arise: are the FIR/sub-mm polarimetric observations measuring magnetically aligned dust grains, or are these observations affected by other dust alignment mechanisms? Is the dependence of the polarization with total intensity due to a loss of dust grain alignment efficiency or intrinsic variations of the B-field?

Theories of grain alignment mechanisms have been in active development since the first discovery of the polarization signature of aligned non-spherical dust grains in the interstellar medium (ISM) by Hiltner (1949) and Hall & Mikesell (1949). The paramagnetic relaxation proposed by Davis & Greenstein (DG; 1951) had been considered as a classical mechanism. However, paramagnetic relaxation has been shown to be inefficient as the rotation of large grains can be easily randomized and then weakly aligned (Hoang & Lazarian 2016a,b), which is opposite to observations. Purcell (1979) showed that the grains could suprathermally rotate with systematic torques, which is due to the desorption of the recoil of H_2 molecules from the grain surface to the

Using Rest-Frame Optical and NIR Data from the RAISIN Survey to Explore the Redshift Evolution of Dust Laws in SN Ia Host Galaxies

Stephen Thorp^{1,2*}, Kaisey S. Mandel^{2,3}, David O. Jones⁴, Robert P. Kirshner^{5,6}, and Peter M. Challis⁷

¹*The Oskar Klein Centre, Department of Physics, Stockholm University, AlbaNova University Centre, SE 106 91 Stockholm, Sweden*

²*Institute of Astronomy and Kavli Institute for Cosmology, Madingley Road, Cambridge, CB3 0HA, UK*

³*Statistical Laboratory, DPMMS, University of Cambridge, Wilberforce Road, Cambridge, CB3 0WB, UK*

⁴*Institute for Astronomy, University of Hawai'i, 640 N. A'ohoku Pl., Hilo, HI 96720, USA*

⁵*TMT International Observatory, 100 West Walnut Street, Pasadena, CA 91124, USA*

⁶*California Institute of Technology, 1200 East California Boulevard, Pasadena, CA 91125, USA*

⁷*Harvard-Smithsonian Center for Astrophysics, 60 Garden Street, Cambridge, MA 02138, USA*

Accepted XXX. Received YYY; in original form ZZZ

ABSTRACT

We use rest-frame optical and near-infrared (NIR) observations of 42 Type Ia supernovae (SNe Ia) from the Carnegie Supernova Project at low- z and 37 from the RAISIN Survey at high- z to investigate correlations between SN Ia host galaxy dust, host mass, and redshift. This is the first time the SN Ia host galaxy dust extinction law at high- z has been estimated using combined optical and rest-frame NIR data (YJ -band). We use the BAYESN hierarchical model to leverage the data's wide rest-frame wavelength range (extending to ~ 1.0 – 1.2 μm for the RAISIN sample at $0.2 \lesssim z \lesssim 0.6$). By contrasting the RAISIN and CSP data, we constrain the population distributions of the host dust R_V parameter for both redshift ranges. We place a limit on the difference in population mean R_V between RAISIN and CSP of $-1.16 < \Delta\mu(R_V) < 1.38$ with 95% posterior probability. For RAISIN we estimate $\mu(R_V) = 2.58 \pm 0.57$, and constrain the population standard deviation to $\sigma(R_V) < 0.90$ [2.42] at the 68 [95]% level. Given that we are only able to constrain the size of the low- to high- z shift in $\mu(R_V)$ to $\lesssim 1.4$ – which could still propagate to a substantial bias in the equation of state parameter w – these and other recent results motivate continued effort to obtain rest-frame NIR data at low and high redshifts (e.g. using the *Roman Space Telescope*).

Key words: supernovae: general – distance scale – dust, extinction – methods: statistical

1 INTRODUCTION

With the advent of the Vera C. Rubin Observatory's Legacy Survey of Space and Time (LSST; Ivezić et al. 2019), and the High-Latitude Time Domain Survey (HLTDS) on the *Nancy Grace Roman Space Telescope* (Spergel et al. 2015; Hounsell et al. 2018; Rose et al. 2021a), cosmology using Type Ia Supernovae (SNe Ia) is set to enter an era of unprecedented precision. However, the success of these future experiments hinges on our ability to account for systematic uncertainties that are not yet fully understood. A particularly challenging and contentious issue is determining the distribution of dust laws in SN Ia host galaxies (see e.g. Brout & Scolnic 2021; Thorp et al. 2021). Galaxy evolution studies tell us that dust properties correlate strongly with stellar mass and star formation (see e.g. Salim et al. 2018; Nagaraj et al. 2022), but the parent stellar populations of SNe Ia also correlate with galaxy properties (e.g. Childress et al. 2014). Either of these effects could cause the accuracy of SN Ia distance estimates to “drift” over cosmic time – a deeply troubling systematic for cosmology. The very latest constraints on the dark energy equation-of-state parameter (w ; see DES Collaboration et al. 2024) from SNe Ia have highlighted the importance of understanding this issue (Vincenzi et al. 2024). In this paper, we analyse new rest

frame near-infrared (NIR) observations of SNe Ia at high redshift from the RAISIN Survey (SNIA in the IR; Jones et al. 2022), using these data in combination with the BAYESN hierarchical model (Mandel et al. 2022; Grayling et al. 2024) to explore how the dust laws in SN Ia host galaxies depends on redshift and mass.

The nature of line-of-sight dust extinction in SN Ia host galaxies has been a topic of significant investigation throughout the history of supernova cosmology, with the correction of this effect being a critical part of SN Ia standardisation. A particular sticking point has been the estimation of the dust law R_V parameter in SN Ia hosts – an issue debated in the literature (e.g. Branch & Tammann 1992; Riess et al. 1996; Tripp 1998; Tripp & Branch 1999, and references therein) since before the first discovery of accelerating expansion (Riess et al. 1998; Perlmutter et al. 1999). As acknowledged in many of these early works (particularly Riess et al. 1996), the estimation of R_V is rendered challenging by the confounding between this quantity and any intrinsic colour–luminosity correlation exhibited by SNe Ia (see Mandel et al. 2017, for extensive discussion of this problem). Considerable progress has been made over the past two and a half decades, with the construction of large optical+NIR SN Ia samples (e.g. Wood-Vasey et al. 2008; Contreras et al. 2010; Stritzinger et al. 2011; Friedman et al. 2015; Krisciunas et al. 2017), and the development of robust statistical methods for analysing these (e.g. Mandel et al. 2009, 2011; Burns et al. 2011, 2014; Mandel et al. 2022).

* E-mail: stephen.thorp@fysik.su.se

How does the radio enhancement of broad absorption line quasars relate to colour and accretion rate?

J. W. Petley¹★, L. K. Morabito¹, A. L. Rankine², G. T. Richards³, N. L. Thomas^{1,4},
D. M. Alexander¹, V. A. Fawcett⁵, G. Calistro Rivera⁶, I. Prandoni⁷, P. N. Best², S. Kolwa⁸

¹Centre for Extragalactic Astronomy, Department of Physics, Durham University, Durham, DH1 3LE, UK

²Institute for Astronomy, University of Edinburgh, Royal Observatory, Blackford Hill, Edinburgh EH9 3HJ, UK

³Department of Physics, Drexel University, 32 S. 32nd Street, Philadelphia, PA 19104, USA

⁴Institute for Computational Cosmology, Department of Physics, Durham University, South Road, Durham, DH1 3LE, UK

⁵School of Mathematics, Statistics and Physics, Newcastle University, Newcastle upon Tyne, NE1 7RU, UK

⁶European Southern Observatory, Karl-Schwarzschild-Str. 2, 85748 Garching bei München, Germany

⁷INAF-IRA, Via P. Gobetti 101, 40129 Bologna, Italy

⁸Physics Department, University of Johannesburg, 5 Kingsway Ave, Rossmore, Johannesburg, 2092, South Africa

Accepted XXX. Received YYY; in original form ZZZ

ABSTRACT

The origin of radio emission in different populations of radio-quiet quasars is relatively unknown, but recent work has uncovered various drivers of increased radio-detection fraction. In this work, we pull together three known factors: optical colour ($g - i$), C IV Distance (a proxy for L/L_{Edd}) and whether or not the quasar contains broad absorption lines (BALQSOs) which signify an outflow. We use SDSS DR14 spectra along with the LOFAR Two Metre Sky Survey Data Release 2 and find that each of these properties have an independent effect. BALQSOs are marginally more likely to be radio-detected than non-BALQSOs at similar colours and L/L_{Edd} , moderate reddening significantly increases the radio-detection fraction and the radio-detection increases with L/L_{Edd} above a threshold for all populations. We test a widely used simple model for radio wind shock emission and calculate energetic efficiencies that would be required to reproduce the observed radio properties. We discuss interpretations of these results concerning radio-quiet quasars more generally. We suggest that radio emission in BALQSOs is connected to a different physical origin than the general quasar population since they show different radio properties independent of colour and C IV distance.

Key words: quasars: general – galaxies: evolution – radio continuum: galaxies

1 INTRODUCTION

Black holes are now key to our understanding of the complex evolution of galaxies, despite being fundamentally simple to characterise (e.g. mass and spin - Kerr 1963). Nearly all galaxies contain a super-massive black hole (SMBHs) and, during rapid growth, black hole systems can stimulate electromagnetic radiation in their surroundings. These black holes are considered to be "active" and referred to as Active Galactic Nuclei (AGN). Combined with the knowledge that SMBHs grow with their galaxies (see Kormendy et al. 2013), AGN have become objects of great interest in many different areas of astronomy today.

Quasars (also known as QSOs) are the brightest of all AGN and are some of the most luminous objects at optical wavelengths in the observable universe (Schmidt et al. 1968). The massive amount of luminosity ($> 10^{44}$ erg/s) that quasars radiate could impact the future evolution of their host galaxies since, at least for a time when we observe them, they have a much greater energetic output than

all the stars in their galaxy. However, it is often difficult to predict what will be observed across the full spectral energy distribution of a quasar even if some wavelength regions or physical properties (eg. accretion rate and black hole mass) are well understood or measured. Since different wavelength ranges offer information about different physical scales and processes, we cannot build a full picture of quasar behaviour without appreciating the longest, as well as the shortest, wavelengths.

Radio emission at low frequencies ($\lesssim 10$ GHz) in quasars is largely dominated by the synchrotron radiation process. Emission is released through the acceleration of electrons moving at relativistic speeds through a magnetic field (Condon et al. 1992). Radio emission is largely unaffected by sources of obscuration which significantly modulate what is observed at shorter wavelengths. For example, we avoid the effects of dust that impact optical and ultra-violet (UV) emission. Radio observations could therefore play a key role in understanding energetic interactions between a black hole and its galaxy. The most widely recognisable sources of synchrotron emission are famous *radio-jet* type galaxies with complex jet and filament type structures which extend well beyond the size of the host galaxy (Fanaroff &

★ E-mail: james.w.petley@durham.ac.uk

Dynamics and potential origins of decimeter-sized particles around comet 67P/Churyumov-Gerasimenko

Marius Pfeifer¹, Jessica Agarwal^{1,2}, Raphael Marschall³, Björn Grieger⁴, and Pablo Lemos^{1,2}

¹ Max Planck Institute for Solar System Research, Justus-von-Liebig-Weg 3, D-37077 Göttingen, Germany
e-mail: pfeifer@mps.mpg.de

² Institute for Geophysics and Extraterrestrial Physics, TU Braunschweig, Mendelssohnstraße 3, D-38106 Braunschweig, Germany

³ CNRS, Laboratoire J.-L. Lagrange, Observatoire de la Côte d'Azur, Nice, France

⁴ Aurora Technology B.V. for ESA, ESAC, Madrid, Spain

Received <date> / Accepted <date>

ABSTRACT

Context. One of the primary goals of the European Space Agency's Rosetta mission to comet 67P/Churyumov-Gerasimenko was to investigate the mechanisms responsible for cometary activity.

Aims. Our aim is to learn more about the ejection process of large refractory material by studying the dynamics of decimeter-sized dust particles in the coma of 67P and estimating their potential source regions.

Methods. We algorithmically tracked thousands of individual particles through four OSIRIS/NAC image sequences of 67P's near-nucleus coma. We then traced concentrated particle groups back to the nucleus surface, and estimated their potential source regions, size distributions, and projected dynamical parameters. Finally, we compared the observed activity to dust coma simulations.

Results. We traced back 409 decimeter-sized particles to four suspected source regions. The regions strongly overlap and are mostly confined to the Khonsu-Atum-Anubis area. The activity may be linked to rugged terrain, and the erosion of fine dust and the ejection of large boulders may be mutually exclusive. Power-law indices fitted to the particle size–frequency distributions range from 3.4 ± 0.3 to 3.8 ± 0.4 . Gas drag fits to the radial particle accelerations provide an estimate for the local gas production rates ($Q_g = 3.6 \cdot 10^{-5} \text{ kg s}^{-1} \text{ m}^{-2}$), which is several times higher than our model predictions based on purely insolation-driven water ice sublimation. Our observational results and our modeling results both reveal that our particles were likely ejected with substantial nonzero initial velocities of around $0.5\text{--}0.6 \text{ m s}^{-1}$.

Conclusions. Our findings strongly suggest that the observed ejection of decimeter-sized particles cannot be explained by water ice sublimation and favorable illumination conditions alone. Instead, the local structures and compositions of the source regions likely play a major role. In line with current ejection models of decimeter-sized particles, we deem an overabundance of CO₂ ice and its sublimation to be the most probable driver. In addition, because of the significant initial velocities, we suspect the ejection events to be considerably more energetic than gradual liftoffs.

Key words. comets: general – comets: individual: 67P/Churyumov–Gerasimenko – zodiacal dust.

1. Introduction

Comets are small Solar System objects that formed in the outer regions of our protoplanetary disk beyond the snowline (e.g., Weissman et al. 2020). At these heliocentric distances, water and other (super-)volatiles like CO₂ can remain solid over astronomical timescales. These ices make up a significant part of cometary material, which otherwise consists mainly of refractory aggregates. Because of this ice content, comets become active once they enter the inner Solar System: their ices start to sublimate. If this happens beneath the cometary surface, the expanding gas can get trapped and build up pressure. Eventually, this pressure may overcome the gravity and tensile strength of the overlying material, expel the gas, and eject some of the refractory material along with it. The released gas and dust then form the characteristic cometary coma, tail, and trail (e.g., Zakharov et al. 2022).

Decimeter-sized particles¹ are likely ejected by CO₂ ice sublimation in deeper surface layers (e.g., Gundlach et al. 2020; Fulle et al. 2020; Wesotowski et al. 2020; Ciarniello et al. 2022;

Davidsson et al. 2022); however, the responsible mechanisms are not yet fully understood (e.g., Zakharov et al. 2022; Bischoff et al. 2023; Agarwal et al. 2023), and even less so for small particles where cohesion forces dominate (e.g., Gundlach et al. 2015; Skorov et al. 2017; Markkanen & Agarwal 2020).

Learning more about these processes was, and still is, one of the primary science goals of the European Space Agency's Rosetta mission to comet 67P/Churyumov–Gerasimenko (e.g., Taylor et al. 2017). The spacecraft rendezvoused with 67P in August 2014 and accompanied the comet through its perihelion passage in August 2015, until Rosetta was set on an intercept course with 67P on September 30, 2016, and landed on its surface. Among the suite of Rosetta's science instruments was the Optical, Spectroscopic, and Infrared Remote Imaging System (OSIRIS), which consisted of a wide-angle and a narrow-angle camera (WAC and NAC, Keller et al. 2007). During the rendezvous phase, these cameras recorded many image sequences of the near-nucleus coma, which also captured the motion of individual dust particles shortly after their ejection. Because the study of their dynamics can help to understand their ejection process, we developed a particle tracking algorithm for OSIRIS images in Pfeifer et al. (2022).

¹ Following the classification of cometary dust by Güttler et al. (2019), we use the term “particle” as a generic term for any unspecified dust particle, independently of its size.